1-1-2013

The design, synthesis, and biological evaluation of aplysinopsin analogs as potential neuromodulators

Kevin Lewellyn
University of Mississippi

THE DESIGN, SYNTHESIS, AND BIOLOGICAL EVALUATION OF APLYSINOPSIN ANALOGS AS POTENTIAL NEUROMODULATORS

A Dissertation
presented in partial fulfillment of requirements
for the degree of Doctor of Philosophy
in the Department of Pharmacognosy
The University of Mississippi

KEVIN LEWELLYN

December 2013

ABSTRACT

Aplysinopsins are tryptophan-derived natural products that have been isolated from a variety of marine organisms and have been shown to possess a range of biological activities. Initial synthesis of a library of 50 aplysinopsin analogs revealed that of the 12 serotonin receptor subtypes and 34 other CNS receptors, aplysinopsin analogs showed a high affinity for the 5-HT_{2B} and 5-HT_{2C} receptor subtypes, with selectivity for 5-HT_{2B} over 5-HT_{2C}. Bromination at C-4 and C-5 of the indole ring resulted in greater binding affinities, with K_i's as low as 35 nM. In addition, biological evaluation of the MAO-A and MAO-B inhibitory activities of these compounds revealed some potent and selective MAO inhibitors. The most active compound **54**, which is brominated at C-6 and methylated at N-2′ and N-4′, showed strong inhibitory activity at MAO-A (IC_{50} of 0.0056 μM) and had an SI of 80.24. Compounds **31**, **51**, and **54** were evaluated in the chick anxiety-depression model to assess their in vivo efficacy. Compound **33** showed a modest antidepressant effect at a dose of 30 nM/kg in the animal model.

In an effort to improve the in vivo efficacy of aplysinopsin analogs, we used an in silico ADME predictor (QikProp) to evaluate and design a new series of analogs with improved ADME properties. We also evaluated the metabolic stability of compound **53** and found that the aplysinopsin scaffold does not appear to be overly susceptible to phase I metabolism, with a $T_{1/2}$ of 61 minutes. We synthesized a new library of 12 analogs and evaluated their affinities at 46 CNS receptors and inhibitory activity at MAO-A and B. We found that *N*-benzyl aplysinopsin analogs had moderate nanomolar-level affinities for 5-HT_{2B} and 5-HT_{2C} receptor subtypes. C-5

Substituted compounds (**88** and **89**) had potent and selective inhibitory activity at MAO-A. Compounds **83**, **88**, and **89** were evaluated in the chick-anxiety depression model to evaluate their in vivo efficacy. Compound **83** showed modest antidepressant activity at a dose of 10 mg/kg and compound **89** showed potent antidepressant activity across all doses (1-10 mg/kg).

DEDICATION

This work is dedicated to my parents and my wife.

ACKNOWLEDGMENTS

I would like to acknowledge my advisor, Professor Jordan Zjawiony, for his continued support and excellent guidance as I worked toward my degree. I would also like to thank my committee members: Dr. Daneel Ferreira, Dr. Mark Hamann, and Dr. Ken Sufka. They were always happy to provide guidance, advice, and helpful discussions whenever I asked.

I would like to extend a special thanks to Dr. Sufka and his lab of graduate and undergraduate researchers for the hard work they put in while performing the chick anxiety-depression assays. Also, Dr. Bryan Roth's lab at the Psychoactive Drug Screening Program at the University of North Carolina-Chapel Hill has been very accommodating in providing screening of compounds at CNS receptors. I would also like to acknowledge Dr. Babu Tekwani and Dr. Narayan Chaurasiya for their efforts in evaluating our compounds for their inhibitory activities of MAO-A and MAO-B. Thanks are also due to Dr. Stephen Cutler and the COBRE program here at Ole Miss that provided me with additional funding during my graduate studies. For their help in performing the QikProp computation analysis, I would like to thank Dr. Robert Doerksen and Gang Fu. Soon to be "Dr." Joonseok Oh is greatly appreciated for his efforts in maintaining our NMR facilities, as well as helping with constructing molecular docking figures.

I would also like to thank Ms. Casey Stauber and all of the staff in the Department of Pharmacognosy office for their tireless work over the years. I do not think we would get much accomplished on a day to day basis without their great efforts.

I would like to extend many thanks to my friends and colleagues that have come and gone during my time in the Department of Pharmacognosy. That includes fellow graduate students and post docs for their support and encouragement in the lab. I have been fortunate to work with so many great scientists who were always happy to answer any question, regardless of how big or small. Finally, I would like to thank my family: my parents, my sister and her family, and my personal friends for their support and encouragement over the years. And last, but not least I would like to thank my wife for being endlessly supportive and understanding of the time I spent pursuing this degree. Thank you all very, very much.

TABLE OF CONTENTS

LIST OF FIGURES

LIST OF TABLES

CHAPTER 1

INTRODUCTION

1. Treatment of depression

The development of treatments for central nervous system disorders is a vast sector of research. The World Health Organization estimates that at the current rate of increase, depression will be the second most disabling condition in the world by 2020.[1] Given this forecast, it is no surprise that pharmaceutical companies are spending vast amounts of time and resources pursuing new leads to treat CNS disorders such as depression and anxiety.[2]

The history of the pharmacological treatment of depression has experienced two revolutionary periods. The first was the 1950s, a decade that saw the launch of the first monoamine oxidase inhibitor, iproniazid, as well as the first of the tricyclic antidepressants used for treatment, imipramine, as shown in Figure 1-1.[3] The second major revolutionary period occurred in the 1980s with the development of the selective serotonin reuptake inhibitor Prozac (fluoxetine), which has become one of the best-selling pharmaceuticals of all time. From the 1950s until today, there have been four general classes of antidepressant drugs used in treatment, each with varying degrees of success and side effect profiles. The four broad categories are: tricyclic antidepressants (TCAs), monoamine oxidase inhibitors (MAOIs), selective serotonin reuptake inhibitors (SSRIs), and atypical antidepressants.

Tricyclic antidepressants primarily function by blocking the reuptake of serotonin and norepinephrine via blockade of the serotonin transporter (SERT) and norepinephrine transporter (NET). These actions result in an increase of the neurotransmitters in the synaptic cleft and thus an increase in neurotransmission.[4] In addition to the inhibition of reuptake, TCAs also exhibit

antagonistic activity at several other receptors, including serotonin subtypes,[5] NMDA,[6] sigma,[7] histamine,[8] and acetylcholine receptors.[5] This wide array of activity/lack of selectivity likely contributes to the side effects of TCAs. Despite being the first antidepressants on the market, TCAs are used less today, as they have been replaced by drugs with better safety and side effect profiles. However, they remain in use for severe cases of depression that do not respond to other classes of antidepressants.[9]

Monoamine oxidase inhibitors were discovered by happenstance when researchers studying the hydrazine iproniazid (Figure 1-1) for the treatment of tuberculosis found that patients who received the drug saw markedly improved psychiatric profiles. Monoamine oxidase (MAO) is an enzyme responsible for the deactivation of neurotransmitters like serotonin, dopamine, and norepinephrine. MAOIs cause a reduction in this enzymatic activity, which results in an increased concentration of neurotransmitters. A more detailed discussion concerning the use of MAOIs in the treatment of depression follows later in this chapter.

Selective serotonin reuptake inhibitors are, as their name implies, drugs that selectively inhibit the reuptake of serotonin from the synapse, much like TCAs. The difference is that they are selective only for serotonin, thus reducing the aforementioned problematic side effects that plague TCAs. The most well know SSRI is Prozac (fluoxetine), shown in Figure 1-1. Unlike TCAs and MAOIs, which were discovered serendipitously, SSRIs were borne out of work surrounding the serotonergic hypothesis, or the serotonin theory, of depression. Essentially this theory postulates that a depletion of serotonin in the brain is responsible for depression. Following this theory, SSRIs, and fluoxetine in particular, became the first rationally designed antidepressants on the market. Fluoxetine and other SSRIs were designed to act on a specific

target (SERT) and to avoid unwanted binding affinities for other receptors/targets, which could lead to the side effects that plagued other antidepressant drug classes. SSRIs possess a much better side effects profile and thus have become some of the best selling drugs in the world, making drugs like Prozac, Celexa (citalopram), and Zoloft (sertraline) household names. These drugs were primary options for the treatment of depression until the recent development of atypical antidepressants.

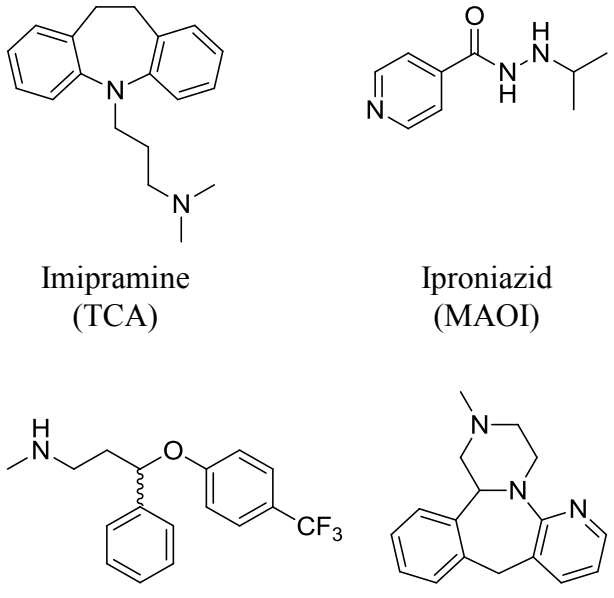

Figure 1-1 Types of antidepressants

Atypical antidepressants are newer drugs that function in different ways from the previously described classic antidepressants. Drugs categorized as atypical do not necessarily share the same mechanism of action. For example, Wellbutrin (buproprion) acts as a type of stimulant more so than a traditional antidepressant. It does so by inhibiting the reuptake of

dopamine and norepinepherine. Another major subgroup of atypical antidepressants, which are of special interest in regards to this dissertation, are drugs that act as agonists/antagonists of specific serotonin receptor subtypes. Buspar (buspirone) and Remeron (mirtazapine) are agonists of serotonin receptor subtype 5-HT_{1A}. Cymbalta (duloxetine) is a representative of the selective serotonin and norepinepherine reuptake inhibitors (SNRIs), which are similar to SSRIs, but also act on norepinepherine uptake in the synaptic cleft. The side effects of atypical antidepressants vary from group to group, as they all have different mechanisms of action. However, in general, they have displayed better side effect profiles and toleration by patients.

Despite the increased safety profile of SSRIs and atypical antidepressants, there are still issues to solve when it comes to antidepressant drug design. First and foremost is the delay in onset of efficacy, which often takes weeks. In addition, it is currently estimated that roughly 30% of patients do not respond to currently available treatment options.[10] Until these issues are solved, the search for safer and more efficacious antidepressant drugs leads will continue.

Natural products as drug sources

Natural products have long been a source of new drugs. In 2003, it was reported that 61% of small-molecule new chemical entities introduced as drugs from 1981 to 2002 could be contributed to natural products.[11] The last decade alone has seen the launch of a broad range of natural product-derived drugs, as shown in Figure 1-2. These include the antibacterial agent Finibax (doripenem), which was launched in 2005 by Shiongi Co. and is used to treat serious kidney and urinary tract infections.

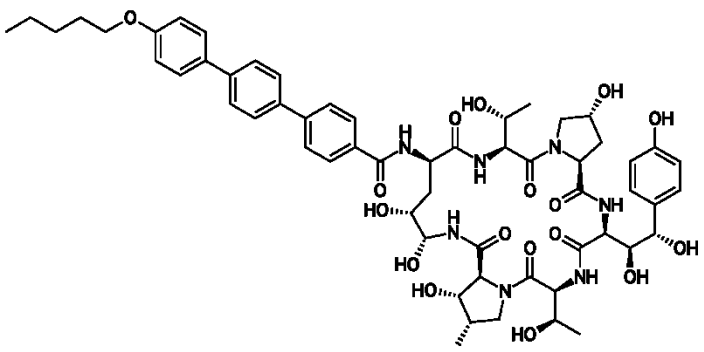

Eraxis (anidulafungin) 2006

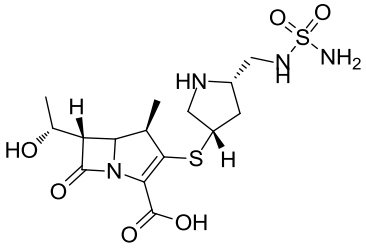

Finibax (doripenem) 2005

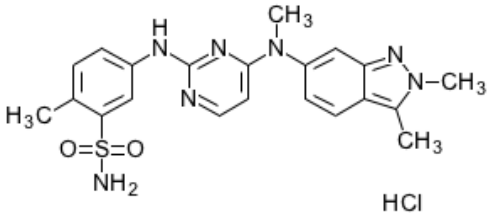

Votrient (pazopanib) 2009

Figure 1-2 Recent natural product-derived drug approvals

The antifungal Eraxis (anidulafungin) was approved by the FDA in 2006 and is marketed by Pfizer. It is commonly used to treat Candida infections in the blood, stomach, or esophagus. The natural product mimic anticancer agent Votrient (pazopanib), launched in 2009, is used against late-stage kidney cancers as well as soft tissue sarcomas. These are just a few examples of natural product-derived drugs to recently gain FDA approval. There are several excellent reviews which cover the broad number and diversity among natural product-derived drug leads either on the market or in the late stages of clinical trials.[12]

Marine natural products

Marine natural products have been a rich source for structurally diverse bioactive secondary metabolites with unique characteristics. More accessible SCUBA technology has made collection easier, which in turn has allowed for increased exploration of marine environments over the last few decades. This has led to the identification of a large number of novel bioactive compounds. There are currently seven marine natural products that are FDA approved, as shown in Table 1-1, the majority of which are anticancer agents. In addition, there are numerous others undergoing further development in clinical trials.[13]

One particular class of marine natural products to garner significant attention from the research community is the marine indole alkaloids. This interest is mostly due to their promising neuromodulatory biological activities. These compounds are structurally similar to endogenous neurotransmitters, so it should come as no surprise that they often possess central nervous system (CNS) activity. There are several indole alkaloids on the market to treat various CNS disorders, such as the triptans, which are used to treat migraines (Figure 1-3).[14] Most drugs in this class are agonists of serotonin receptor subtypes 5-HT_{1B} and 5-HT_{1D}. It is clear that the structural homology between these indole alkaloids and the body's natural neurotransmitters opens up a therapeutic niche to possibly treat CNS disorders such as depression and anxiety.

Name	Natural Source	Treatment
Brentuximab vedotin (SGN-35)	Cyanobacterium	Cancer[15]
Trabectedin (ET-743)	Tunicate	Cancer[16]
Cytarabine (Ara-C)	Sponge	Cancer[17]
Eribulin mesylate (E7389)	Sponge	Cancer[18]
Ziconotide	Cone Snail	Pain[19]
Omega-3-acid ethyl esters	Fish	Hypertriglyceridemia[20]
Vidarabine (Ara-A)	Sponge	Antivrial[21]

Table 1-1 FDA approved marine natural product drugs

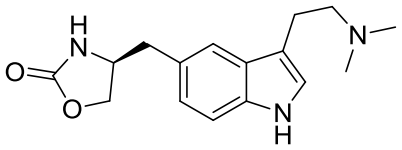

Zolmitriptan

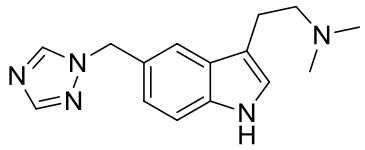

Rizatriptan

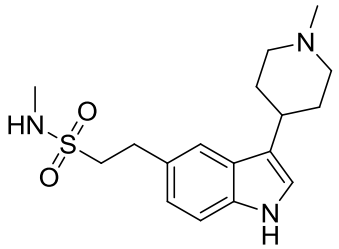

Naratriptan

Figure 1-3 Triptans used to treat migraine headaches

Targeting serotonin receptor subtypes

Serotonin, or 5-hydroxytryptamine (5-HT), is an indoleamine with a chemical structure similar to the amino acid tryptophan. Tryptophan actually serves as a precursor in the biosynthetic pathway of serotonin via a two-step pathway, as shown in Figure 1-4. The first, and rate-limiting step, involves the hydroxylation of position C-5 of tryptophan. The final step is the decarboxylation of 5-hydroxytryptophan to serotonin.

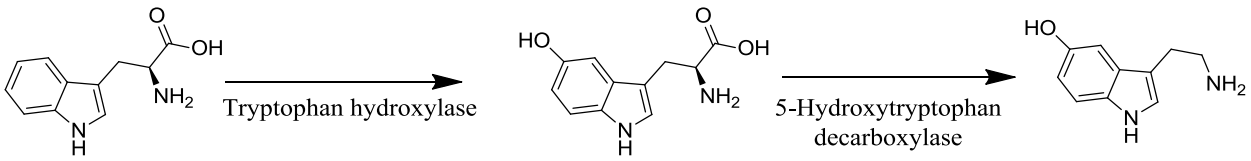

Figure 1-4 Serotonin biosynthesis

As mentioned previously, the serotonin receptor system has been widely recognized as a key element in the pathophysiology of depression and as a mediator of the therapeutic action of antidepressants.[22] Dysfunction of the serotonin receptor system has been implicated in a wide array of psychiatric disorders, including anxiety, depression, and schizophrenia.[23] The role of serotonin in mood control, appetite, sleep, and pain has also been extensively studied.[24] The life cycle of serotonin can be simplified to the following steps. First, serotonin is released into the synaptic cleft where it binds to pre- or postsynaptic serotonin receptor subtypes. Next, it is released and subsequently taken up by SERT. Then, it is recycled into the vesicular pool or degraded by monoamine oxidase A.

Serotonin functions in the body are mediated by a large family of receptors.[25] There have been seven families of serotonin receptors identified, 5-HT_1 – 5-HT_7. Each of these is further subdivided into subtypes. Overall there are 14 subtypes of serotonin receptors, as shown in Figure 1-5. All of these subtypes, except for 5-HT_3, are G-protein coupled receptors (GPCR). 5-HT_3 is a ligand-gated ion channel receptor.

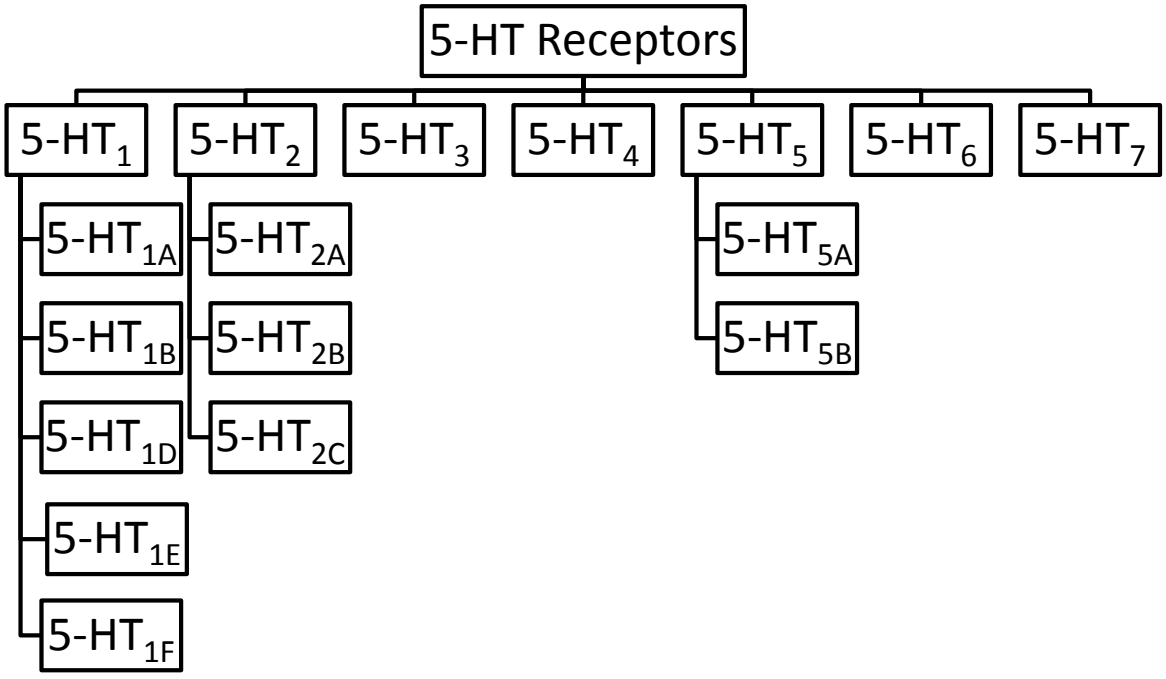

Figure 1-5 Serotonin receptor subtypes

Owing to the serotonin receptor subtypes sharing a high degree of structural homology, research efforts are aimed at finding receptor ligands with a high affinity and selectivity among serotonin receptor subtypes. The discovery of potent and selective ligands could provide not only drug leads but also increased understanding of the functions of each receptor subtype. Owing to the structural homology between serotonin and marine indole alkaloids, these natural products and their derivatives represent interesting scaffolds to explore new leads for the treatment of CNS disorders.

MAO inhibitors

As mentioned previously, MAOIs are another class of drugs that have received significant use in the clinical setting to treat CNS disorders. After their discovery in the 1950s, they were used as first line treatment for depression for several decades. However, their

extensive side effects and food and drug interactions led to a decline in use. The dietary restrictions imposed by the FDA include the following common foods to avoid while using MAOIs: aged cheeses and meats, draft beer, sauerkraut, kimchee, soybean products, and wine. In addition, the list of drugs to avoid is also quite long, but in general, the idea is to avoid dangerous drug-drug interactions that could lead to the development of serotonin syndrome. Serotonin syndrome results when an MAOI is taken in combination with serotonin enhancing drugs like SSRIs or St. John's wort. These restrictions, coupled with the development of new and safer antidepressants, led MAOIs to be relegated to third or fourth-line treatment options for depression in the last two decades.

There are two isoforms of MAO: MAO-A and MAO-B.[26] They have been found to vary in their distribution in the body, but both are found in various regions in the brain. The two isoforms also have different preferred substrates. The preferred MAO-A substrates are serotonin and norepinephrine, while MAO-B preferentially breaks down phenylethylamine and histamine. Dopamine and tyramine are substrates for both isoforms.

MAOIs can be classified into three categories: nonselective, selective, and reversible inhibitors. The early MAO inhibitors such as phenelzine were neither reversible nor selective, hence, their extensive side effects profile and dietary restrictions. Newly developed selective and reversible MAOIs have given this class of antidepressants new life. These selective inhibitors allow the other isoform to metabolize substances such as tyramine, thus avoiding potentially harmful side effects. Ligands that bind reversibly can also be displaced by other substrates, such as the aforementioned tyramine. Thus, selective and reversible MAOIs could potentially be used without the cumbersome dietary restrictions of older MAOIs. Selegiline

(Figure 1-6) is an example of a selective and reversible MAO-B inhibitor, which has been approved to be used in a transdermal patch system that requires no dietary restrictions. Selective and reversible inhibitors of MAO-A (RIMAs) like moclobemide are on the market internationally but not currently in the US. Like their selective and reversible MAO-B counterparts, they too lack the cumbersome dietary restrictions that made older MAOIs less appealing to doctors and patients. These new classes of MAOIs increased the demand for new drugs that are potent and selective for one MAO isoform and which also bind reversibly.

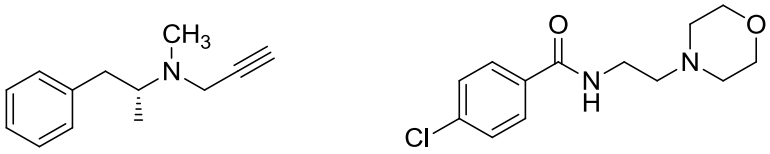

Selegiline
MAO-B inhibitor

Moclobemide
MAO-A inhibitor

Figure 1-6 Selective and reversible MAOIs

Aplysinopsins

Aplysinopsins are tryptophan-derived marine natural products that were first isolated in 1977 from several Indo-Pacific sponge species from the genera *Thorecta*.[27] Those species have since been reassigned as the *Aplysinopsis* genera. Since their initial isolation, aplysinopsins have been isolated from sponges in several geographic locations such as the Caribbean[28] and the Mediterranean.[29] In addition to being isolated from sponges, aplysinopsins have also been isolated from corals,[30] mollusks,[31] and sea anemones.[32]

The general structure of aplysinopsin derivatives is shown in Table 1-2. It is comprised of an indole moiety coupled with an imidazolidinone. There are several common themes among natural derivatives of aplysinopsins. First is the variation in the bromination pattern on the

indole moiety. In all but one of the naturally occurring aplysinopsin derivatives, bromination occurs at C-6. The only exception is that of 5,6-dibromo-2′-demethylaplysinopsin (**1**), which is brominated at C-5 and C-6.[33] The number and position of *N*-methylations on the C ring can also vary. There have been compounds isolated with one (**2, 3**), two (**4, 5**), and three (**6**) methyl groups present.

The stereochemistry of the C-8-C-1′ double bond is another source of variation among natural derivatives. The earliest reports of aplysinopsins and the subsequent biological investigations either did not address this issue, or just described the aplysinopsin analog as the *E* geometrical isomer. The work of Guella *et al.* nicely elucidated this issue and provided an NMR technique by which the two isomers may be readily differentiated.[34] They found that one can use the ^{1}H, ^{13}C heteronuclear coupling constants between H-8 and C-5′ to determine the predominant isomer. A larger coupling constant (9 - 11 Hz) indicates the presence of the *E* isomer, while the coupling constant is usually smaller (4 - 5.5 Hz) for the *Z* isomer.

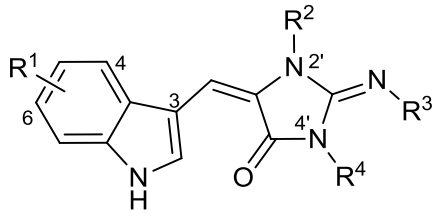

General Structure of Aplysinopsin Analogs

CMPD	Name	R^1	R^2	R^3	R^4
1	5,6-dibromo-2′-demethylaplysinopsin	4,6-Br	H	H	CH_3
2	2′-de-*N*-methyl-aplysinopsin	H	H	H	CH_3
3	6-bromo-2′-de-*N*-methylaplysinopsin	6-Br	H	H	CH_3
4	6-bromoaplysinopsin	6-Br	CH_3	H	CH_3
5	6-bromo-4′-de-*N*-methylaplysinopsin	6-Br	CH_3	H	H
6	methylaplysinopsin	H	CH_3	CH_3	CH_3

Table 1-2 Structures of aplysinopsins 1-6

1′,8-dihydroaplysinopsins and C-1′ substituted derivatives have also been isolated (**7**-**11**) (Table 1-3). The oxidation state of the C ring is a source of variety, as derivatives (**12**, **13**) have been isolated with different oxidation states at C-3′ of the imidazolidinone moiety (Table 1-4).[34a] Analogs which are substituted at N-1′ have been reported from sponges (**14**)[30] and anthozoans (**15**).[35] Lastly, aplysinopsin dimers have been isolated from a coral species, as seen in Figure 1-7.[36]

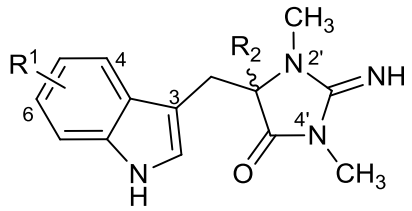

CMPD	Name	R^1	R^2
7	1′,8-dihydroaplysinopsin	H	H
8	6-bromo-1',8-dihydroaplysinopsin	6-Br	H
9	6-bromo-1'-hydroxy-1',8-dihydroaplysinopsin	6-Br	OH
10	6-bromo-1'-methoxy-1',8-dihydroaplysinopsin	6-Br	OCH_3
11	6-bromo-1'-ethoxy-1',8-dihydroaplysinopsin	6-Br	OCH_2CH_3

Table 1-3 Structures of aplysinopsins 7-11

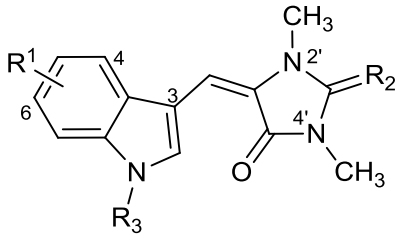

CMPD	Name	R^1	R^2	R^3
12	3′-deimino-3′-oxoaplysinopsin	H	O	H
13	6-bromo-3′-deimino-3′-oxoaplysinopsin	6-Br	O	H
14	N-propionylaplysinopsin	H	NH	$OCCH_2CH_3$
15	N-methylaplysinopsin	H	HH	CH_3

Table 1-4 Structures of aplysinopsins 12-15

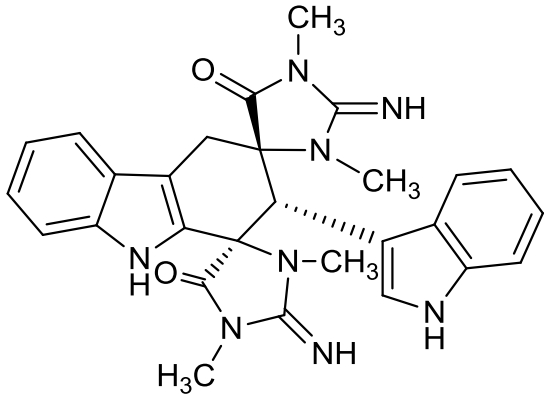

Figure 1-7 Aplysinopsin dimer

Biological activity of aplysinopsins

Aplysinopsins have been shown to possess a wide range of biological activities. Their first reported biological activity was antitumor activity seen in mice. Using a bioassay guided fractionation approach, aplysinopsin (**16**) (Figure 1-8) was isolated from the sponge *Verongia spengelli*.[37] In in vitro assays, compound **16** was shown to have an inhibitory activity against P388 lymphocytic leukemia in mice at a dose of 200 mg/kg. Another aplysinopsin analog, isoplysin A (**17**), was also found to possess some antineoplastic activity. It was found to inhibit the growth of murine lymphoma LH-1210 cells, with an IC_{50} value of 11.5 μg/mL. In the same study, aplysinopsin and methylaplysinopsin (**6**) also showed moderate cytotoxicity against the LH-1210 cell line with IC_{50} values of 2.3 and 3.5 μg/mL, respectively.[35]

A series of aplysinopsin analogs, isolated from the sponge *Smenospongia aurea,* were evaluated for their in vitro antimalarial activity.[38] These compounds were tested against *Plasmodium falciparium*, and several compounds showed moderate activity and selectivity. 6-Bromoaplysinopsin (**4**) had an IC_{50} of 0.34 μg/mL. Isoplysin A (**17**) and 6-bromo-2′-de-*N*-

methylaplysinopsin (**3**) also showed moderate activity, with IC_{50}'s of 0.97 and 1.1 μg/mL, respectively. However, in subsequent in vivo testing, compound **4** was found to be inactive.[39]

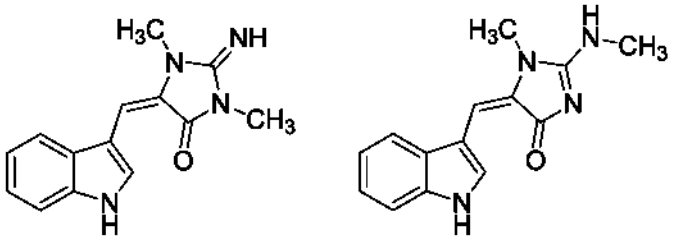

Aplysinopsin (16) **Isoplysin A (17)**

Figure 1-8 Structures of aplysinopsin and isoplysin A

Marine organisms have been a rich source of antimicrobial drug leads in the past,[40] so it is no surprise that aplysinopsins have been evaluated for their potential antimicrobial activities. There are several reports of mostly weak inhibitory properties against various microbes. A mixture of 6-bromoaplysinopsin (**4**) and 6-bromo-4′-de-*N*-methylaplysinopsin (**5**) was found to inhibit *Bacillus subtillis*,[41] and in a separate report, compound **4** was found to also inhibit growth of the fungus *Trichophyton mentagrophytes*.[42] In addition, compounds **16** and **4** were found to inhibit the growth of *Staphylococcus aureus*.

Despite the aforementioned biological activities, our main interest in aplysinopsins lies in their ability to modulate neurotransmissions. Since their discovery, their structural similarity to endogenous neurotransmitters has led to them being investigated for neuromodulatory activity. As mentioned previously, several marine indole alkaloids have already been found to have potential to treat depression by acting on various neurotransmitters. Aplysinopsins have been implicated in acting on both the serotonin receptor system as well as the monoamine oxidase

system.

An early study found that methylaplysinopsin (**6**) was able to inhibit MAO activity in a mouse brain homogenate model. In the same study, an evaluation of the binding kinetics revealed this inhibition to be short-term and reversible.[43] Compound **6** had a moderate ability to displace serotonin with an IC_{50} of 160 μM. Methylaplysinopsin was also evaluated for its ability to influence norepinephrine uptake and was found to have no significant effect.

A 2002 study by Hu et al. evaluated aplysinopsin analogs isolated from the Jamaican sponge *Smenospongia aurea* for their affinity for human serotonin 5-HT_2 receptor subtypes 5-HT_{2A} and 5-HT_{2C}.[38] These subtypes were of special interest due to their involvement in the pathophysiology of anxiety and depression. The 5-HT_2 receptor subfamily share highly conserved sequences (80%),[25] thus the study was aimed at not only finding ligands with high affinity, but also selectivity among the two receptor subtypes studied. Their SAR analysis pointed to a significance of functional groups at C-6, C-2′ and C-3′ in binding to human 5-HT_2 receptors. Bromination at C-6 and the increased length of the alkyl chain at C-3′ enhanced affinity. In addition, the bromination enhanced the selectivity for 5-HT_{2C} over the 5-HT_{2A} subtype. On the other hand, the methylation at N-2′ increased affinity to the 5-HT_{2A} receptor.

In another study of a synthetic library of aplysinopsin analogs, it was shown that the aplysinopsin scaffold can be manipulated such that selection between 5-HT_{2A} and 5-HT_{2C} can be achieved.[44] Cummings et al. found that alkylation at N-2′ and N-4′ coupled with various halogenation patterns can yield highly selective ligands. More specifically, substitution at C-6 with a chlorine or bromine resulted in a preference for 5-HT_{2C} binding. However, if C-6 is left unsubstituted or substituted with a fluorine, there was a preference for 5-HT_{2A}. It is proposed

that the size of the halogen plays a key role in this selectivity.

There are few reports of in vivo evaluations of aplysinopsin analogs, especially concerning their neuromodulatory activity. In a recent study, aplysinopsin (**16**) was evaluated in the Porsolt forced swim test but did not exhibit any antidepressant activity.[45] This result highlights an important problem in CNS drug discovery, *i.e.*, compounds that possess potent in vitro activities but fail to show significant efficacy in animal models due to poor absorption, distribution, metabolism, excretion and toxicity (ADMET) properties. CNS agents must pass through the blood-brain barrier (BBB), and this requirement leads to the failure of many CNS drug candidates. For this reason, assessment of BBB permeability should be done as early as possible in drug discovery. There are several ways to evaluate BBB permeability, including in vivo, in silico, and in vitro methods.[46]

As mentioned previously, the number of people diagnosed with depression and/or complications arising from depression is growing, fueling a need for new antidepressant drugs which are more efficacious as well as safer. The current treatment options are not effective in large segments of the population, and, even in those individuals who do respond to treatment, it often takes weeks to see the effects.[47] Despite these initial negative results in in vivo testing, aplysinopsins represent a promising scaffold for the development of potential therapeutically valuable compounds to treat depressive disorders.

CHAPTER 2

IN VITRO STRUCTURE-ACTIVITY RELATIONSHIPS OF APLYSINOPSIN ANALOGS AND THEIR IN VIVO EVALUATION IN THE CHICK ANXIETY-DEPRESSION MODEL

Adapted from: Lewellyn, K.; Bialonska, D.; Chaurasiya, N. D.; Tekwani, B. L.; Zjawiony, J. K. *Bioorg. Med. Chem. Lett.* **2012**, *22*, 4926 and Lewellyn, K.; Bialonska, D.; Loria, M. J.; White, S. W.; Sufka, K. J.; Zjawiony, J. K. *Biorg. Med. Chem.* **2013**, *21*, 7083 with permission.

2. Introduction

Depression effects nearly 1 in 10 adults in the US according to a CDC study.[48] The WHO estimates that by 2020 depression will be the second most disabling condition in the world.[1] Based on these statistics there is a clear need for new drug candidates for the treatment of depression.[49] Aplysinopsins have received considerable attention as promising neuromodulators, with significant affinity to serotonin receptors[38] and the potential to inhibit MAO activity.[43] Since these two mechanisms are known to be involved in antidepressant action, aplysinopsins represent potentially useful candidates in antidepressant drug development.

Dysfunction of the serotonin receptor system can lead to a wide array of psychiatric disorders including anxiety, depression and schizophrenia.[23] The role of serotonin in mood control, appetite, sleep, thermoregulation and pain has also been extensively studied.[24] In addition to CNS disorders, the 5-HT receptor system has also been implicated in disorders of the cardiovascular and pulmonary systems.[50] With the increased understanding of how serotonin and its receptors function in multiple systems throughout the body, we must take into account the potentially wide ranging side effects of drugs on systems other than the CNS. This problem further underscores the need to develop drug leads which are potent, but also highly selective among the serotonin receptor subtypes.

A group of aplysinopsins isolated the from Jamaican sponge *Smenospongia aurea* exhibited an affinity for human serotonin 5-HT_2 receptor subtypes 5-HT_{2A} and 5-HT_{2C} expressed in a mammalian cell line.[38] These subtypes were of interest as possible targets in the treatment of schizophrenia, depression, anxiety, and obesity.[51] It has been shown that 5-HT_{2C} receptor knockout mice exhibit obesity, epilepsy, and cognitive disorders.[52] The three receptor subtypes

of the 5-HT_2 family (2A, 2B, 2C) share highly conserved sequences (80%); thus, designing ligands which are potent and selective remains a challenge.

A major problem in the development of 5-HT_{2C} ligands has been a lack of selectivity over 5-HT_{2A} and 5-HT_{2B} subtypes. Activation of 5-HT_{2A} receptors may lead to hallucinations and activation of 5-HT_{2B} can result in cardiac insufficiency and pulmonary hypertension (e.g. fenfluramine case).[53] Thus, discovery of highly selective 5-HT_{2C} ligands could provide new and safer drugs. A good example of this is lorcaserin (Belviq) (Figure 2-1), a recently approved anti-obesity drug.[54] It was developed based on the potent 5-HT_{2C} agonist dexfenfluramine, which was approved as a weight loss agent in 1996. However, cardiovascular side effects stemming from 5-HT_{2B} agonist activity led to dexfenfluramine's withdrawal from the market just one year later.[55] Using a medicinal chemistry approach, lorcaserin was developed to retain its potent 5-HT_{2C} agonism, but also be selective for 5-HT_{2C} over 5-HT_{2B}. Lorcaserin has high affinity (K_i = 15 nM) to human 5-HT_{2C} receptors and exhibits 18- and 104-fold selectivity over 5-HT_{2A} and 5-HT_{2B}, respectively.[56]

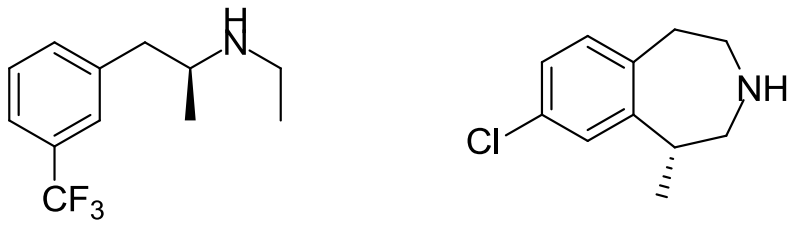

Dexfenfluramine Lorcaserin

Figure 2-1 5-HT_{2C} ligands dexfenfluramine and lorcaserin

To date, there has been little published regarding the structure activity relationship between aplysinopsin analogs and their serotonin binding affinities and selectivity. A preliminary SAR analysis of naturally occurring aplysinopsins pointed to significance of

functional groups at positions 6, 2′ and 3′ in binding to human 5-HT_2 receptors.[38] Bromination at C-6 and the increased length of the alkyl chain at C-3′ enhanced affinity. In addition, the bromination enhanced the selectivity to 5-HT_{2C} over the 5-HT_{2A} subtype. On the other hand, methylation at C-2′ increased affinity to the 5-HT_{2A} receptor. In another study of a synthetic library of aplysinopsin analogs, it was shown that the aplysinopsin scaffold can be manipulated such that selection between 5-HT_{2A} and 5-HT_{2C} can be achieved.[44] Cummings et al. found that alkylation at C-2′ and C-4′ coupled with various halogenation patterns can yield highly selective ligands. More specifically, C-6 substitution with a chlorine or bromine resulted in a preference for 5-HT_{2C} binding. However, if C-6 is left unsubstituted or substituted with a fluorine there was a preference for 5-HT_{2A}. It is proposed that the size of the halogen plays a key role in this selectivity. Both of these studies are promising results that suggest a potential therapeutic value for aplysinopsin analogs. However, both also use a limited number of analogs and only evaluate affinity at 5-HT_{2A} and 5-HT_{2C}, ignoring potential binding at not only other serotonin receptor subtypes, but also at other CNS receptors. The small library size also limits the amount of SAR information that is able to be gathered from the study. We will add to these promising reports by working with a larger library of compounds and evaluating their activity on a larger number of serotonin receptor subtypes and thirty four other CNS receptors as well (see Table 2-1). Evaluating the library at a large number of CNS receptors beyond serotonin receptor subtypes may reveal potentially deleterious off-site activity.

Alpha1A	Beta2	D5	H4	MOR
Alpha1B	Beta3	DAT	KOR	NET
Alpha1D	BZP Rat Brain Site	DOR	M1	SERT
Alpha2A	D1	GABAA	M2	Sigma1
Alpha2B	D2	H1	M3	Sigma2
Alpha2C	D3	H2	M4	
Beta1	D4	H3	M5	

Table 2-1 List of additional CNS receptors evaluated.

Monoamine oxidase inhibitors (MAOIs) initially were first line medications in the treatment of depressive illness, however, due to serious side effects, the interest in these drugs diminished.[57] When the two isoforms, MAO-A and MAO-B, were discovered, interest was renewed in their potential therapeutic use and several new generations of selective MAO inhibitors have been developed.[58] Today, much more is known about the use of selective MAO inhibitors to treat various mental disorders such as depression, anxiety, and Parkinson's and Alzheimer's disease.[59] Owing to this increased understanding of neurological disease states, there is an increased interest in development of potent and selective MAOIs.

Structurally, aplysinopsins are made up of two distinct moieties: an indole and an imidazolidinone ring. The indole scaffold is known to contribute to MAO inhibitory activities (see Figure 2-2), and many analogs have been prepared using this scaffold.[60] Furthermore, a recent study has shown that imidazolines possess potent and selective activity at both MAO isoforms.[61] Based on this data and the previous study examining the effects of methylaplysinopsin (**6**) on MAO activity,[43] it is clear that the aplysinopsin scaffold represents a potential source of new MAOI drug candidates.

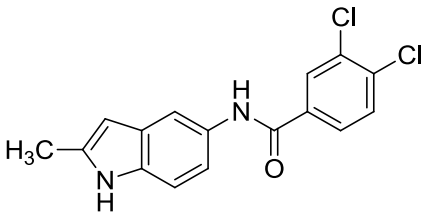

MAO-B IC_{50} = 0.06 μM

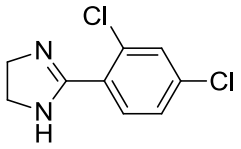

MAO-B K_i = 1.49 μM

Figure 2-2 Known indoles and imidazolines with MAO inhibitory activities.

In the present study, 50 aplysinopsin analogs (**31-80**) (Table 2-2) have been obtained synthetically and screened for affinity to 12 human serotonin as well as 34 additional CNS receptors. The library was also evaluated for inhibitory activity at MAO isoforms A and B. Tested analogs varied in the substitution pattern of the indole ring and the imidazolidinone moiety (see Figure 2-3). The indole ring was either non-brominated or brominated in the 4, 5, 6, or 7 positions. The imidazolidinone was not substituted, or methylated in one (2′, 3′, 4′), two (2′, 3′; 2′, 4′; and 3′, 4′), or three positions (2′, 3′, and 4′).

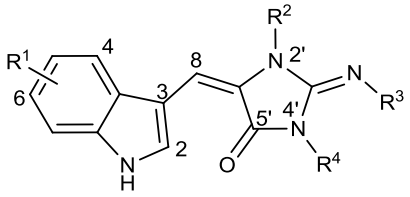

Figure 2-3 General structure of aplysinopsin analogs.

There have been a limited number of studies examining the biological activities of aplysinopsins in vivo. The number of neuromodulatory studies is even less. One early study did use an ex vivo system to examine MAO inhibition and perform preliminary pharmacokinetic studies.[43] They found that the MAO activity was short-term and reversible and that the biological activity correlated with the disappearance of methylaplysinopsin from the plasma. In

a more recent study, aplysinopsin (**51**) was tested in the Porsolt forced swim test but did not exhibit any antidepressant activity.[45] Considering these results, following in vitro evaluation of our library, we wanted to evaluate several lead compounds in an appropriate animal model to determine if their in vitro efficacy translated to an in vivo model. Three compounds (**33**, **51**, and **54**) were screened in the chick anxiety-depression model.[62] This hybrid social isolation stress paradigm is capable of screening for both anxiolytic and anti-depressant activity.

Synthesis of aplysinopsin analogs

Synthesis of 3-formylindoles

Aplysinopsins consist of an indole moiety coupled with a corresponding imidazolidinone. There have been several papers published reviewing the various synthesis strategies to obtain aplysinopsin analogs.[63] Most synthesis strategies involve the synthesis of the desired 3-formylindole followed by condensation with the appropriate imidazolidinone.

The 3-formylindoles **18-22** were initially prepared using a variation of the Batcho-Leimgruber indole synthesis[64] as shown in Figure 2-4. Briefly, the appropriate bromonitrotoluenes were added to a mixture of *N*,*N*-dimethylformamide dimethyl acetal and pyrrolidine in DMF and heated to 110°C until the substrate was consumed. The resulting crude enamines were reduced and cyclized with zinc in acetic acid. The brominated indoles were converted to 3-formylindoles via a Vilsmeier-Haack reaction. In some cases, for subsequent synthesis of larger quantities of aplysinopsin analogs, commercially available 3-formylindoles were used.

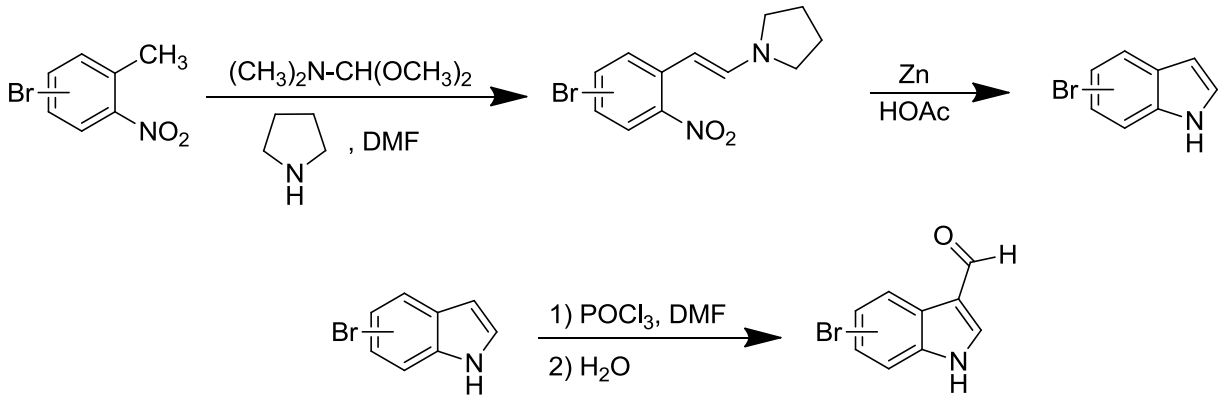

Figure 2-4 Synthesis of 3-formylindoles

Synthesis of imidazolidinones

The synthesis of the imidazolidinones **23-30** were carried out according to published procedures as shown in Figures 2-4 - 2-5, except for creatinine (**24**), which was available commercially. Briefly, creatinine (**24**) was methylated using iodomethane to yield 1,3-dimethyl-2-imino-4-imidazolidinone (**28**). Compound **28** was subsequently refluxed in methanol to yield the isomerized 1-methyl-2-(methylamino)-2-imidazolin-4-one (**27**). Compound **27** was methylated to yield the trimethylated 1,3-dimethyl-2-(methylimino)- 4-imidazolidinone (**30**).[65]

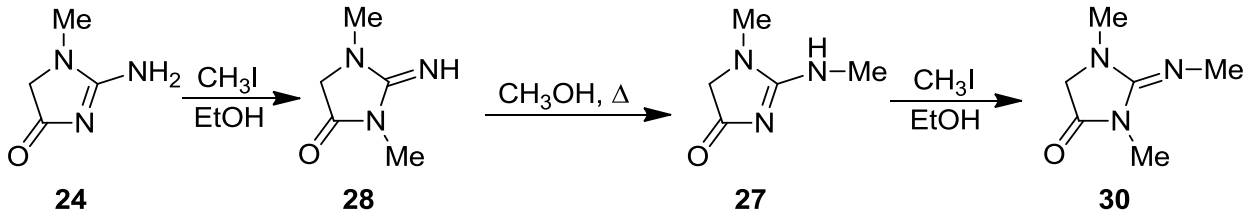

24 **28** **27** **30**

Figure 2-5 Synthesis of imidazolidinones 24, 27, 28, and 30

Compound **23** was synthesized from guanidinoacetic acid according to the procedure from Bengelsdorf as shown in Figure 2-6.[66] Compound **23** was methylated to yield **26**. Our attempts to obtain the imidazolidinone **25** following the published procedure[65] and the

condensation of glyoxal with *N*-methylguanidine[67] failed.

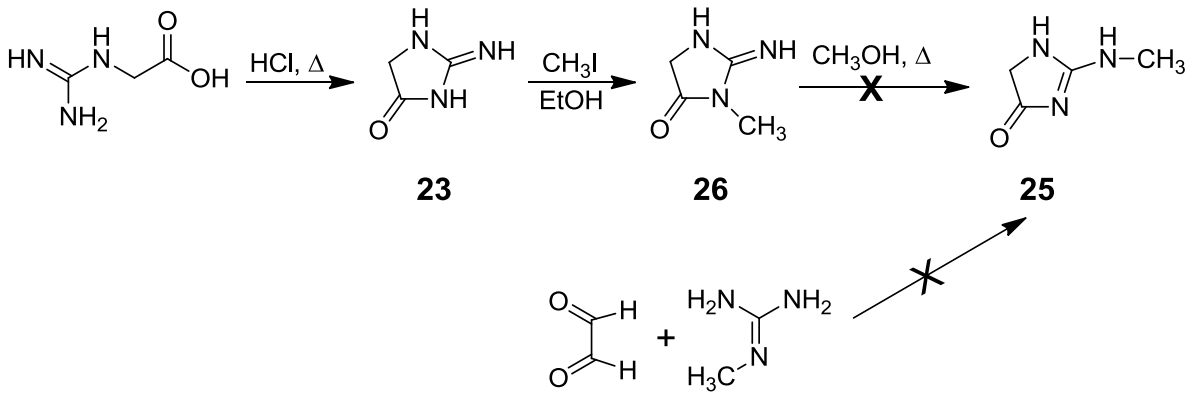

Figure 2-6 Synthesis of imidazolidinones 23 and 26

Eventually, the analogs with methylamine substitution, **76-80**, were synthesized via condensation of the corresponding 3-formylindoles **18-22** with thiohydantoin,[68] methylation of intermediate thiones **66-70**,[69] followed by substitution of thioethers **71-75** with methylamine as shown in Figure 2-7.

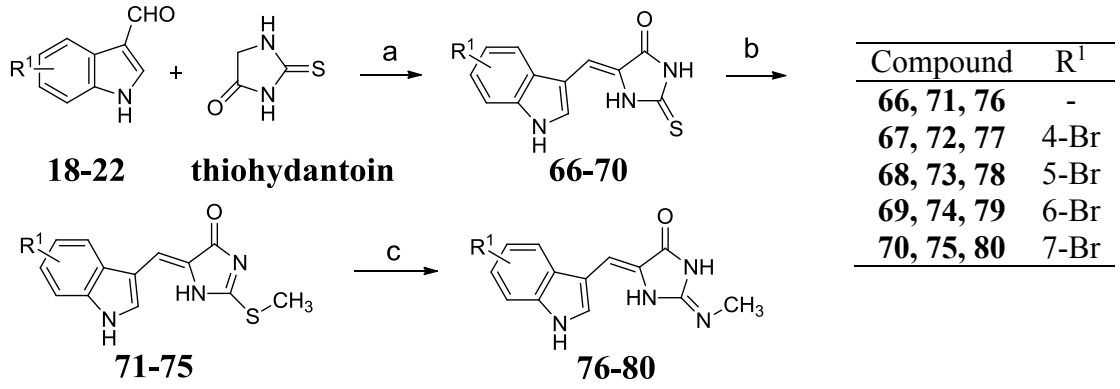

Compound	R^1
66, 71, 76	-
67, 72, 77	4-Br
68, 73, 78	5-Br
69, 74, 79	6-Br
70, 75, 80	7-Br

Reagents and conditions: (a) ETA, EtOH, reflux, 1h; (b) CH_3I, NaOH, MeOH, RT, 18h; (c) CH_3NH_2, EtOH, sealed vessel, 70ºC, 24h.

Figure 2-7 The synthesis of 3′-*N*-methylamineaplysinopsin analogs (76-80).

The general scheme for the synthesis of aplysinopsin analogs **31-65** is shown in Table 2-2. The condensation of 3-formylindoles with the appropriate imidazolidinones was carried out according to the procedure from Djura and Faulkner.[28] Briefly, equimolar amounts of the appropriate indole aldehydes **18-22** and imidazolidinones **23-30** were mixed under nitrogen and heated over an open flame until the reaction mixture began effervescing. Several minutes after effervescence stopped, the mixture was cooled to room temperature. The crude mixture was extracted with MeOH and insoluble materials filtered off. The solution was concentrated and loaded on to silica gel for purification.

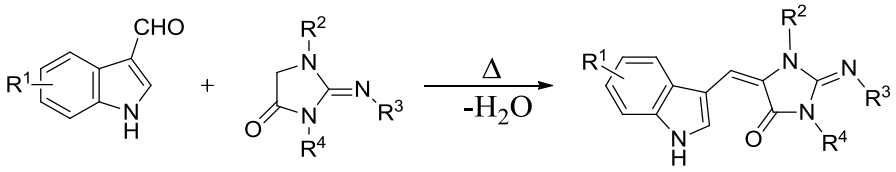

18-22 **23-30** **31-65**

Compd	R^1	Compd	R^2	R^3	R^4
18	-	**23**	H	H	H
19	4-Br	**24**	Me	H	H
20	5-Br	**25**	H	Me	H
21	6-Br	**26**	H	H	Me
22	7-Br	**27**	Me	Me	H
		28	Me	H	Me
		29	H	Me	Me
		30	Me	Me	Me

Compd	R^1	R^2	R^3	R^4	Compd	R^1	R^2	R^3	R^4
31	-	H	H	H	**48**	5-Br	Me	Me	H
32	4-Br	H	H	H	**49**	6-Br	Me	Me	H
33	5-Br	H	H	H	**50**	7-Br	Me	Me	H
34	6-Br	H	H	H	**51**	-	Me	H	Me
35	7-Br	H	H	H	**52**	4-Br	Me	H	Me
36	-	Me	H	H	**53**	5-Br	Me	H	Me
37	4-Br	Me	H	H	**54**	6-Br	Me	H	Me
38	5-Br	Me	H	H	**55**	7-Br	Me	H	Me
39	6-Br	Me	H	H	**56**	-	H	Me	Me
40	7-Br	Me	H	H	**57**	4-Br	H	Me	Me
41	-	H	H	Me	**58**	5-Br	H	Me	Me
42	4-Br	H	H	Me	**59**	6-Br	H	Me	Me
43	5-Br	H	H	Me	**60**	7-Br	H	Me	Me
44	6-Br	H	H	Me	**61**	-	Me	Me	Me
45	7-Br	H	H	Me	**62**	4-Br	Me	Me	Me
46	-	Me	Me	H	**63**	5-Br	Me	Me	Me
47	4-Br	Me	Me	H	**64**	6-Br	Me	Me	Me
					65	7-Br	Me	Me	Me

Table 2-2 Synthesis route to aplysinopsin analogs (31-65)

In vitro evaluation of library

Serotonin receptor affinity

A series of 50 synthesized compounds (**31-80**) were evaluated by the NIMH Psychoactive Drug Screening Program (PDSP) at the University of North Carolina-Chapel Hill. Briefly, compounds were first evaluated in a primary radioligand binding assay for 12 serotonin receptor subtypes. A "hit" is defined as an inhibition > 50 % in the primary assay. Secondary assays are used to determine the affinity constants (K_i) of hits at the specified serotonin receptor subtypes. K_i's are calculated using the Cheng-Prusoff equation.[70]

A cursory overview of the in vitro binding data reveals that the majority of the activity among the 12 receptor subtypes lies in the 5-HT_2 family, specifically at 5-HT_{2B} and 5-HT_{2C}. Selected secondary binding highlights are shown in Table 2-3. Complete in vitro secondary assay results for all compounds and receptors can be found in the supplementary material.

The library of compounds can be organized into eight groups of analogs based on the substitution pattern of their imidazolidinone moiety. In each of those eight groups there are five analogs, one non-brominated and four analogs brominated at positions 4, 5, 6, and 7 of the indole ring. As shown in Table 2-3, the "A group", with no *N*-methylations present on the imidazolidinone moiety, showed the lowest K_i values, but with varying degrees of selectivity among the 5-HT_2 family of receptor subtypes. Compound **33** showed the highest affinity overall, with a K_i = 35nM at 5-HT_{2C}, however, it lacked selectivity among the 5-HT_2 family. The same can be said for compounds **31** and **34**, both of which possess nanomolar level affinities for 5-HT_{2B} and 5-HT_{2C}, but were not notably selective for either one over the other.

Cmpd	Structure	Binding affinity (K_i nM ± S.D.)		
		5-HT_{2A}	5-HT_{2B}	5-HT_{2C}
31	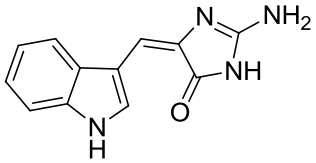	1169 ± 158	232 ± 22	349 ± 44
33	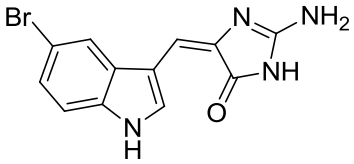	58 ± 6	51 ± 7	35 ± 4
34	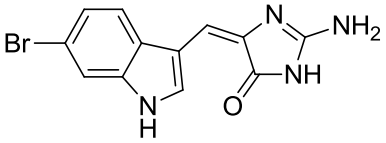	3128 ± 317	269 ± 34	201 ± 24
43	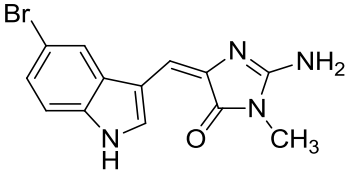	279 ± 21	94 ± 9	1271 ± 168
47	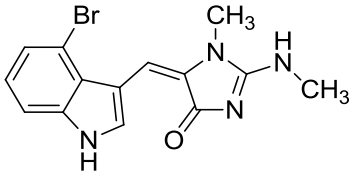	662 ± 92	99 ± 10	320 ± 61

Table 2-3 Selected serotonin receptor subtype binding affinities

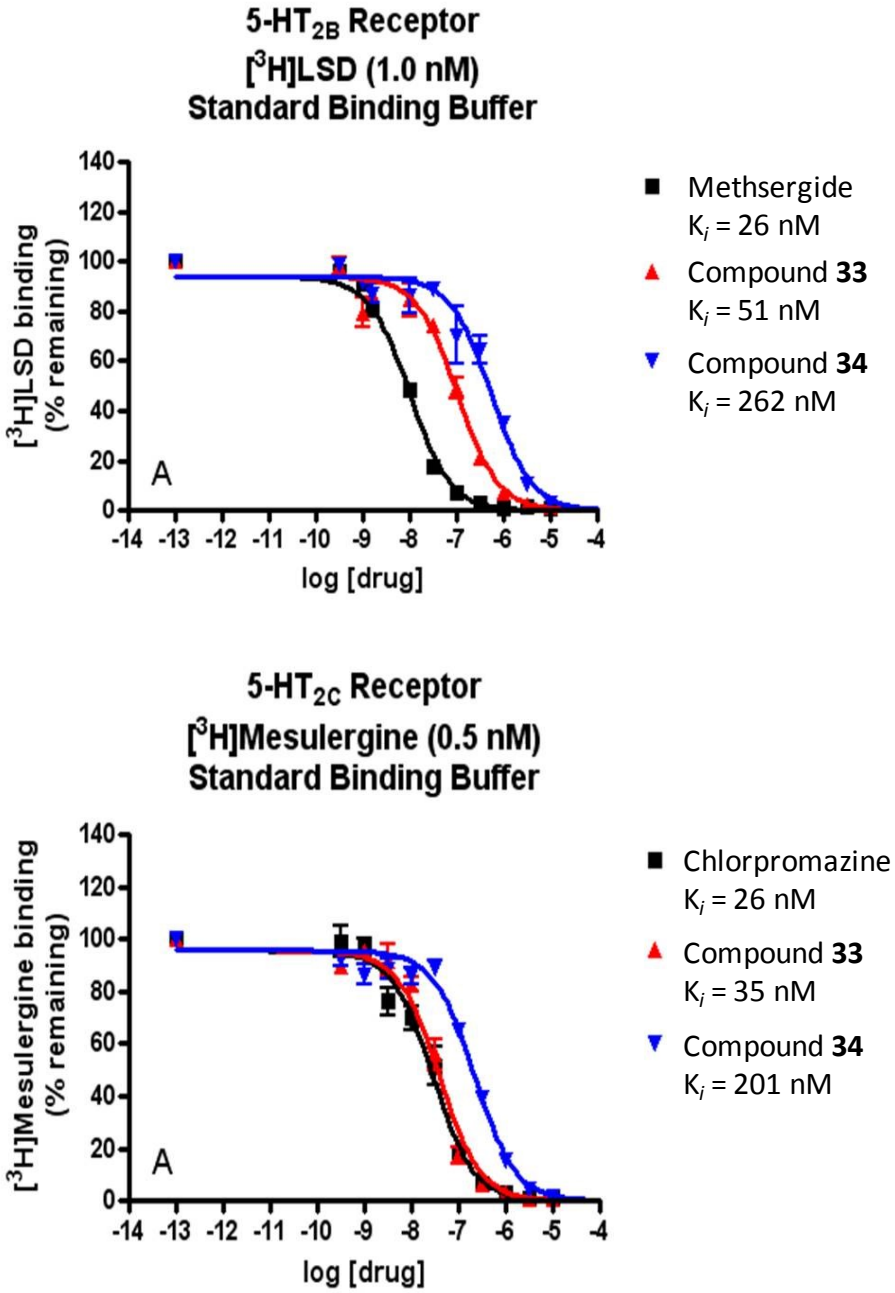

Figure 2-8 Binding affinity graphs for compounds 33, 34, and positive controls towards 5-HT$_{2B}$ and 5-HT$_{2C}$ receptors.

A general trend across all sub-groups of the library was that among each series of compounds it was shown that brominated compounds possessed lower (or better) K_i values than

their non-brominated counterparts. This was in line with previous reports that various halogenations improved K_i values.[38, 44] More specifically, we found that compounds brominated at C-4 and C-5 possess higher binding affinities in general. This is intriguing as there have been no reports of aplysinopsin analogs, synthetic or natural, halogenated at C-4. All of the naturally occurring aplysinopsin derivatives are either halogenated at C-6 or are di-brominated at C-5 and C-6. Concerning selectivity, across the entire library there was a noticeable selectivity for 5-HT_{2B} over 5-HT_{2C}. The average relative selectivity index (**SI**) for 5-HT_{2B} over 5-HT_{2C} was 4.32. A K_i value of 10,000 nM was assumed for compounds which were not tested in secondary binding assays to determine the relative SI. As mentioned earlier, the previous aplysinopsin SAR studies[38, 44] examining 5-HT receptor activity have failed to evaluate binding affinity for the 5-HT_{2B} receptor subtype, therefore it is difficult to make comparisons between the two data sets based on selectivity among 5-HT_2 receptor subtypes.

Concerning the effects of *N*-methylation of the imidazolidinone moiety, our results were in contrast to previous reports that showed an importance of *N*-alkylation in selectivity among 5-HT_2 receptor subtypes.[44] We did not observe a clear pattern of an increase in potency or selectivity among serotonin receptor subtypes based on variation in *N*-methylation. In fact, our most active compound subset was the group which had no alkylations of the imidazolidinone moiety. Again, comparison to previous SAR studies[38, 44] regarding imidazolidinone substitution patterns is difficult, as they did not evaluate any analogs which were unsubstituted on the imidazolidinone moiety.

MAO inhibitory activity

The 50 aplysinopsin analogs were also evaluated for their MAO-A and MAO-B

inhibitory activities (see Table 2-4). In addition, clorgyline and deprenyl (Figure 2-9) were evaluated as reference compounds. The results, expressed as IC_{50} and SI (selectivity index given by the MAO B IC_{50} / MAO A IC_{50} ratio) values are summarized in Table 2-4. In general we found that most aplysinopsin analogs showed greater inhibitory activity at MAO-A compared to MAO-B, with IC_{50} values ranging from 0.0056-26.12 μM for MAO-A and 0.207-100 μM for MAO-B. In particular, compound **54** displayed excellent MAO-A inhibitory activity, with an IC_{50} value of 0.0056 μM and an SI of 80.24. It possesses a lower MAO-A IC_{50} than reference compound clorgyline (0.0067 μM).

clorgyline deprenyl

Figure 2-9 Reference compounds for MAO inhibitory assay

In general, we found that analogs which did not have *N*-methyl groups on the imidazolidinone moiety displayed less inhibitory activity at both MAO-A and MAO-B, indicating that *N*-methylation of the imidazolidinone moiety is important for MAO inhibitory activity. Furthermore, mono-*N*-methylated compounds (**36-45**, **76-80**) did not possess significant activity at MAO-A or MAO-B. Advancing to di-*N*-methylated analogs (**46-60**), revealed an overall increase in MAO inhibitory activity. The aforementioned **54** as well as **49** and **51**, all displayed potent inhibition of MAO A with IC_{50} values of 0.0056 μM, 0.029 μM, and 0.035 μM respectively. Compounds **51** and **54** are identical in their *N*-methylation pattern on the imidazolidinone, with positions N-2′ and N-4′ methylated, but differ in their indole bromination pattern.

Compound	MAO-A	MAO-B	SI[a]	Compound	MAO-A	MAO-B	SI[a]
	IC_{50} (μM)	IC_{50} (μM)			IC_{50} (μM)	IC_{50} (μM)	
31	12.750±0.250	33.000±2.000	2.59	**57**	5.475±0.125	26.833±1.041	4.9
32	2.467±0.208	28.333±0.577	11.49	**58**	3.250±0.563	16.767±0.751	5.16
33	5.867±0.551	11.333±0.289	1.93	**59**	1.123±0.587	25.733±1.537	22.91
34	3.683±0.448	25.333±1.041	6.88	**60**	1.080±0.364	4.260±0.177	3.94
35	5.517±0.511	27.800±0.721	5.04	**61**	0.098±0.024	9.017±0.076	92.32
36	12.167±0.764	43.167±3.055	3.55	**62**	0.623±0.153	5.217±0.257	8.37
37	26.167±1.756	>100	-	**63**	0.085±0.006	0.370±0.017	4.38
38	8.000±0.781	24.500±1.803	3.06	**64**	0.018±0.001	0.207±0.015	11.19
39	6.075±0.175	35.667±1.607	5.87	**65**	0.153±0.008	2.817±0.076	18.37
40	6.107±0.257	34.333±0.577	5.62	**66**	14.333 ± 0.577	24.333 ± 4.041	1.69
41	1.967±0.153	34.333±1.893	17.46	**67**	0.267 ± 0.029	0.450 ± 0.095	1.68
42	1.517±0.126	37.000±1.000	24.4	**68**	1.233 ± 0.252	2.567 ± 0.176	2.08
43	0.327±0.025	4.300±0.200	13.16	**69**	1.533 ± 0.153	2.567 ± 0.208	1.67
44	0.165±0.039	3.800±0.100	23.03	**70**	0.543 ± 0.038	1.237 ± 1.614	2.27
45	1.197±0.090	14.267±0.681	11.92	**71**	2.783 ± 0.202	59.333 ± 4.041	21.31
46	3.075±0.075	33.833±2.363	11	**72**	0.677 ± 0.050	3.733 ± 0.321	5.51
47	2.583±0.362	26.333±0.577	10.19	**73**	7.133 ± 0.321	8.750 ± 0.250	1.22
48	0.263±0.025	11.633±0.777	44.18	**74**	0.533 ± 0.035	1.417 ± 0.202	2.65
49	0.029±0.001	2.667±0.153	91.95	**75**	0.627 ± 0.843	2.433 ± 0.115	3.88
50	1.900±0.050	12.833±0.666	6.75	**76**	13.333 ± 1.422	6.000 ± 0.819	0.45
51	0.035±0.001	10.017±0.076	290.34	**77**	1.800 ± 0.173	7.033 ± 1.419	3.9
52	2.067±0.208	51.167±1.607	24.76	**78**	1.200 ± 0.265	2.000 ± 0.781	1.66
53	0.236±0.307	2.700±0.050	11.44	**79**	4.433 ± 0.231	20.700 ± 2.858	4.66
54	0.0056±0.0002	0.447±0.035	80.24	**80**	3.900 ± 0.794	26.000 ± 1.000	6.66
55	0.052±0.001	3.117±0.126	60.52	**clorgyline**	0.0067±0.002	-	
56	5.817±0.535	30.467±0.896	5.24	**deprenyl**	-	0.045±0.01	

[a] The values are IC_{50s} computed from dose response curves and are mean ± S.D. of at least triplicate observations.

[b]The relative selectivity for MAO-A is defined by the ratio of IC_{50} (MAO-B)/IC_{50} (MAO-A) for each compound.

Table 2-4 Aplysinopsin analogs tested for inhibition (IC_{50}) of human MAO-A and MAO-B activities in vitro

All three (**49**, **51**, **54**) are di-*N*-methylated, with one of the *N*-methylations occurring at N-2′, which appears to play a large role in activity, as similar di-*N*-methylated compounds **56-60**,

which are unsubstitiuted at N-2′, are significantly less active. All three of the aforementioned compounds also possess a high SI, especially **51**, which has an SI of 290.34.

The series of five tri-*N*-methylated analogs (**61-65**) yielded the two lowest MAO-B IC_{50} values in compounds **63** and **64** (0.370 μM and 0.207 μM respectively). These compounds lacked selectivity though, with each possessing strong inhibitory activity towards MAO-A as well.

Concerning the bromination pattern, we found that bromination at C-5 and C-6 resulted in the lowering of IC_{50} values across all eight groups of analogs. This is not surprising considering that most naturally occurring halogenated aplysinopsin analogs are brominated at these positions,[71] and this is in agreement with a recent SAR study of indole analogs which revealed that substitution at C-5 lead to increased potency and selectivity for MAO-B.[72] Bromination at C-6 appears to be especially crucial for MAO-A inhibition, as halogenation at that position resulted in the lowest IC_{50} values for each group of compounds.

Another area of interest was the relationship between the geometry of the C-8-C-1′ double bond and MAO inhibitory activity. During synthesis of the analogs, the *E* or *Z* configuration is determined by the presence, or lack thereof, of a substituent at N-2′.[34a] If N-2′ is substituted with a methyl or bulkier group, the condensation will result in a double bond with predominantly *E* configuration. If N-2′ is non-methylated, bearing either a hydrogen atom or a lone pair, the major product will be *Z*-configured at the C-8-C-1′ double bond. This stereochemical outcome is confirmed using ^{1}H, ^{13}C heteronuclear coupling constants between H-8 and C-5′.[34b] The *E* isomer possesses a larger H-8, C-5′ heteronuclear coupling constant (9-11 Hz) compared to the *Z* isomer (4-5.5 Hz). It appears that an *E* configuration is important for

MAO-A selectivity and potency. The aforementioned three most active groups (**47-50**, **51-55**, and **61-65**) are all *E* configured due to their N-2′ methylation. Compounds **56-60**, which are also di-methylated, but *Z* configured, are significantly less active, insinuating that *E* configuration is an important SAR factor.

MAO inhibitors, which are potent and selective in addition to reversible, are of special interest to researchers. Thus, we evaluated three potent and selective analogs to assess their pharmacokinetic binding profiles. Compound **54** was selected due to its potent and selective MAO-A inhibition, and compounds **63** and **64** due to their being the most potent MAO-B inhibitors we assayed. Notably, compounds **63** and **64** were also potent inhibitors of MAO-A. Compound **54** inhibited MAO A through a reversible competitive mechanism with a K_i value in the range of 13.5 to 18. 9 nM, while the analog **63** inhibited MAO A through a reversible mixed-type inhibition mechanism with a K_i value in the rage of 20.7 to 26.2 nM. All three compounds tested inhibited MAO B through a reversible uncompetitive mechanism with K_i values in the range of 0.185 to 1.648 uM.

An overview of both 5-HT and MAO in vitro data reveals that the most potent and selective MAO-A inhibitors (**51** and **54**) did not possess significant affinities for any serotonin receptor subtypes. Furthermore, we found that analogs with the lowest K_i values for serotonin receptor subtypes (**33**, **43**, and **47**) did not possess significant MAO-A or MAO-B inhibitory activity. This is important because acting on both targets could lead to issues such as serotonin syndrome, as discussed in Chapter 1.

In vivo evaluation of lead compounds

The previous study assessing in vivo efficacy of aplysinopsins found that despite potent

in vitro CNS activity, aplysinopsins displayed diminished or non-existent in vivo activity.[45] Kochanowska et al. evaluated the parent compound aplysinopsin (**51**) in a Porsolt forced swim test. It did not display any significant antidepressant activity. Based on these findings we sought to evaluate our compounds in a different behavioral model. We chose the chick anxiety-depression model. It is different from the aforementioned forced swim test in that it acts as both a panic model to simulate anxiolytic conditions[62] and as a behavioral despair model to evaluate a depression-like state.[73] Further, the model shows solid face,[74] construct,[75] and predictive validity.[75-76] The chick anxiety-depression model entails isolation of socially raised chicks isolated at 5-6 days post-hatch. Chicks tested with conspecifics show low rates of vocalization throughout the session whereas chicks tested in isolation show high rates of distress vocalizations (DVocs) during the first 5 minutes (i.e., the anxiety-like phase; see ref 62) which decline over the next 20 minutes by 40-50% of the initial rate and remain steady throughout the remaining isolation period (i.e., depression-like phase). The reduced DVoc rates during this latter phase mirror the pattern seen in traditional behavioral despair depression models.

In addition to using a new behavioral model, we assessed whether key structural changes (e.g. halogenations and *N*-methylations) would result in increased in vivo efficacy profiles. Based on our in vitro results, we chose three lead compounds (**33**, **51**, **54**) to be evaluated in the in vivo anxiety-depression model.[62] Compounds **51** and **54** showed nanomolar level affinity for MAO-A and both had a high selectivity index for MAO-A over MAO-B.[77] Despite its limited selectivity among 5-HT_2 receptor subtypes, compound **33** was chosen due to its potency and ability to serve a good primary representative of the general aplysinopsin pharmacophore in initial in vivo screening to assess bioavailability.

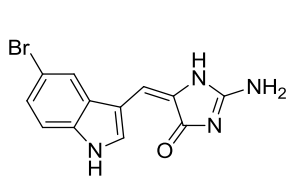

CMPD **33**
Notable Binding 5-HT Ki's:
$5\text{-}HT_{2A}$ = 58 ± 6 nM
$5\text{-}HT_{2B}$ = 51 ± 7 nM
$5\text{-}HT_{2C}$ = 35 ± 4 nM

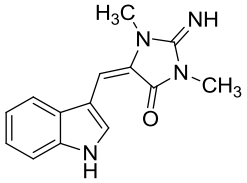

CMPD **51**
Notable MAO-A inhibitory activity/selectivity:
IC_{50} = 35 ± 1
SI MAO-B/MAO-A= 290.34

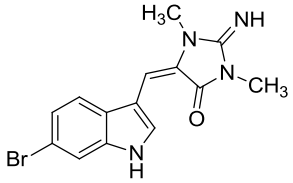

CMPD **54**
Notable MAO-A inhibitory activity/selectivity:
IC_{50} = 5.6 ± 0.2
SI MAO-B/MAO-A= 80.24

Figure 2-10 Lead compounds selected for in vivo screening

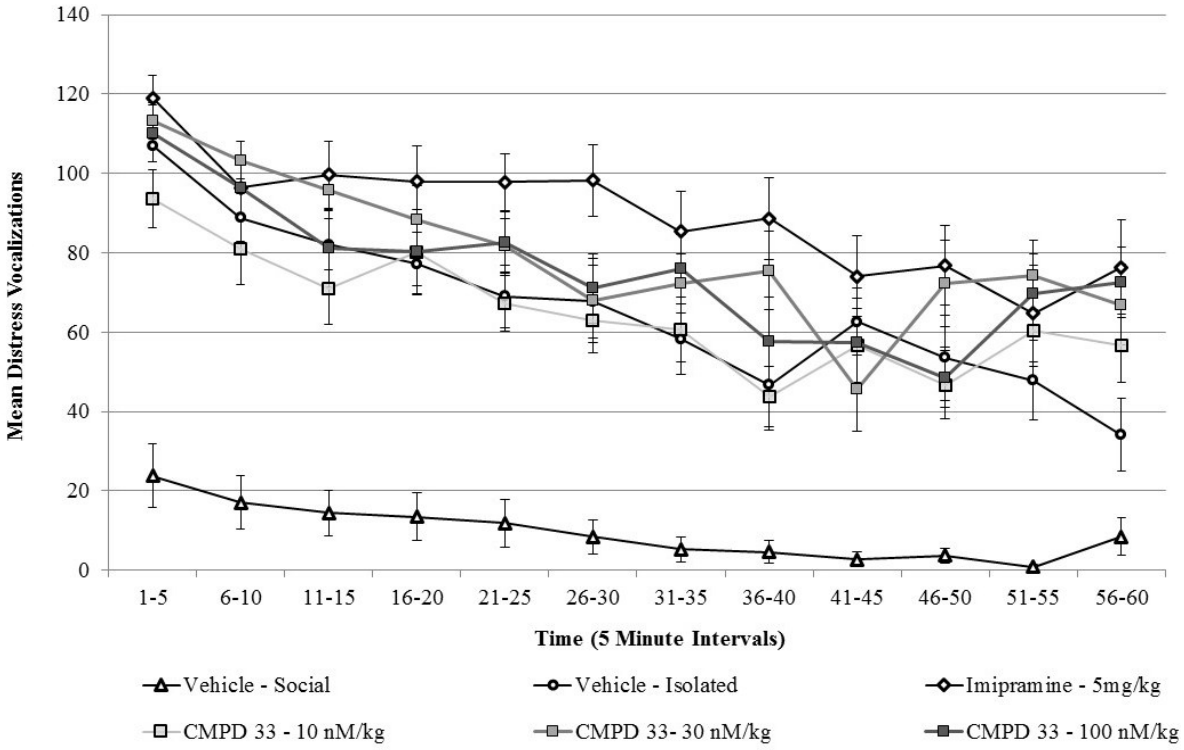

Figure 2-11 Mean distress vocalizations as a rate/minute function (+/- SEM) for time in five minute intervals.

Compounds were screened in the chick anxiety-depression model at 10, 30, and 100

nM/kg concentrations. Of the three compounds tested, **33** displayed the most promising activity. The pattern of distress vocalization rates across the isolation stressor for the various treatment conditions are summarized in Figure 2-11 for compound **33**. Socially tested chicks given vehicle displayed few DVocs across the test session. Vehicle-isolated chicks exhibited high DVoc rates during the first five minute block (anxiety-like phase) that declined over the next 25-30 minute period to approximately 50% of the initial rate and remained relatively stable for the remaining of the test session (depression-like phase). During the anxiety-like phase, none of the tested compounds altered DVocs. Imipramine attenuated the decline in DVocs during the depression-like phase (i.e., antidepressant effect). Further, the 30 nM/kg dose of **33** produced modest attenuation of the depression-like phase. Consistent with these observations, a two-way ANOVA revealed a significant drug treatment effect $F(5,726)=23.44$, $p<0.0001$, a significant isolation time effect $F(11,726)=35.43$, $p<0.0001$, and a significant drug x isolation interaction $F(55,726)=2.05$, $p<0.0001$.

These findings prompted an additional set of analyses to evaluate drug treatment effects during the anxiety-like phase (0-5 m), the first half (30-45 m) of the depression-like phase, and the second half (45-60 m) of the depression-like phase. These analyses for compound **33** are summarized in Figure 2-12, Figure 2-13, and Figure 2-14. A one-way ANOVA of the DVoc data from the anxiety-like phase (0-5 min block; see Figure 2-12) revealed a significant treatment effect $F(5,66)=32.86$, $p<0.0001$. Fisher's post-hoc analyses revealed that the mean DVoc rate of the isolated-vehicle group was higher than mean DVoc rate of the social-vehicle group, $p<0.0001$. All other relevant comparisons failed to reach statistical significance.

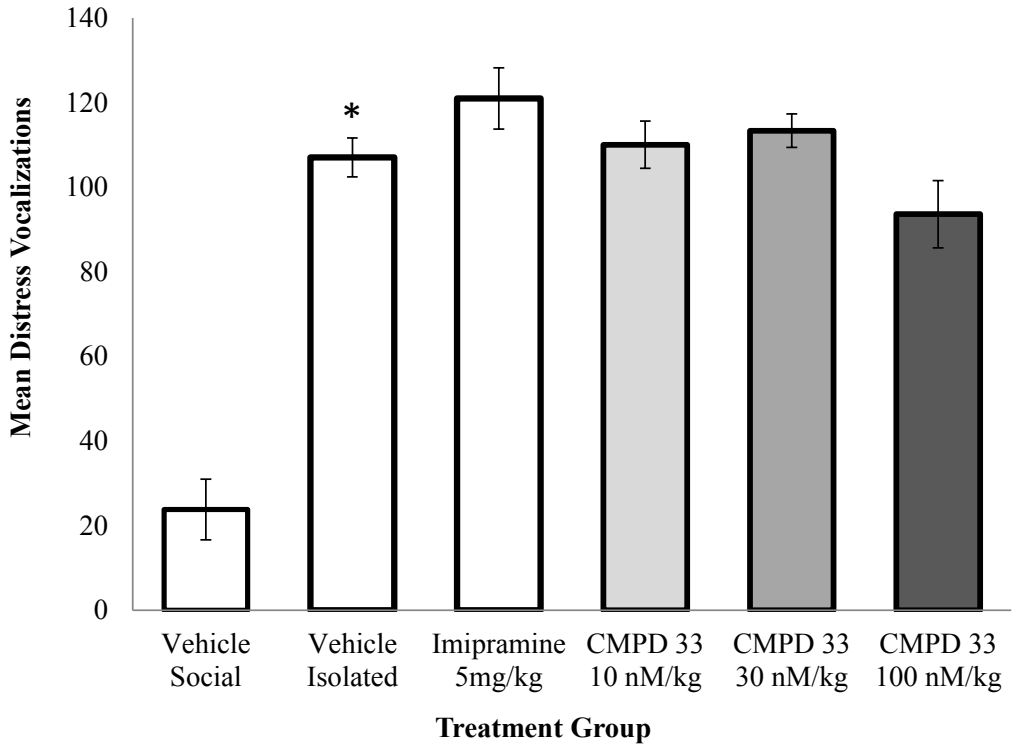

Figure 2-12 The effects of social separation on mean DVocs (+/- SEM) in each drug treatment condition under the anxiety-like phase (minutes 1-5).

A one-way ANOVA of the DVoc data from the first half of the depression-like phase (see Figure 2-13) revealed a significant treatment effect $F(5,66)=17.605$, $p<0.0001$. Post-hoc analyses (paired t-test) revealed that in the isolated-vehicle group the mean DVoc rate for the depression-like phase was lower than in the anxiety-like phase, $p<0.0001$ and that Fisher's least significant differences (LSD) demonstrated imipramine attenuated this decline, $p<0.0001$. All other relevant comparisons failed to reach statistical significance.

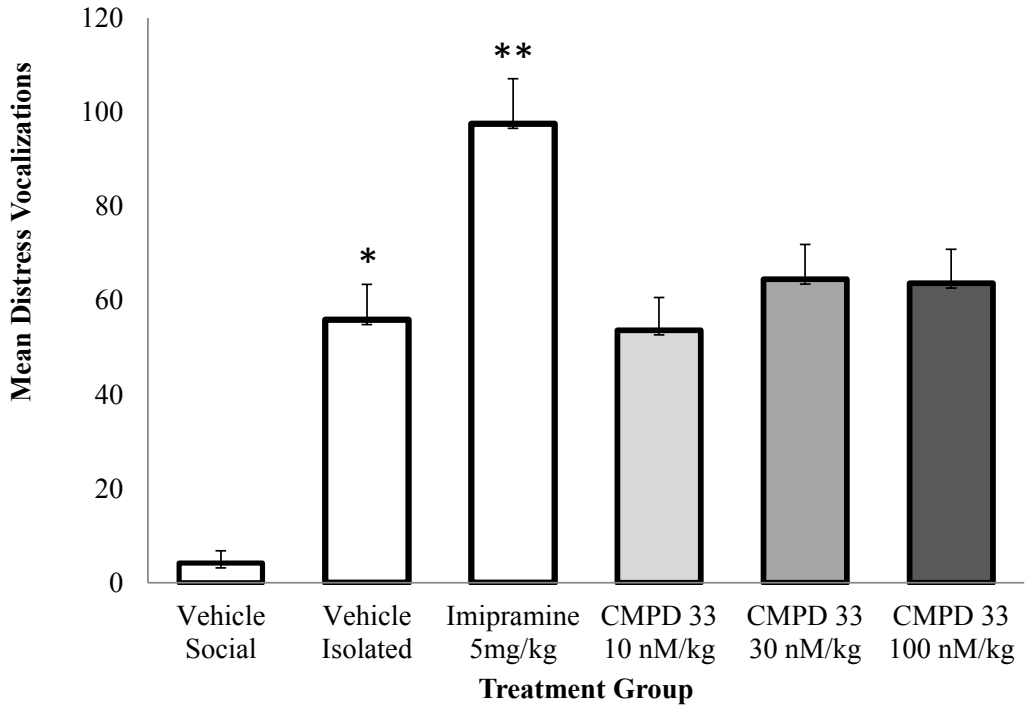

Figure 2-13 The effects of social separation on mean DVocs (+/- SEM) in each drug treatment condition under the first depression-like phase (minutes 31-45).

Analysis of the second half of the depression-like phase (see Figure 2-14) showed a significant treatment effect $F(5,66)=14.344$, $p<0.0001$. A paired t-test revealed that in the isolated-vehicle group the mean DVoc rate for the depression-like phase was lower than in the anxiety-like phase, $p<0.0001$. Fisher's LSD revealed that the mean DVoc rates of the imipramine group ($p=0.0002$) and 30 nM/kg **33** ($p=0.017$) were higher than the mean DVoc rate of the isolated-vehicle group.

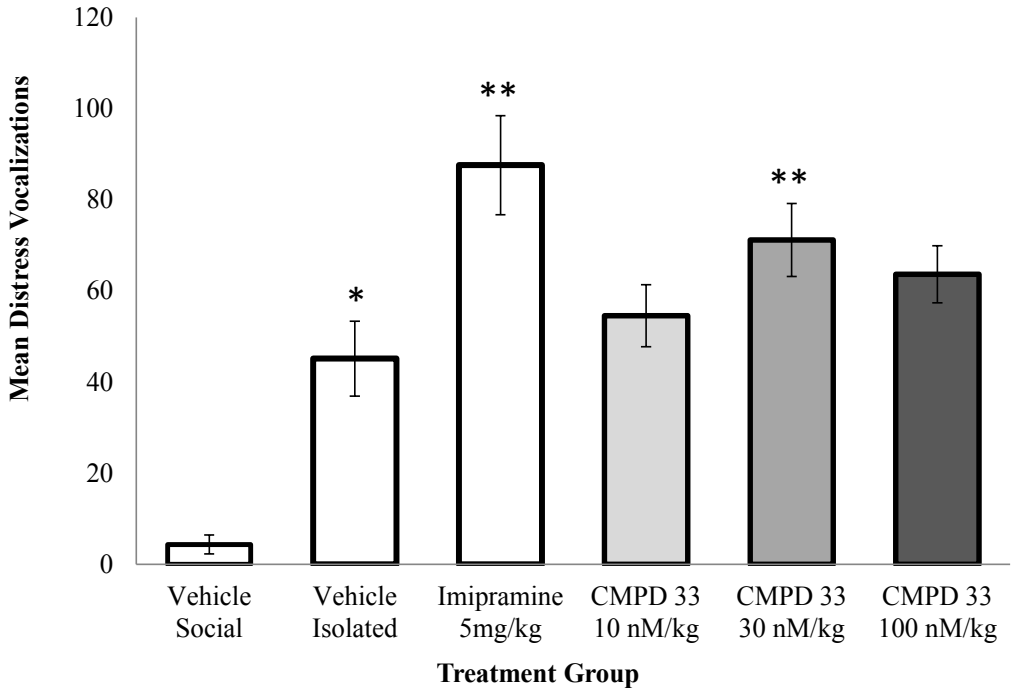

Figure 2-14 The effects of social separation on mean DVocs (+/- SEM) in each drug treatment condition under the second depression-like phase (minutes 46-60).

Data from the in vivo screening demonstrated that isolation stress produced sequential anxiety-like and depression-like phases and that the positive control imipramine produced antidepressant effects in the model. A modest antidepressant effect was seen with compound **33** at the intermediate dose during the latter half of the depression phase. This late onset of action may reflect the interaction of this compound at serotonin receptors and that an isolation test session beyond the 60 minute may reveal more robust effects.[74]

Conclusion and Discussion

In conclusion, we report the synthesis of 50 aplysinopsin analogs which were evaluated for their affinity at 12 serotonin receptor subtypes and 34 other CNS receptors, in addition to inhibitory activity of MAO isoforms A and B. Previous reports indicated that aplysinopsin analogs possessed affinity and selectivity for serotonin receptor subtypes.[38, 44] Both of these reports pointed to key structural features that allowed analogs to have a high degree of selectivity for 5-HT_{2C} over 5-HT_{2A}. Among those were C-6 halogenation. Both studies found that the inclusion of a larger halogen (bromine or chlorine) at C-6 led to an increased binding affinity and selectivity for 5-HT_{2C}. If C-6 was substituted with a smaller halogen (fluorine) or left unsubstituted, the molecules were selective for 5-HT_{2A}. As mentioned previously, both of the previous studies only evaluated affinity at those two receptor subtypes.

Bromination of the indole moiety increased aplysinopsins' binding affinity for the 5-HT_2 subfamily of receptors. More specifically, bromination at C-4 and C-5 increased affinity the most. In general, analogs showed a selectivity for 5-HT_{2B} over 5-HT_{2A} and 5-HT_{2C}. This finding is important, as aplysinopsins have previously not been evaluated for their 5-HT_{2B} affinity, and increased affinity at this receptor can often lead to undesirable side effects. As more information becomes available, such as the recent report of a 5-HT_{2B} crystal structure with ergotamine bound[78], we should be able to better understand the binding behavior of 5-HT_{2B} selective ligands and design more selective ligands. In comparing our results to the previous studies regarding selectivity between 5-HT_{2A} and 5-HT_{2C}, we also observed a general trend of increased selectivity for 5-HT_{2C} when C-6 was brominated compared to unsubstituted. The previous report by Cummings *et al.*[44] also noted that halogenation (of any type) at C-5 resulted in

a lack of affinity for either receptor. Analogs with bromination at C-5 were actually some of the most active and selective analogs in our library. Possible explanations for these conflicting results could be differences in the assay and cell culture conditions.

The other area of modification was the substitution of the imidazolidinone moiety. Our results showed no clear pattern regarding the effect of *N*-alkylation of the imidazolidinone moiety as far as serotonin affinity and selectivity were concerned. In fact, we observed the most potent affinities in the subgroup which had no *N*-alkylations of the imidazolidinone moiety. Both of the previous studies found that alkylation of R2 and R4 were important for binding to serotonin receptor subtypes 5-HT_{2A} and 5-HT_{2C}. However, neither of these studies evaluated analogs which were unsubstituted on the imidazolidinone moiety, so comparison of data is not possible.

Biological evaluation of the MAO-A and MAO-B inhibitory activities of these compounds revealed some potent and selective MAO inhibitors. The most active compound **54**, which is brominated at C-6 and methylated at N-2′ and N-4′, showed strong inhibitory activity at MAO-A (IC_{50} of 5.6 nM) and had an SI of 80.24. We found several factors important in selectivity and potency. The first is multiple *N*-methylations of the imidazolidinone moiety, one of which should be the methylation of N-2′, in addition to either N-3′ or N-4′. Secondly, bromination at C-5 or C-6 is important for MAO-A potency and selectivity. These results suggest that the aplysinopsin scaffold may be useful in designing selective MAO inhibitors.

Based on the in vitro screening findings, we chose to evaluate three compounds in an in vivo model. Similarly to previous in vivo studies of aplysinopsins using different depression models, we were unable to reproduce the in vitro efficacy in an animal model. However, one

compound, **33**, did exhibit a modest antidepressant effect in the later stages of the evaluation period. It is clear that the aplysinopsin scaffold has potential to generate leads to treat CNS disorders or serve as molecular probes to further investigate the underlying selectivity issues among 5-HT receptor subtypes and MAO isoforms A and B.

Experimental

Chemistry

Unless specified all reagents were purchased from commercial sources and used without further purification. Compounds were purified via column chromatography using Sorbtech silica gel, 60A, 40-63um from Sorbent Technologies. Whatman silica gel F254 polyester backed plates were used for TLC and visualized with UV light and/or ninhydrin, vanillin, and anisaldehyde. NMR spectra were recorded on a 400 MHz Bruker instrument (400 UltraShield, 54 mm standard magnet bore, Billerica, MA) with 3mm direct carbon probe. ^{1}H-NMR and ^{13}C-NMR spectra were recorded at 400 MHz and 100 MHz, respectively. Chemical shifts were standardized to TMS and solvent signals. All biologically evaluated compounds were found to possess ≥ 95% purity by HPLC (UV detection at 210 and 254 nm). Purified samples were analyzed by LC-MS (Bruker Daltonik microTOF, Leipzig Germany) using a 150 x 4.6 mm C8 column (Luna Phenomenex). HR-ESI-MS analysis was done in positive ionization mode.

General procedures for the synthesis of aplysinopsin analogs and full characterizations of three compounds evaluated in vivo are provided below. Analytical data for all other compounds can be found in the Supplementary Data section.

General procedure for the synthesis of aplysinopsin analogs 31-65 (GP1)

Equimolar amounts of the appropriate 3-formylindoles **18-22** and imidazolidinones **23-30** were mixed under N_2 and heated over an open flame until the reaction mixture began effervescing. Several minutes after the effervescence stopped, the mixture was cooled to room temperature. The crude mixture was extracted with MeOH and insoluble materials filtered off. The solution was concentrated and loaded on to silica gel for purification using.

General procedure for the synthesis of aplysinopsin analogs 66-70 (GP2)

Equimolar amounts of the appropriate 3-formylindoles **18-22** and thiohydantoin **4** were dissolved in abs. EtOH and 1 mL of ethanolamine was added. The mixture was heated at reflux for 1 h. After cooling the precipitate was filtered off and dried to yield compounds **66-70**, which were used without further purification.

General procedure for the synthesis of aplysinopsin analogs 71-75 (GP3)

To a solution of appropriate intermediates **66-70** (1.5 mmol) and NaOH (1.5 mmol) in 5 mL of MeOH and 0.5 mL H_2O was added MeI (1.5 mmol). The mixture was stirred at room temperature for 18h. The resulting precipitant was filtered and dried to yield compounds **71-75**, which were used without further purification.

General procedure for the synthesis of aplysinopsin analogs 76-80 (GP4)

Compounds **71-75** were dissolved in abs. EtOH and 2x molar equivalents of CH_3NH_2 was added. The mixture was heated to 70ºC in a sealed vessel for 24h. After cooling the crude mixture was purified on silica gel.

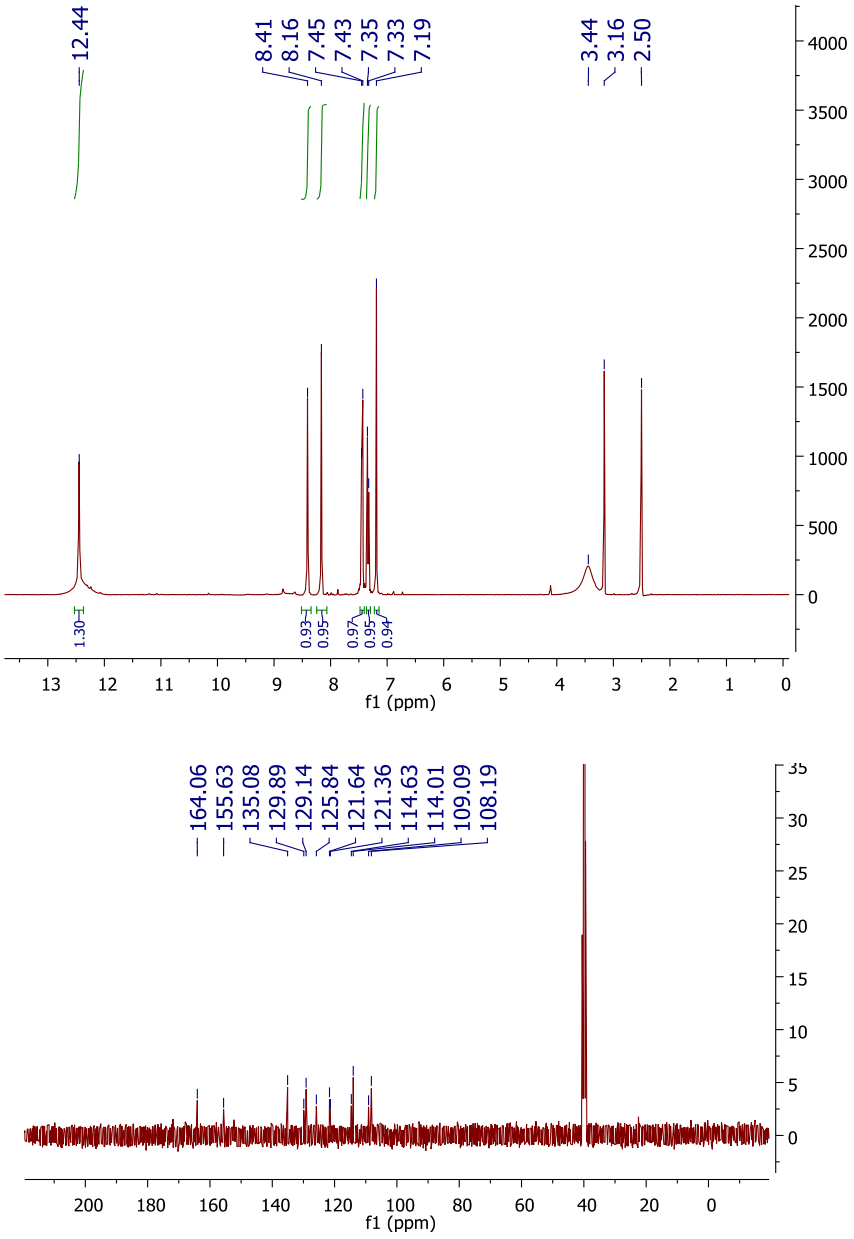

Figure 2-15 ^{1}H and ^{13}C NMR spectra of compound 33.

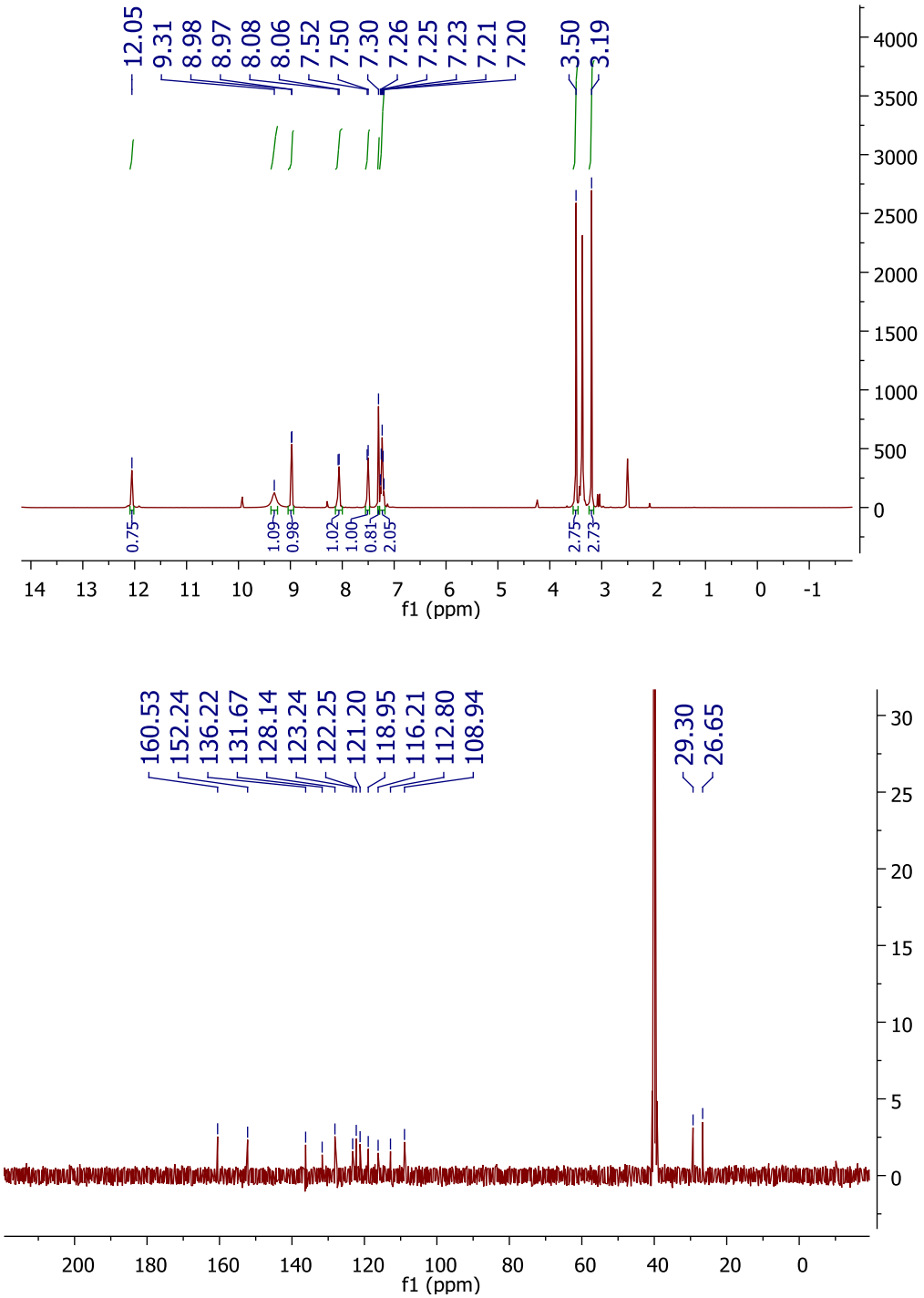

Figure 2-16 ^{1}H and ^{13}C NMR spectra of compound 51.

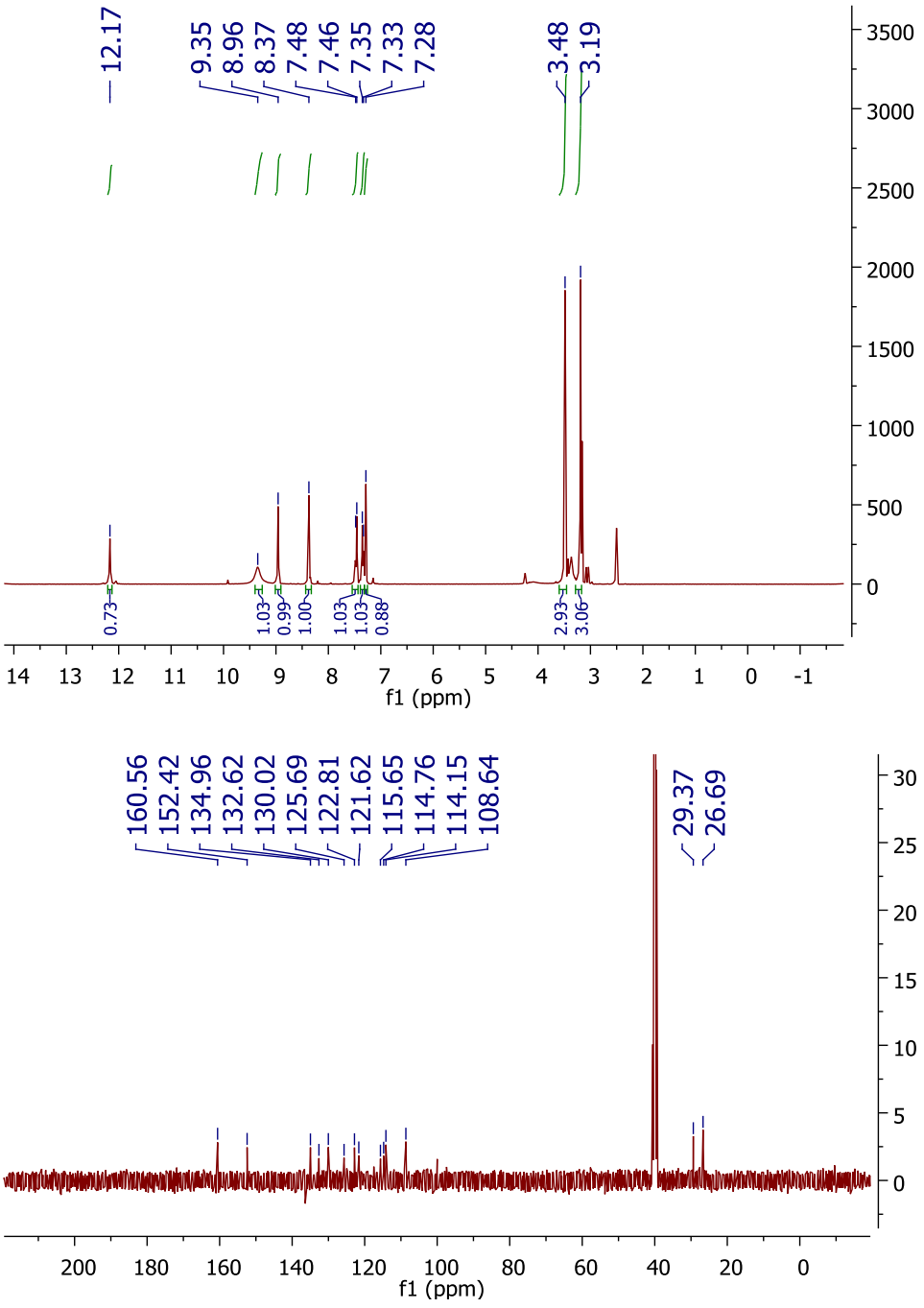

Figure 2-17 ^{1}H and ^{13}C NMR of compound 54.

(Z)-2-Amino-5-[(5-bromo-*1H*-indol-3-yl)methylene]-*1H*-imidazol-4(*5H*)-one (33)

5-Bromo-3-formylindole (448 mg, 2 mmol) and demethylcreatinine (198 mg, 2 mmol) were reacted according to **GP1** to yield **33** (380 mg, 62% yield). ^{1}H NMR (400 MHz, DMSO) δ 12.44 (s, 1H), 8.41 (s, 1H), 8.16 (s, 1H), 7.44 (d, *J* = 8.6 Hz, 1H), 7.34 (d, *J* = 8.6 Hz, 1H), 7.19 (s, 1H). ^{13}C NMR (101 MHz, DMSO) δ 164.06, 155.63, 135.08, 129.89, 129.14, 125.84, 121.64, 121.36, 114.63, 114.01, 109.09, 108.19. HRESMS *m/z* calcd 305.0038 ($M^{\cdot+}$ +H); found: 305.0040.

(E)-5-[(*1H*-indol-3-yl)methylene]-2-imino-1,3-dimethylimidazolidin-4-one (51)

3-formylindole (290 mg, 2 mmol) and 1,3-dimethyl-2-imino-4-imidazolidinone (254 mg, 2 mmol) were reacted according to the above **GP1** to yield **51** (365 mg, 72% yield). ^{1}H NMR (400 MHz, DMSO) δ 12.05 (s, 1H), 9.31 (s, 1H), 8.97 (d, *J* = 2.4 Hz, 1H), 8.07 (d, *J* = 7.4 Hz, 1H), 7.51 (d, *J* = 7.4 Hz, 1H), 7.30 (s, 1H), 7.28 – 7.18 (m, 2H), 3.50 (s, 3H), 3.19 (s, 3H). ^{13}C NMR (101 MHz, DMSO) δ 160.53, 152.24, 136.22, 131.67, 128.14, 123.24, 122.25, 121.20, 118.95, 116.21, 112.80, 108.94, 29.30, 26.65. HRESMS *m/z* calcd 255.1246 ($M^{\cdot+}$ +H); found: 255.1290.

(E)-5-[(6-Bromo-*1H*-indol-3-yl)methylene]-2-imino-1,3-dimethylimidazolidin-4-one (54)

5-Bromo-3-formylindole (448 mg, 2 mmol) and 1,3-dimethyl-2-imino-4-imidazolidinone (254 mg, 2 mmol) were reacted according to the above **GP1** to yield **54** (312 mg, 47% yield). ^{1}H NMR (400 MHz, DMSO) δ 12.17 (s, 1H), 9.35 (s, 1H), 8.96 (s, 1H), 8.37 (s, 1H), 7.47 (d, *J* = 8.5 Hz, 1H), 7.34 (d, *J* = 8.5 Hz, 1H), 7.28 (s, 1H), 3.48 (s, 3H), 3.19 (s, 3H). ^{13}C NMR (101 MHz, DMSO) δ 160.56, 152.42, 134.96, 132.62, 130.02, 125.69, 122.81, 121.62, 115.65, 114.76, 114.15, 108.64, 29.37, 26.69. HRESMS *m/z* calcd 333.0351 ($M^{\cdot+}$ +H); found: 333.0352.

Note: For physical data of all compounds tested, see Chapter 4.

Bioassays

In vitro evaluation of serotonin binding affinity

K_i determinations were generously provided by the National Institute of Mental Health's Psychoactive Drug Screening Program. Briefly, compounds are initially evaluated in a primary binding assay, in which they are tested at a final concentration of 10 μM. They are tested in quadruplicate and compounds that show > 50% inhibition are deemed hits and advance to secondary radioligand binding assays. Here compounds are tested at eleven concentrations (0.1, 0.3, 1, 3, 10, 30, 100, 300 nM, 1, 3, 10 μM) to determine the K_i values at specific receptors. For complete experimental details please refer to the PDSP web site http://pdsp.med.unc.edu/ and click on "Binding Assay" on the menu bar.

In vitro evaluation of MAO inhibitory activity

An in vitro assay was designed to measure the effect of aplysinopsin analogs on MAO-A and B activity. Recombinant human MAO-A and B were obtained from BD Biosciences (Bedford, MA, USA). Kynuramine bromide, 4-hydroxyquinoline, clorgyline and R-(-)-deprenyl were purchased from Sigma (St Louis, MO, USA). Aplysinopsin analogs (10^{-9} to 10^{-2}M), clorgyline and deprenyl (10^{-12} to 10^{-5}M) were tested for inhibition of human MAO-A and B activity. MAO-activity was assessed by a modification of the fluorometric method of Kralj[79] and was adopted for 96 well plate's format. The 200 μL reaction mixtures containing recombinant human MAO-A or MAO-B (5 μg/mL) and the test compounds in KH_2PO_4 buffer (100 mM; pH 7.4) were pre-incubated at 37ºC for 15 min. The reactions with positive control wells with standard MAO inhibitors and controls without inhibitors were also set up simultaneously. The

reaction was initiated by addition of kynuramine (250 μM) in potassium KH_2PO_4 (100 mM; pH 7.4) and incubated further at 37°C for 20 min. After incubation the reaction was stopped by the addition of 75 μL of 2N NaOH. The deaminated product of kynuramine, which spontaneously cyclizes to 4-hydroxyquinoline, was determined fluorometrically at 320 nm excitation and 460 nm emission wavelengths in a plate reader (SpectraMax M5, Molecular Devices, Sunnyvale, CA, USA). Wells receiving no test compounds were used as controls to calculate the inhibition percentage. The IC_{50} values were computed from the dose response inhibition curves prepared by GraphPad.

In vivo evaluation of aplysinopsin analogs

All procedures involving animals were performed as approved by the Institutional Animal Care and Use Committee of The University of Mississippi. Cockerels (Production Red, Ideal Poultry, Cameron, TX, USA) were received into the laboratory at 2 days post hatch and housed in 34 x 57 x 40 cm cages with 12 chicks per cage. Food and water are available ad libitium via gravity feeders. Daily maintenance that entails the replacement of tray liners and filling food and water gravity feeders is conducted during the hour that precedes the animal's dark cycle. Lights are operated on a 12:12 light dark cycle. Supplemental heating sources are provided to maintain appropriate housing temperatures in the range of 32 +/- 1°C.

Testing equipment

A six unit testing apparatus containing Plexiglas chambers (25 x 25 x 22 cm) surrounded by sound attenuating media is used to record separation-induced vocalizations. Each unit is lined with acoustical fiber media, illuminated by a 25-W light bulb, and ventilated by an 8-cm-diameter rotary fan (Model FP-108AX S1, Commonwealth Industrial Corp., Taipei, Taiwan).

Miniature video cameras (Model PC60XP, SuperCircuits, Inc., Liberty Hill, TX) mounted in the sound-attenuating enclosures at floor level and routed through a multiplexor (Model PC47MC, SuperCircuits, Inc.) provided televised display of the chicks for behavioral observation. To record DVocs, microphones (Radio Shack Omnidirectional Model 33-3013 modified for AC current) are mounted at the top of the Plexiglas chamber. These vocalizations are routed to a computer equipped with custom designed software for data collection.

Methods

Squads of six chicks were taken from their home cage and placed within a lidded plastic transport container. To track subject assignment to treatment conditions, chicks are marked using colored felt pens and body weight is determined for each chick to determine dosing and identify outliers (i.e., low body weight). Drugs were administered IP 15 minutes prior to behavioral testing. Chicks were placed into individual testing units for a 60 minute session. Following the completion of the session chicks were removed from the testing apparatus and returned to their home cage.

CHAPTER 3

DESIGN OF A SECOND GENERATION OF APLYSINOPSIN ANALOGS WITH IMPROVED IN VIVO EFFICACY

3. Introduction

Our previous results showed that the aplysinopsin scaffold has potential to yield drug leads which have neuromodulatory activities. The previous results also showed that future drug design efforts would need to focus on improving the in vivo efficacy as well as maintaining serotonin receptor affinity and MAO inhibitory activities. We were able to identify lead compounds which possessed nanomolar level affinities for 5-HT receptor subtypes and MAO isoforms A and B. However, the lack of in vivo efficacy indicates that the compounds are not reaching the target tissue, in this case the brain, with a high enough plasma concentration to elicit significant effects. There are a number of possible reasons for the loss of efficacy from cell based assays to an animal model. Most pharmaceutical companies have entire divisions devoted to solving these issues and improving the in vivo efficacy of lead compounds. As medicinal chemists continue to explore new chemical space in terms of lipophilicity and solubility, there is a constant push to find ways to improve bioavailability, especially as it pertains to CNS drugs.

Poor bioavailability is one of the leading causes of drug failure in pre-clinical and clinical development.[80] This lack of bioavailability can generally be traced back to the relationship between physiochemical properties (e.g. logP, MW, PSA, etc) and the ADME (absorption, distribution, metabolism, and excretion) characteristics of lead compounds. There are numerous reviews about the physiochemical properties associated with successful CNS-active drugs.[81] Out of those, several guidelines, or "rules" have emerged as standards for evaluating the likeliness of a drug to cross the Blood-Brain Barrier (BBB) and be CNS-active. First and foremost is Lipinski's "Rule of Five," which asserts that if all five of the following conditions are met, then a drug is likely to have good bioavailability:[82]

- Molecular weight ≤ 500
- LogP is ≤ 5
- Hydrogen bond donors ≤ 5 (sum of OHs and NHs)
- Hydrogen bond acceptors ≤ 10 (sum of Ns and Os)
- Number of rotatable bonds ≤ 10

Lipinski's rules have been validated by numerous studies to be accurate and useful for predicting a drug's bioavailability.[83] Several years after his initial proposal of the "Rule of Five," Lipinski put forth an additional, more constrictive set of rules specifically for CNS penetration.[84] As discussed earlier, drugs which must penetrate the CNS have a narrower window of physical properties. Lipinski proposed that CNS penetration is likely if the following parameters are met:

- Molecular weight ≤ 400
- LogP ≤ 5
- Hydrogen bond donors ≤ 3
- Hydrogen bond acceptors ≤ 7

Another set of similar rules are those of Clark,[85] who proposed that potential CNS drugs should meet the following criteria:

- N + O < 6
- Polar surface area < 60-70 $Å^2$
- MW < 450
- Log D = 1-3
- ClogP – (N + O) > 0

Clark's rules bear some similarity to Lipinski's rules. There are also numerous other sets of "rules" or guidelines to follow when designing a library of drug leads. The key for greatly adopted use of these guidelines is their ease of use. For the most part, medicinal chemists are able to quickly tabulate these properties and use the results to aid in compound library design.

When looking at the various parameters that contribute to the ADME profile, we wanted

to evaluate which parameters might be diminishing the in vivo efficacy of our aplysinopsin analogs. For a CNS drug to cross the BBB and reach its therapeutic target, there are several obstacles that must be overcome. First is avoiding excessive metabolism. We made use of an in vitro stability study and metabolism profiling assay to assess the metabolism of aplysinopsin analogs. If a drug is excessively metabolized before it reaches the BBB, it will likely not be active. Second is permeability once it reaches the BBB. The BBB is a major detriment to CNS drug development. There are essentially three ways that drugs can cross the BBB: passive paraceullar diffusion, passive transcellular diffusion, and active transport (influx and efflux). Paracellular diffusion is uncommon due to the epithelial cells which form tight junctions in the BBB. Due to this, the most common way for drugs to diffuse across the BBB is transcelluar diffusion. There are currently a variety of in vitro, in vivo, and in silico methods used to investigate BBB permeability of drug candidates.[86] An in silico (QikProp by Schrödinger) method was used to evaluate several predicted permeability parameters. Last, but not least, is the ability of efflux pumps to pump out compounds which are able to successfully cross the BBB. The multidrug-resistance transporter (MDR-1), also known as P-glycoprotein, is the most widely studied of the efflux pumps. MDR-1 is found ubiquitously through the body, not just in the BBB. Many drugs have been found to be substrates of MDR-1, and it plays an important role in the development of CNS drug candidates. An in vitro MDR-1 assay was used to assess whether aplysinopsins were subjected to MDR-1 transport, which could explain their lack of in vivo efficacy.

Design of Second Library of Aplysinopsin Analogs

Poor ADMET properties account for the failure of nearly 40% of drug candidates in clinical trials.[87] Being able to predict these failures earlier can help save time, money, and resources. Current technology allows us to predict these properties quickly and accurately without using costly and time consuming methods such as high-throughput screening. Using programs such as QikProp by Schrodinger, we can evaluate not only classic ADME parameters like Lipinki's "Rule of Five," but also other pharmaceutically relevant properties such as polar surface area (PSA), log S (solubility in water), log P (partition in octanol/water mixture), log BB (blood-brain partition coefficient), Caco-2 and MDCK cell permeabilities, and TSW (toxicity structural warnings). QikProp is able to compute these pharmaceutically relevant properites with high degrees of precision, as shown in Figure 3-1, where the QikProp predicted water/octanol partition coefficients are compared to the experimental values. They were found to be in excellent agreement with an R^2 value of 0.92. Similar R^2 results were found for all QikProp predicted properties. QikProp can perform calculations rapidly, analyzing thousands of compounds in very short periods of time depending on computing power available.

When building a virtual library of aplysinopsin compounds to analyze using QikProp, we had to consider which areas of the aplysinopsin scaffold are available to be modified. In general, they can be classified into three groups: 1) substitution of the indole ring, 2) substitution at the indole nitrogen, 3) alterations of the substitution pattern on the imidazolidinone moiety (see Figure 3-2).

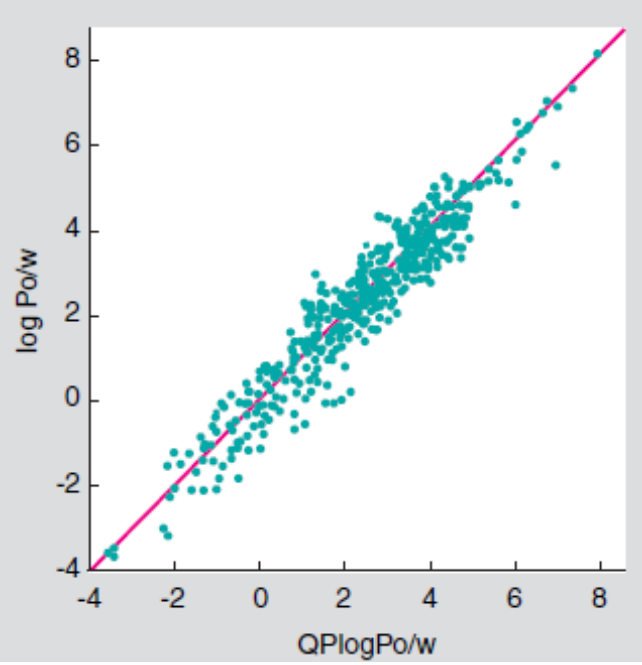

Figure used with permission from Schrodinger.

Figure 3-1 QikProp-predicted water/octanol partition coefficients plotted against experimental values.

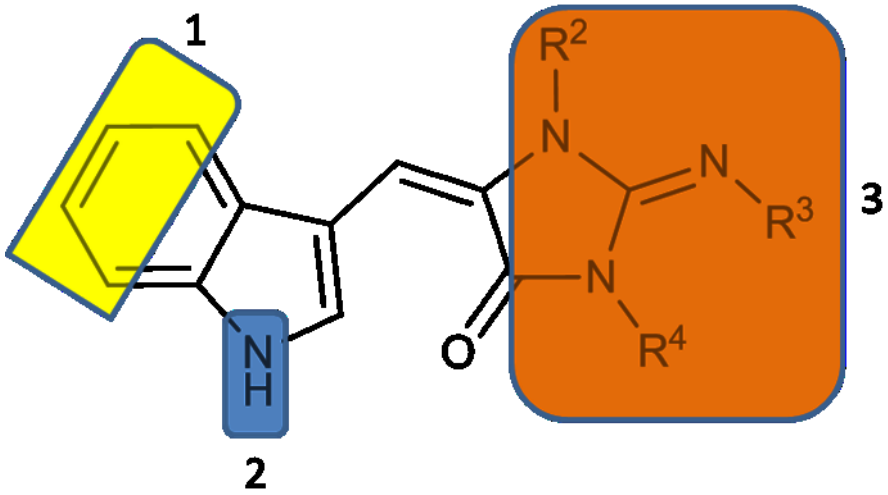

Figure 3-2 Possible sites of modification of aplysinopsins scaffold.

Because we are only looking at a limited amount of chemical space (only the aplysinopsin scaffold), we are unlikely to see a great deal of variation in any one individual parameter.

However, we can still observe measurable changes in the physicochemical properties analyzed. Thus, we can see which structural changes might lead to improvements in the overall ADME profile of the compounds.

We screened a library of over 400 aplysinopsin analogs with modifications at the aforementioned positions, using known modifications to triptamines, indoles, and other CNS alkaloid drugs. One drawback to these in silico programs is that they generate a wealth of data which is often hard for medicinal chemists to interpret. For this reason, we chose to focus on a set of properties and predictors which could give us clear information to guide the construction of our new library. The properties we chose to focus on, as well as a brief description of each, are listed below in Table 3-1. We were especially interested in the various permeability predictors (QPPMDCK, QPlogBB). As in vitro and in vivo models of BBB permeability are cost prohibitive to run in a HTS manner for most academic groups, we relied on the predicted values from QikProp to guide us in terms of permeability measurements. In addition, we were also interested in the ability to predict toxicity issues, such as the blockage of HERG (human ether-a-go-go-related) K+ channels. Drugs which interfere with this voltage-gated K+ channel can cause potentially fatal cardiac side effects, including TpD. This has led to several drugs being pulled off the market, such as the antipsychotic sertindole.[88] Also, HERG blockage is a major cause of drug development delays, delays in approval, and in some cases removal from the market or black box warnings.[89] Patch-clamp assays to measure HERG blockage are complex and expensive,[90] therefore accurate in silico methods to predict possible HERG interference are quite useful.

Another interesting pharmacokinetic parameter evaluated was the rate of protein binding.

Excessive binding to human serum albumin (HSA) can lead to drug safety issues, and more importantly in our case, decreased brain penetration.[91] Since only free/unbound drug is able to passively diffuse across the BBB, a higher rate of HSA binding by a drug reduces the concentration of free drug available to cross the BBB. Evaluation of the QPlogKhsa values could give us valuable insight into possible causes of the lack of brain penetration.

Property of Descriptor	Description	Range/Recommended Values
#stars	Number of property or descriptor values that fall outside the 95% range of similar values for known drugs. A large number of stars indicates that a drug is less drug-like that molecules with fewer start.	0-5
CNS	Predicted CNS activity on a -2 (inactive) to +2 (active) scale.	-2 - +2
QPlogHERG	Predicted IC50 value for the blockage of HERG K+ channels.	Concern below -5
QPPCaco	Predicted Caco-2 cell permeability. Caco-2 cells are a model for the gut-blood barrier.	<25 poor, >500 great
OPlogBB	Predicted brain/blood partition coefficient.	-3.0 – 1.2
QPPMDCK	Predicted apparent MDCK cell permeability. MDCK cells are considered a good mimic for the blood-brain barrier.	<25 poor, >500 great
QPlogKhsa	Prediction of binding to human serum albumin.	-1.5 – 1.5
RuleOfFive	Number of violations of Lipinski's rule of five.	Maximum is 5.

Table 3-1 QikProp properties and descriptors.

QikProp analysis results

Initially we considered the overall predicted CNS activity, which QikProp evaluates on a -2 to +2 scale. This value is calculated by compiling multiple other calculated properties and evaluating them against a test set of known CNS compounds and their physicochemical properties. The higher the number the better, thus a result of +2 would equate to a drug that had a high probability of being CNS active, and -2 would be a drug that was not likely CNS active. Our best predicted value was a 0. The range was 0 to -2. This was not surprising as the polar nature of the aplysinopsin scaffold makes it an unlikely candidate to cross the BBB and be CNS active, as we observed with our first set of lead compounds in in vivo studies. However, we used these values as a tool to exclude some compound for further consideration. Going forward we focused on compounds with a CNS values of 0 or -1. For clarity, each property or descriptor discussed will now be done based on the area of the aplysinopsin which is modified as show in Figure 3-2, with group 1 being those substituted on the indole moiety, group 2 those substituted on the indole nitrogen, and group 3 being modifications of the substitution pattern on the imidazolidinone ring.

It should be noted that we observed little change in the overall properties with any of the substitutions made to the imidazolidinone ring. In fact, the highest/best values were when the imidazolidinone was dimethylated, as in compound **28**. For ease of discussion, it should be assumed that unless noted otherwise, all compounds are alkylated at R2 and R4.

Next, we examined several permeability factors. We were most interested in those permeability measurements that concerned CNS activity: QPlogBB and QPPMDCK. QPlogBB is a measure of the predicted blood/brain partition coefficient, so the larger the number the better

chance that the drug would have a higher concentration in the brain vs. the blood. The QPPMDCK is the predicted MDCK cell permeability. MDCK (Madin-Darby canine kidney) cells are widely used as models for the cerebral endothelial cells that make up the BBB due to their similar cell structures, which includes tight junctions.[92]

For QPPMDCK, we observed a range of values from 6.842 all the way to 7687.354. QikProp defines a score of <25 as being poor and >500 as being good. The 7687.354 value was an outlier, as most of our values were in the range of 200-1500, with our statistical average being a value of 944. In terms of group 1 modifications (those made to the indole ring), we observed that the addition of polar groups (for example hydroxy groups) resulted in a drastic decrease in QPPMDCK values. This should not be surprising, as the endogenous ligand serotonin, with its 5-hydroxy group, is not able to cross the BBB itself. The two best QPPMDCK values for group 1 compounds were from the 5-methoxyaplysinopsin analog (**89**) which had a QPPMDCK value of 563.564, and 5-fluoroaplysinopsin analog (**88**), with QPPMDCK value of 967.232. Compared to other halogen substituted analogs, the fluoro-substituted analog had the best QPPMDCK value, perhaps due to its smaller size compared to other halogens, thus reducing the overall bulk of the molecule.

Examining the QPPMDCK values for group 2 analogs (those substituted at the indole nitrogen), the best values were observed for the *N*-benzylaplysinopsin analogs (**81-85**). On average, these five analogs had a QPPMDCK value of 1829. The highest values were found with the *para*-chloro-*N*-benzyl analog (2637) and the *para*-nitro-*N*-benzyl analog (1938). Looking at similarly substituted analogs, the *N*-phenyl substituted analogs had substantially lower values. For example, the *para*-cyano-*N*-phenyl analog had a QPPMDCK value of 189.

Other groups examined included chloromethyl and chloroethyl substituted analogs, as well as methylamino analogs. All of these exhibited lower QPPMDCK values than the *N*-benzyl analogs.

Next we examined the QPlogBB values, which are representative of the steady state distribution of a compound between the brain tissue and plasma. We found an average value of -0.7969. It is somewhat difficult to discuss negative values being "positive," however, compounds with great BBB penetration profiles often have negative logBB values, for example the logBB value of caffeine is -0.219. With that in mind, we examined compounds with values > -1. Using that number as a threshold we essentially cut our library in half. The range of values was from -2.453 to 0.086, with an average of -0.7969.

Looking at group 1 substations (on the indole moiety), we observed some of the lowest values. Similar to the QPPMDCK values, addition of polar groups to the indole moiety drastically lowers the QPlogBB values. In general, all of the proposed new analogs substituted on the indole moiety scored relatively low compared to other analogs. We did observe that some of our higher values obtained for this value were done with analogs from the first library of compounds (**30-80**), suggesting that the halogenation of the indole moiety can improve this QPlogBB value.

In regards to substitutions at the nitrogen atom of the indole, many of the same trends for QPlogBB values were observed as with the QPPMDCK values. The *N*-benzyl series of analogs provided some of the highest values, with *para*-chloro-*N*- benzyl scoring -0.281, a value similar to that of the aforementioned caffeine. The *N*-methylaplysinopsin analog also scored well, with a QPlogBB value of -0.299. We observed a limited SAR of this type of substitution, with a

decreased QPlogBB value as the *N*-alkyl chain was lengthened to *N*-ethyl (-0.371) and *N*-propyl (-0.452).

As mentioned previously, our primary motivation for using this ADME calculator was to be able to assess permeability issues while using a rational approach in the design of our next series of compounds. After reviewing the data generated by QikProp a "short list" of 50 compounds was assembled based on positive permeability data. Beyond the permeability data, we were also looking at several other properties. First, were the basic Rule of Five properties as discussed earlier. We did not observe frequent violations of these five rules, likely due to the fact that while designing possible compounds for the QikProp assay, we did not propose molecules that had blatant violations of any of the rules. However, there were a few proposed structures that violated at least one rule. In most cases, this was due to a molecular weight over 500 or a LogP > 5.

We were also interested in examining the potential for excessive HSA binding, which can lead to dramatic decreases in the amount of free/unbound drug in circulation. QPlogKhsa values for our library ranged from -0.688 to 0.884, with an average of 0.447. For reference, it is useful to know that many antidepressants used in the clinic today have relatively higher logKhsa values, for example imipramine has a logKhsa of 0.75. The antidepressants trifluprom azine and chlorpromazine have logKhsa values of 1.05 and 1.1, respectively. Looking at the groups that had positive permeability values, the previously discussed *N*-benzyl analogs had similar values to those of the current antidepressant drugs, with an average of 0.7994 among that subset of proposed analogs. The lowest values were for analogs which had polar substituents on the indole ring (e.g. –OH) and halogenation at all positions (4, 5, 6, 7) of the indole ring as well.

Concerning the predicted HERG K+ channel blockage IC_{50} values, we found a very small variation in values across all compounds examined. The entire library of compounds only covered the range of -6.004 to -4.26, with an average of -4.9787. QikProp notes that a QPlogHERG below -5 should be a concern. As mentioned previously, HERG K+ blockage by the pharmaceutical sertindole caused Long QT syndrome, a heart rhythm disorder that results in fast, chaotic heartbeats. These side effects have prevented it from being approved by the FDA in the US. Based on the structural similarity between sertindole and the aplysinopsin scaffold, values at or below -5 are not surprising. If the aplysinopsin scaffold should advance further in clinical development these concerns would definitely need to be further evaluated and addressed properly.

Considering all of the above data, the synthetic feasibility of each potential group of analogs was assessed. Based on that data, three groups of analogs were selected for synthesis in order to further evaluate in in vitro and in vivo assay systems. These 12 compounds are shown in Figure 3-3. The highlighted QikProp values for each of the proposed analogs are shown in Table 3-2.

CMPD	CNS	MW	QPlogHERG	QPPCaco	QPlogBB	QPPMDCK	QPlogKhsa	RuleOfFive
81	0	344.415	-6.011	2030.987	-0.442	1064.008	0.715	0
82	0	378.86	-5.938	2038.425	-0.281	2637.092	0.833	1
83	0	378.86	-6.08	1786.328	-0.409	1635.765	0.817	0
84	0	389.4073	-5.419	2131.378	-0.301	1938.391	0.821	0
85	0	289.4073	-5.252	2045.582	-0.354	1872.032	0.811	0
86	0	279.2966	-4.83	940.391	-0.62	639.294	0.141	0
87	-1	296.328	-4.951	706.915	-0.751	340.043	-0.21	0
88	0	272.281	-4.668	1074.116	-0.417	967.232	0.034	0
89	0	284.317	-4.628	1128.129	-0.575	563.564	0.016	0
90	0	268.318	-4.859	1949.152	-0.299	1017.745	0.204	0
91	0	282.344	-4.954	1963.825	-0.371	1026.029	0.306	0
92	0	296.371	-5.171	1972.863	-0.452	1031.133	0.423	0

Table 3-2 Selected QikProp values for compounds 81-92

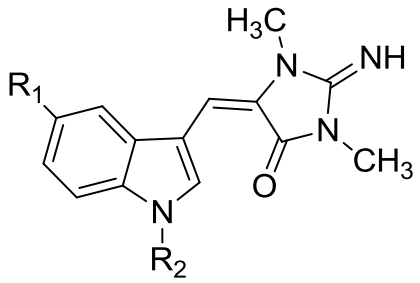

Compound	R1	R2	Compound	R1	R2
81	H	H	87	H	$COCH_3$
82	H	*p*-Cl	88	F	H
83	H	*o*-Cl	89	OCH_3	H
84	H	*p*-NO2	90	H	CH_3
85	H	*o*-NO2	91	H	CH_2CH_3
86	CN	H	92	H	$CH_2CH_2CH_3$

Figure 3-3 Structures of proposed new library of aplysinopsin analogs

Metabolic stability of aplysinopsins

While concurrently evaluating a new library of analogs in the QikProp ADME prediction program, we also assessed the in vitro metabolic stability of aplysinopsins. Compound **53** was evaluated in an in vitro stability study and metabolism profiling assay. Metabolism greatly influences the bioavailability of a drug. Rapid metabolism is a common cause of failure of a drug to reach sufficient concentrations at the target tissue. Metabolism can be divided into two phases: phase I and phase II. For this study, focus will be on phase I, where drugs are subjected to oxidation by the CYP superfamily of enzymes. These enzymes are responsible for the metabolism of the majority of marketed drugs.[93] Liver microsomes (in our case, rat microsomes) are commonly used to evaluate phase I metabolism. Using this in vitro system, intrinsic hepatic

clearance (CL_{int}) and metabolic half-life ($T_{1/2}$) were determined. In addition, any major metabolites produced are able to be evaluated. This may give direction in terms of telling which part of the structure is undergoing metabolism, therefore we can make structural modifications to reduce the susceptibility of a compound to metabolic turn-over if necessary.

Results of microsomal stability study

To determine the intrinsic rate of clearance (CL_{int}) and metabolic half-life ($T_{1/2}$), compound **53** was incubated with rat liver microsomes with appropriate cofactors (NADPH), and the level of the parent compound remaining was monitored at multiple time points. The results for CL_{int} and $T_{1/2}$ are shown below in Figure 3-4. In general a CL_{int} of <40 μL/min/mg is considered ideal.[94] Compound **53**'s rate of clearance of 23 μL/min/mg is well below that threshold. Concerning half-life values, our $T_{1/2}$ value of 61 minutes is good, as the longer the half-life the better. Compound **53**'s $T_{1/2}$ is comparable to that of imipramine (66 minutes), which is used as the control in the chick/anxiety depression model we use to evaluate our compounds. In addition, diazepam, which is used to treat anxiety and panic attacks, has a $T_{1/2}$ of 54 minutes. Thus, there is nothing about the observed CL_{int} or $T_{1/2}$ values that would indicate that microsomal stability problems are the cause of aplysinopsins' poor bioavailability. Despite compound **53**'s extended $T_{1/2}$ there was one primary metabolite detected during GC/MS analysis using Metabolynx software from Waters. The metabolite, with MW difference of +16, was determined to be the result of an oxidation of the indole ring. See Figure 3-5.

Compound	Incubation conc (μM)	Species	NADPH-dependent Clint (μl min^{-1} mg^{-1})	NADPH-dependent $T_{1/2}$ (min)	NADPH free incubation
Aplysinopsin	5.0	Rat	23	61	No metabolism observed at 60 min

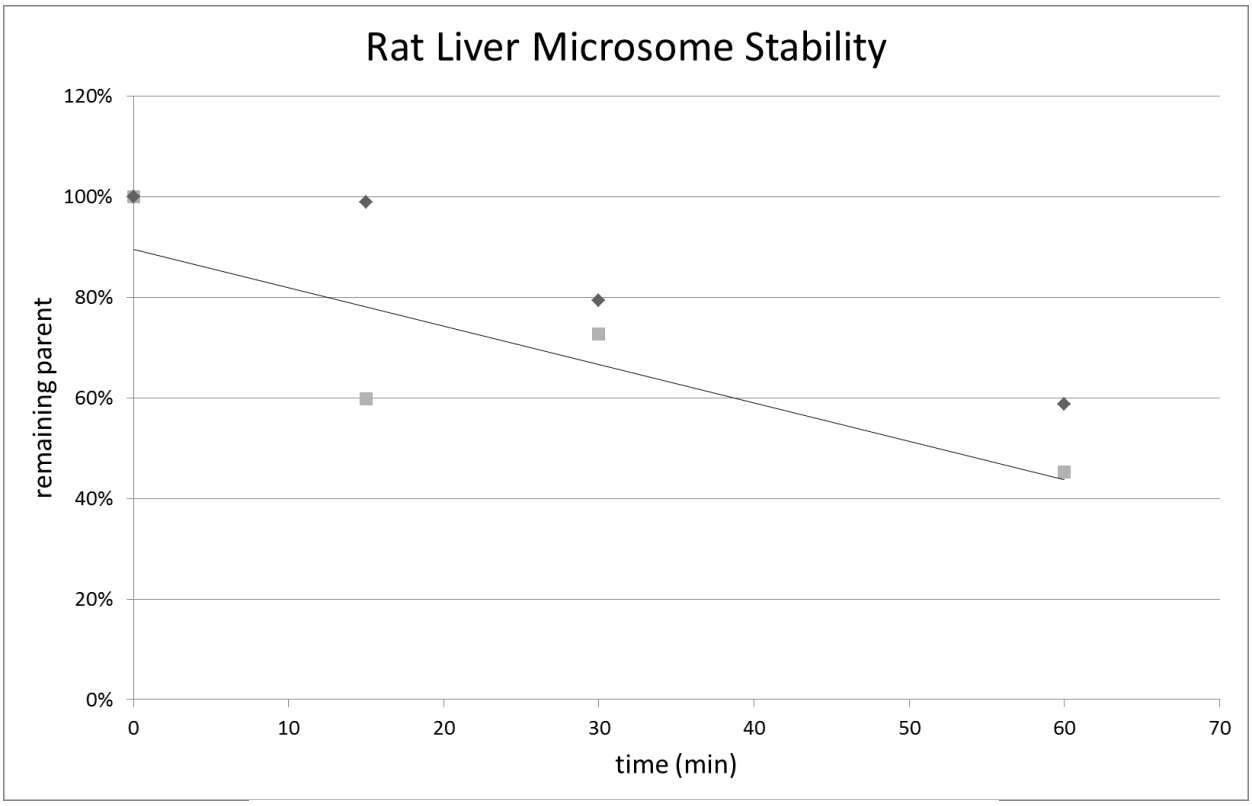

Time (min)	Parent % (1)	Parent % (2)	Average
0	100%	100%	100%
15	60%	99%	79%
30	73%	79%	76%
60	45%	59%	52%

Figure 3-4 Evaluation of the microsomal stability of compound 53

m/z	Retention time (min)	MW difference	Daughter ions detected
333	4.3	parent	318, 234, 197, 170, 155
349	3.7, 3.8	+16	334, 250, 186, 171

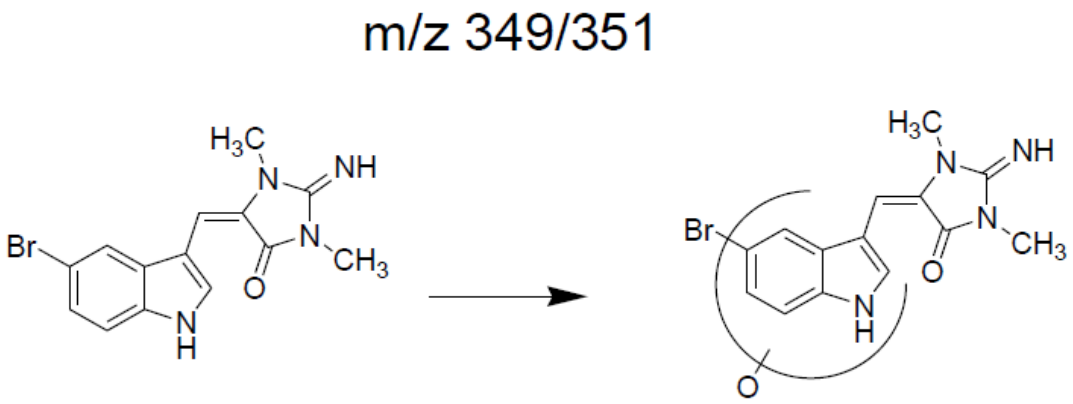

Figure 3-5 Metabolite structural hypothesis

Synthesis of second generation aplysinopsin analogs

Following analysis of results obtained with QikProp and evaluation of the metabolism of aplysinopsins, that data was used to select a new library of analogs to synthesize. The library can be sub-divided into three basic groups: *N*-benzyl analogs (**81**-**85**), analogs which are substituted on the indole moiety (**86**, **88**, and **89**), and analogs which are substituted on the nitrogen of the indole moiety (**87**, **90-92**). The general strategy for the synthesis is similar to the previous work, with the synthesis of the 3-formylindole with the appropriate substitution first. This is then followed by condensation of the 3-formylindoles with the imidazolidinone **28**.

Synthesis of *N*-benzyl analogs (81-85)

Initial efforts towards the synthesis of the *N*-benzyl aplysinopsin analogs focused on the use of phase-transfer catalytic (PTC) conditions to introduce the benzyl group to 3-formylindole, followed by the use of microwave irradiation for the condensation step (see Figure 3-6 and Figure 3-7).[95] The catalyst used was triethyl benzyl ammonium chloride (TEBA). Using this method the *N*-benzyl-3-formylindoles were obtained in moderate yields (~50%), which was much lower than the previously reported 90% yields using this methodology. Furthermore, the use of microwave irradiation for the condensation of *N*-benzyl-3-formylindoles with imidazolidinone **28** was much less efficient than previous methods used for the condensation reaction. Considering these lower yields, an alternative approach for the synthesis of the *N*-benzyl analogs was sought. A report from Ottoni et al. suggested that the *N*-benzyl-3-formylindoles could be obtained in high (>90%) yields and in short reaction times with facile workup conditions.[96] This method uses a mild base (NaOH) and treatment of 3-formylindole with the appropriate benzyl bromide in acetone. Upon addition of the benzyl bromide, a precipitate forms almost immediately, which is filtered off and the solution concentrated to yield the targeted N-benzyl-3-formylindoles, which can be used without further purification.

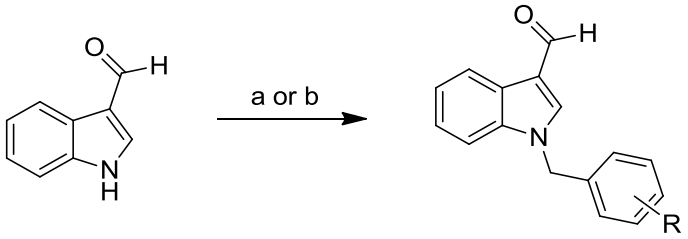

Reagents and conditions: (a) appropriate benzyl bromide, NaOH, CH_2Cl_2, TEBA,2H; (b) KOH (EtOH); acetone, appropriate benzyl bromide.

Figure 3-6 Synthesis of *N*-benzyl-3-formylindole intermediates

As mentioned, the microwave irradiation method for the condensation was quite inefficient, with yields lower than 30%. Using the previous condensation method of Djura and Faulkner also produced low yields and significant decomposition of the *N*-benzyl starting materials. Following this, several acid and base catalyzed condensation conditions were utilized, all with equally low yields. The method of Boyd and Sperry,[97] which used ethylene glycol as the solvent (see Figure 3-7), was successful in produced a high yield condensation step. Their report also cites high rates of decomposition of starting materials, which they suggest is due to the instability of the starting material to the presence of acid or base at high temperatures. In seeking a neutral reaction solvent, ethylene glycol was used and led to a successful condensation reaction. Using the same solvent system produced the targeted products in moderate yields (~70%).

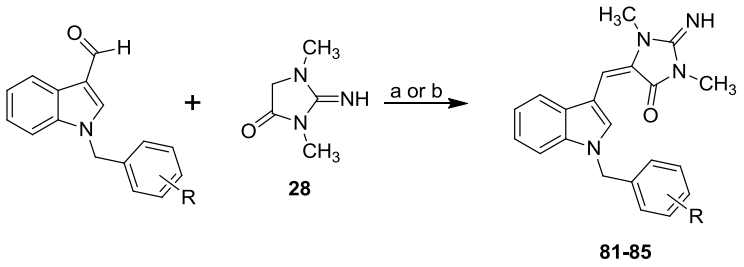

Compound	R
81	H
82	*p*-Cl
83	*o*-Cl
84	*p*-NO_2
85	*o*-NO_2

Reagents and conditions: (a) ethylene glycol, 130°, 4h;
(b) sodium acetate, acetic acid, microwave irradiation, 60s

Figure 3-7 Condensation of *N*-benzylaplysinopsin analogs 81-85

Synthesis of analogs substituted on the indole moiety

Compounds **86**, **88**, and **89** were synthesized using commercially available appropriately substituted 3-formylindoles (see Figure 3-8). Using the method of Djura and Faulkner[28], condensation was carried out between the 3-formylindoles and the imidazolidinone **28** to yield the desired target substituted aplysinopsin analogs.

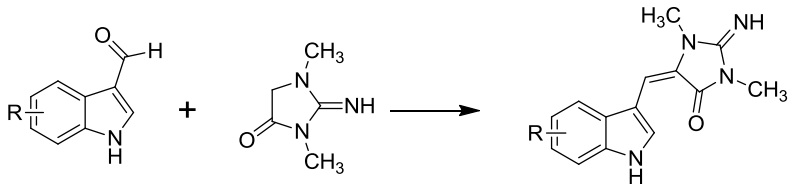

Compound	R
86	5-CN
88	5-F
89	5-OMe

Figure 3-8 Synthesis of compounds 86, 88, and 89

Synthesis of analogs substituted at the indole nitrogen

Compounds **90-92** were synthesized via alkylation of the nitrogen of the indole, using the appropriate alkyl iodides in DMSO (see Figure 3-9). The *N*-substituted 3-formylindole intermediates were obtained in the crystalline form and then subjected to the condensation conditions, making use of ethylene glycol as the solvent. Compound **87**, the *N*-acetyl aplysinopsin analog, was prepared using commercially available *N*-acetyl-3-formylindole, which was then subjected to condensation conditions.

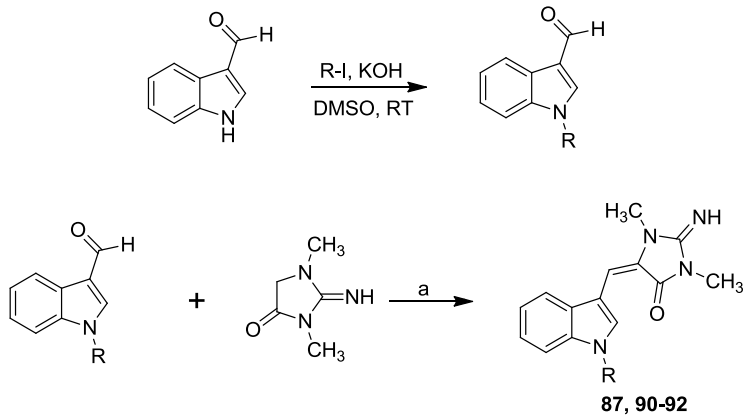

Compound	R
87	$-COCH_3$
90	$-CH_3$
91	$-CH_2CH_3$
92	$-CH_2CH_2CH_3$

Reagents and conditions: (a) ethylene glycol, 130°, 4h

Figure 3-9 Synthesis of compounds 87 and 90-92.

In vitro serotonin receptor binding

The series of new analogs (**81-92**) were evaluated in the NIMH PDSP at UNC-Chapel Hill. They were evaluated for their serotonin receptor affinity, as well as their affinity for 34 other CNS receptors (see Table 2-1). As before, they were initially evaluated in a primary radio ligand binding assay, and hits which possessed inhibition > 50% in the primary assay were evaluated in a secondary assay to determine their K_i values. A summary of these results is shown below in Table 3-3.

Cmpd	Binding affinity (K_i nM ± S.D.)				
	5-HT_{2A}	5-HT_{2B}	5-HT_{2C}	5-HT_3	KOR
81		1,282	3,849		
82		900		539	384
83		787	493	247	932
84		1,067		344	666
85					2,058
86					
87					
88					1,195
89					2,405
90					
91	7,883	1,782	1,632		
92		3,272			

Table 3-3 Selected CNS receptor in vitro binding affinities for compounds 81-92.

Compounds **81** through **85** represent the N-benzylaplysinopsin derivatives. Most of the activity was contained in this group of five analogs. Moderate activity at serotonin receptor subtypes 5-HT_{2B} and 5-HT_{2C} was observed. These analogs, however, did not possess the in vitro potency of the leads from the first library (see Table 2-3). The most active compound in terms of 5-HT_2 affinity, was compound **83**, the *N-ortho*-chlorobenzyl-aplysinopsin analog. It showed moderate affinity for both 5-HT_{2B} (787 nM) and 5-HT_{2C} (247 nM). (See Figure 3-10)

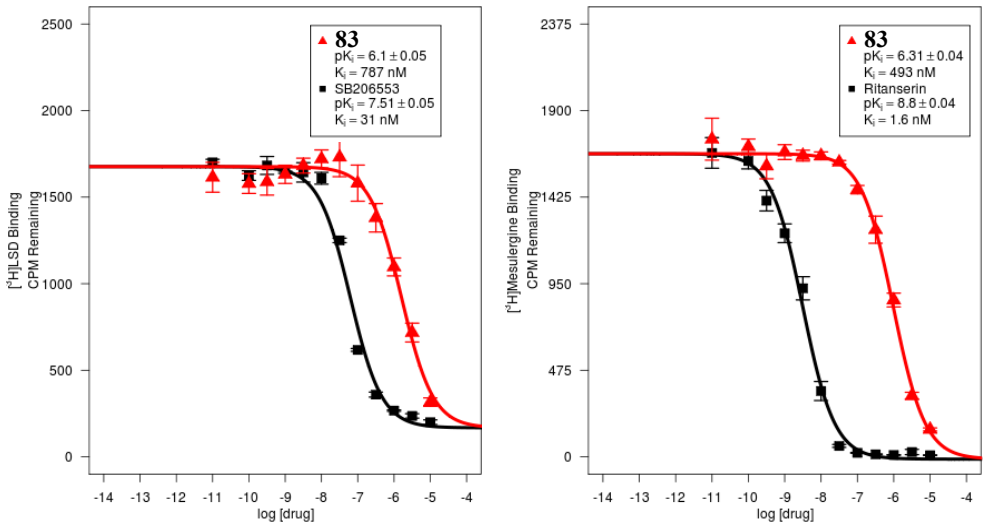

Figure 3-10 Binding affinity graphs for compound 83 positive controls towards 5-HT$_{2B}$ and 5-HT$_{2C}$ receptors.

An interesting note is the activity of these compounds at the 5-HT$_3$ receptor, as well as the κ-opioid receptor. The activity at 5-HT$_3$ is especially interesting, as aplysinopsins have never been reported to possess activity at this serotonin receptor subtype. Furthermore, unlike all of the other serotonin receptor subtypes which are G-protein coupled receptors, 5-HT$_3$ is a ligand-gated ion channel receptor. The 5-HT$_3$ receptor subtype, like other serotonin subtypes, has been implicated in multiple CNS disorders.[98] However, it has also received significant attention from the pharmaceutical industry due to the ability of 5-HT$_3$ antagonists to suppress chemotherapy- and radiotherapy-induced vomiting.[99] Three of the *N*-benzyl analogs showed nanomolar level affinity for the 5-HT3 receptor subtype, with the two most potent being compound **83**: *ortho*-Cl (247 nM) and compound **84**: *para*-NO_2 (344 nM). See Figure 3-11.

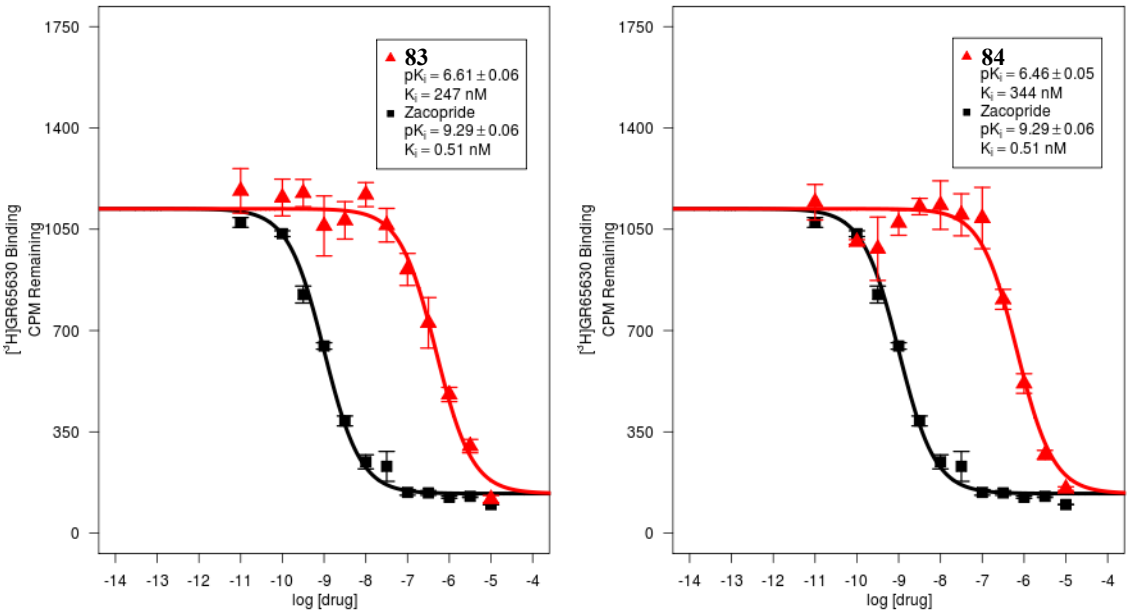

Figure 3-11 Binding affinity graphs for compounds 83, 84, and positive controls towards 5-HT3.

This is also the first report of aplysinopsins possessing affinity for the kappa opioid receptor (KOR). The KOR system has drawn considerable attention from researchers who are interested in its possible analgesic properties. Furthermore, researchers are especially interested in possible opioid receptor ligands which may have better side effect profiles than the mu opioid receptor agonists, such as morphine. Previous efforts to use KOR agonists as analgesics have been slowed by their side effect profiles, which often includes sedation and dysphoria. Recently, research has shifted its focus on possibly targeting the KOR in the peripheral nervous system, with a view of avoiding some of these unwanted side effects.[100] In a recent report, Bruchas et al. describe how the kappa opioid receptor system may be implicated in regulating the serotonin system in the brain via p38 mitogen-activated protein kinase (p38 MAPK).[101] Compounds **82-84** showed nanomolar level affinity for the κ-opioid receptor (see Figure 3-12). It is important to note that none of these compounds showed significant affinity for any of the other opioid

receptor subtypes.

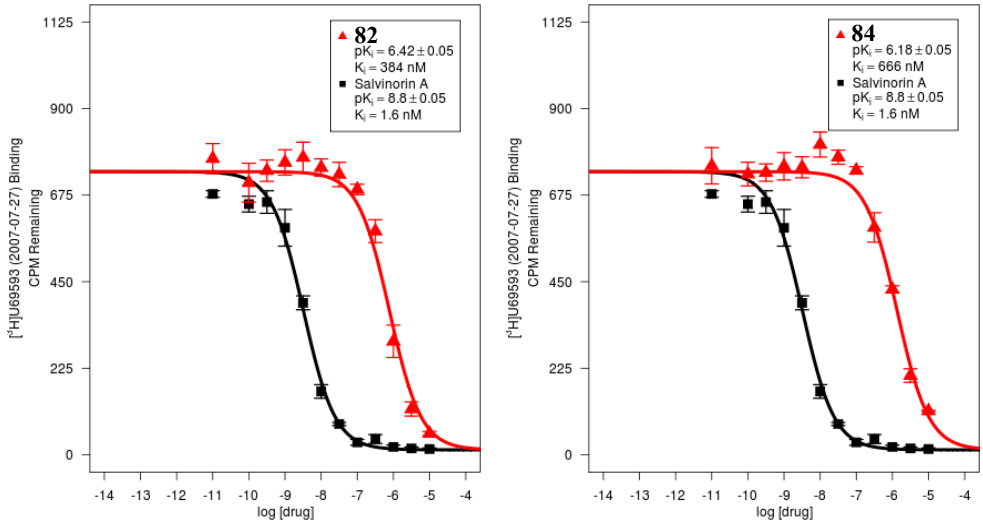

Figure 3-12 Binding affinity graphs for compounds 82, 84, and positive controls towards KOR.

In vitro inhibition of MAO isoforms A and B

Compounds **81-92** were also evaluated for their MAO-A and MAO-B inhibitory activities (see Table 3-4). Compared to the first library of compounds analyzed (see Table 2-4), less potent overall inhibitory activities were observed. Once again, compounds were selective for MAO-A over MAO-B, except for three compounds (**82**, **84**, and **85**), which were selective for MAO-B.

Compound	MAO-A	MAO-B	SI[a]
	IC_{50} (μM)	IC_{50} (μM)	
81	41.811 ± 9.49	>100	2.39
82	21.193 ± 0.15	1.02 ± 0.31	0.04
83	2.154 ± 0.13	8.25 ± 0.07	3.83
84	1.114 ± 0.12	0.48 ± 0.09	0.43
85	8.165 ± 0.59	5.64 ± 0.70	0.69
86	2.880 ± 0.08	41.60 ± 0.27	14.44
87	1.685 ± 0.10	84.16 ± 2.46	49.95
88	0.204 ± 0.01	20.34 ± 3.65	99.71
89	0.547 ± 0.04	29.16 ± 1.44	53.31
90	29.864 ± 1.01	>100	3.34
91	16.023 ± 1.37	65.84 ± 3.87	4.11
92	12.613 ± 0.27	41.30 ± 0.67	3.27
Clorgylin	0.003 ± 0.0004	-	
Deprenyl	-	0.08 ± 0.02	

[a]The relative selectivity for MAO-A is defined by the ratio of IC_{50} (MAO-B)/IC_{50} (MAO-A) for each compound.

Table 3-4 Aplysinopsin analogs 81 - 92 tested for inhibition of human MAO-A and MAO-B activities.

The most active compounds at MAO-A, **88** and **89**, were similar to the previous library of aplysinopsin analogs, with substitutions at C-5. Reviewing the MAO inhibitory activities of the N-benzylaplysinopsin derivatives (**81** – **85**) reveals that overall these compounds were not very potent. This group did yield the three aforementioned compounds which were more selective for MAO-B over MAO-A. This is unique, as only one compound of the first series of 50 analogs (**76**) was selective for MAO-B over MAO-A. There are no significant structural similarities between these compounds and compound **76** other than their being unsubstituted on the indole ring. Compound **84** was the most potent and selective MAO-B inhibitor out of both sets of analogs. There were other compounds which possessed lower IC_{50} values for MAO-B than compound **84**, however, they were all even more potent inhibitors of MAO-A. For example, compound **54** had an IC_{50} of 0.447 μM for MAO-B, but also had a 0.0056 μM IC_{50} value for

MAO-A.

Compounds **86**, **88**, and **89** closely resembled the first library of analogs. They were substituted at C-5 with cyano, fluoro, and methoxy groups, respectively. Compounds **88** and **89** were especially active, with IC_{50} values in the low micromolar range. These compounds also displayed significant selectivity for MAO-A over MAO-B, with SI's of 99 and 54, respectively.

Compounds **87** and **90-92** were all substituted at the indole nitrogen atom. They were all selective for MAO-A over MAO-B. Compound **87**, the N-acetyl derivative, was especially selective for MAO-A, with an SI of 50. Among the N-alkyl analogs, we observed that the longer the length of the alkyl chain, the more potent inhibitor of MAO-A the compounds were, with the N-propyl analog possessing the lowest IC_{50} of 12.61 μM.

Assessment of MDR-1 efflux pump susceptibility

Efflux pumps are a major obstacle in BBB penetration. Efflux of a drug out of the brain by the MDR-1 efflux pump could be a cause for the poor in vivo efficacy of lead compounds. Based on this we sought to evaluate the interaction of aplysinopsin analogs with the MDR-1 efflux pump. This was done in collaboration with the PDSP at UNC-Chapel Hill. They have developed a live cell assay that allows measurement of the interaction of compounds with the MDR-1 transporter. It is a fluorescence-based assay that is performed in Caco-2 cells (see Figure 3-13). Briefly, the assay is based on the ability of MDR-1 to transport calcein acetoxymethyl ester (calcein-AM) out of cells, but not the free form of calcein. Calcein-AM is able to passively diffuse into Caco-2 cells, where an esterase can then hydrolyze calcein-AM to calcein, which is unable to be pumped out. This calcein molecule is highly fluorescent, whereas calcein-AM is not. Thus, if an assayed compound is subjected to efflux from the cell via MDR-

1, it will compete with calcein-AM for MDR-1, thus it will lower the amount of calcein-AM pumped out, and result in a higher rate of conversion of calcein-AM to calcein, and subsequently increased fluorescence. Hence, the more the compound interacts with MDR-1, the higher the increase in fluorescence.

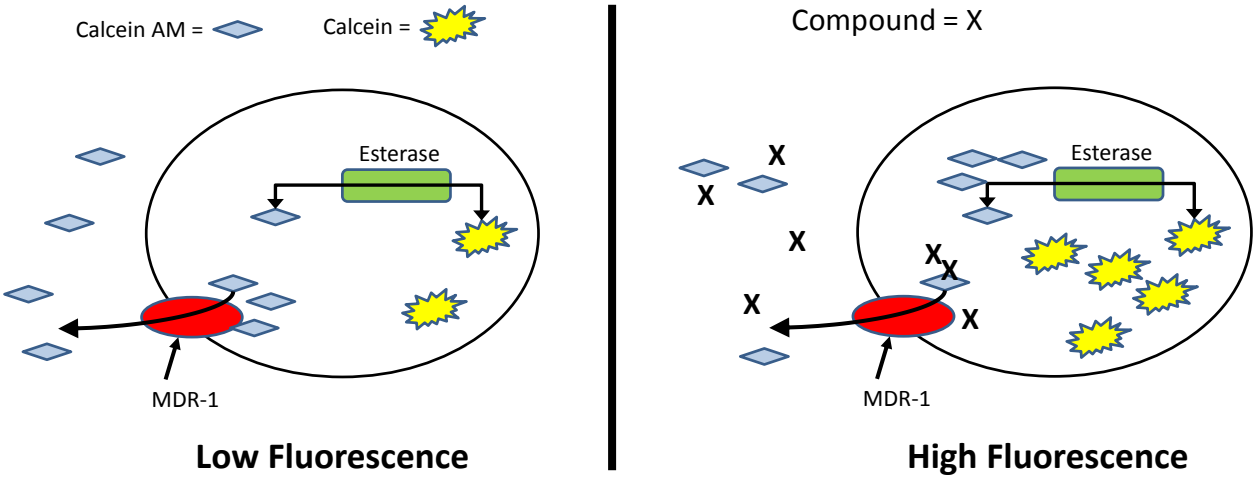

Figure 3-13 MDR-1 susceptibility assay

Ten analogs were initially assayed for their MDR-1 susceptibility, however, problems establishing statistically relevant signal windows with control compounds have slowed the work, and some of the results are still pending. Preliminary results for three of the 10 compounds (compounds **83**, **88**, and **89**) are known of November 24, 2013, there are still some questions regarding the statistical significance of these results, but they are presented here because they provide valuable preliminary insights into the possible MDR-1 susceptibility of aplysinopsins. Re-testing of these three, and testing of the other seven compounds is to be undertaken pending the reestablishment of the correct assay parameters.

The results of each compound tested are shown below in Figure 3-14. Ideally the positive control cyclosporin A, a known MDR-1 inhibitor, shows a large increase in

fluorescence, however, as you can see in Figure 3-14 we only observed a marginal increase in fluorescence in cells treated with cyclosporin A. This limited signal window from the positive control makes it difficult to make firm conclusions regarding the percentage increase in fluorescence due to our compounds. However, it should be noted that based on the small signal window available none of the three compounds evaluated showed a significant increase in fluorescence, indicating that they would not be MDR-1 substrates.

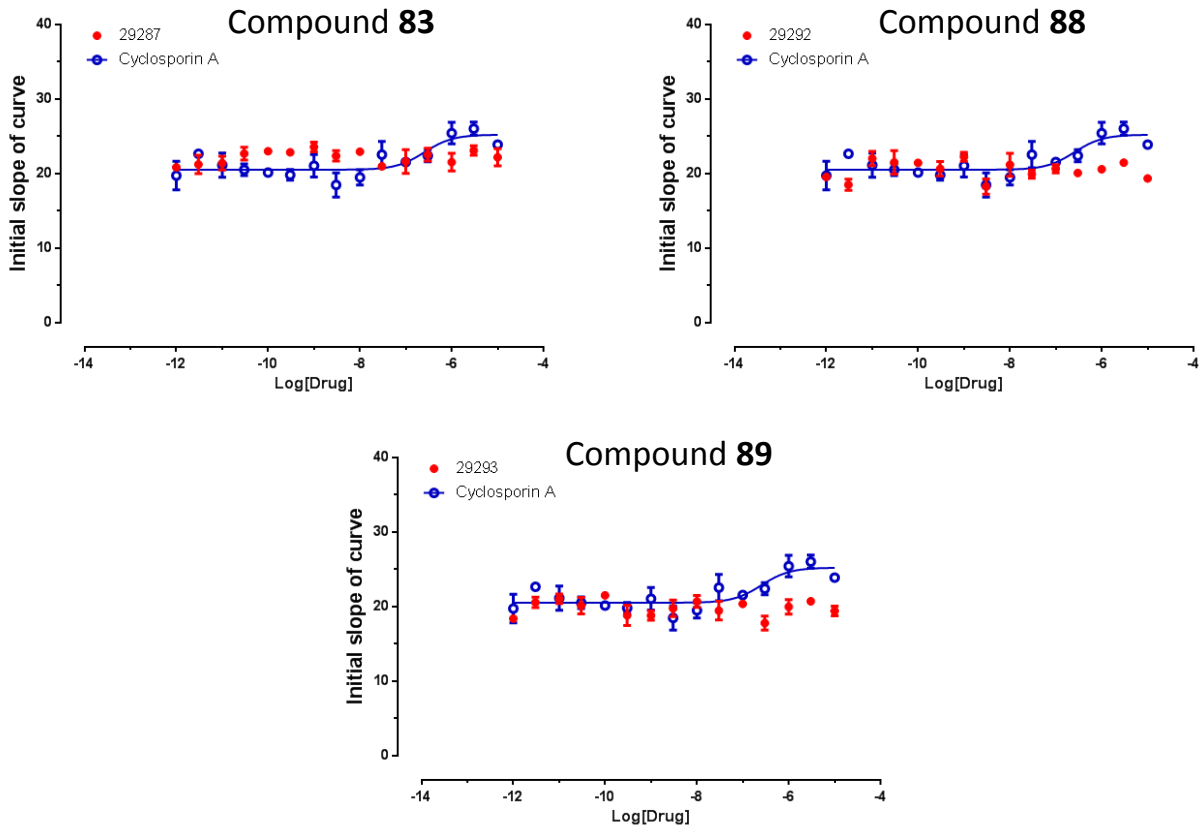

Figure 3-14 MDR-1 susceptibility of compounds 83, 88, and 89.

In vivo evaluation of second generation lead compounds

Based on the in vitro binding data and information from the MDR-1 assay and metabolic stability assays, three new lead compounds were evaluated in the chick anxiety-depression model to assess their potential anti-depressant activities. For background and detailed experimental methodology please see Chapter 2.

Compounds (**83**, **88**, and **89**) were evaluated in this round of in vivo testing. Compound **83** was chosen based on it the fact that it was the most potent 5-HT ligand from the second group of analogs, with a Ki of 493 nM for 5-HT_{2C}. Compounds **88** and **89** were potent and selective inhibitors of MAO isoform A, with IC50 values of 0.204 μM and 0.547 μM, respectively. In addition, both were highly selective for MAO-A over MAO-B, with SI values of 99 and 53, respectively.

In addition to new compounds, other aspects of the assay were altered. During this round of testing, evaluation periods were extended from 60 to 90 minutes, to observe antidepressant effects which were missed previously due to delayed onset of effects. Compounds were evaluated at 1, 3, and 10 mg/kg doses for this round of testing and the positive control was imipramine at a dose of 1 mg/kg.

Distress vocalizations rates across the isolation test were compiled into five phases that included the anxiety-like phase (0-3 min) and four quarters of the depression like phase (30-90 min). ANOVAs were performed at each to examine treatment difference of **83**, **88** and **89**. None of the test articles showed significant treatment effects in the anxiety-like phase (data not shown). Further, **88** did not show significant treatment effects during any segment of the depression-like phase (data not shown). However, **83** and **89** show significant treatment effects

in the last 2 and 3 quarters of the depression-like phase, respectively; such differences reflect different onsets of action of these two test articles. For clarity, the data presented below summarize the treatment effects for the final 2 quarters of the depression-like phase (60-90 min).

The effects of imipramine and **83** on DVocs during the depression-like phase are summarized in Figure 3-15.

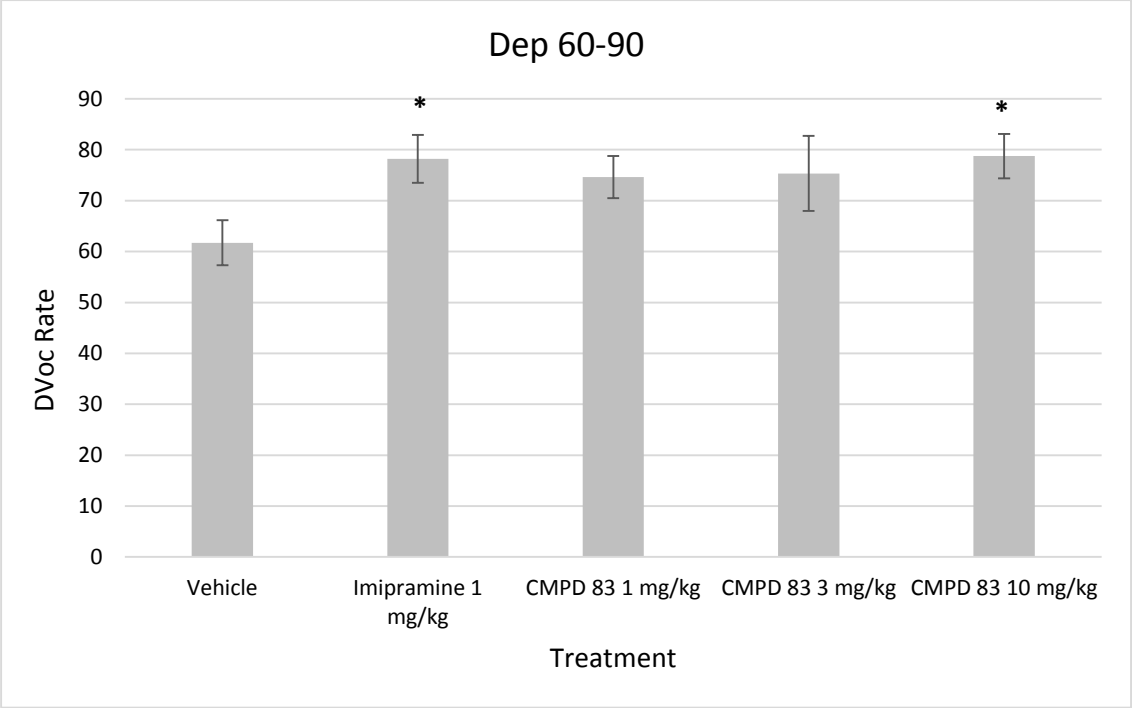

Figure 3-15 The effects of 83 on isolation-induced distress vocalizations (DVocs) for the final 30 min of the isolation period. Values represent mean ±SEM (n= 17-18). * indicates significant increase in DVoc compared with vehicle condition.

Chicks tested in the vehicle condition displayed a DVoc rate of 124 in the anxiety phase that declined to 62 in the depression-like phase illustrating behavioral despair. Imipramine and 10 mg/kg **83** showed anti-depressant activity by attenuating the onset of behavioral despair. A 1-way ANOVA on these data failed to reveal a significant treatment effect, $F_{5, 89}= 1.877$, $p=0.122$. However, planned comparisons using Fisher's LSD analyses revealed that DVocs in the

imipramine and 10 mg/kg **83** groups were significantly higher than the vehicle group ($P < 0.05$).

The effects of 1 mg/kg imipramine and three doses of **89** on DVocs during the depression-like phase are summarized in Figure 3-16. Chicks tested in the vehicle condition displayed a DVoc rate of 118 in the anxiety phase that declined to 50 in the depression-like phase illustrating behavioral despair. Imipramine and all doses of **89** showed anti-depressant activity by attenuating the onset of behavioral despair. Consistent with these observations the 1-way ANOVA on these data approached significance, F=2.107, p=0.087. Further, Fisher's LSD analyses showed that DVocs in the imipramine, and all **89** groups were significantly higher than vehicle ($P < 0.05$).

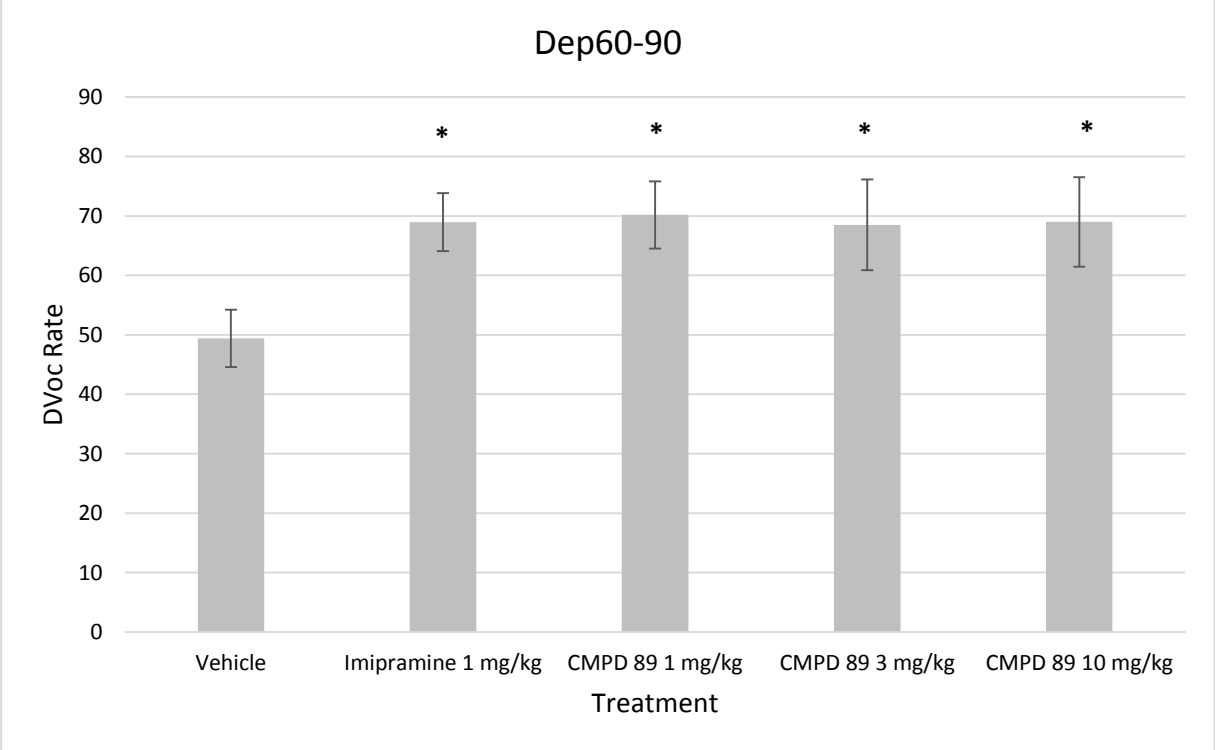

Figure 3-16 The effects of 89 on isolation-induced distress vocalizations (DVocs) for the final 30 min of the isolation period. Values represent mean ±SEM (n = 17-18). * indicates significant increase in DVoc compared with vehicle condition.

Conclusions and discussion

We report the design and synthesis of 12 aplysinopsin analogs which were evaluated for their affinity at 12 serotonin receptors subtypes and 34 other CNS receptors, in addition to inhibitory activity of MAO isoforms A and B. Potential compounds were first evaluated using the QikProp ADME evaluation program. Using this program, several predicted permeability properties of 400 hundred potential analogs were assessed to improve the in vivo efficacy of aplysinopsin analogs. In addition to this in silico analysis of potential analogs, the metabolic stability of compound **53** was evaluated using a rat liver microsomal study. The aplysinopsin scaffold was not especially labile to phase I metabolism, possessing a $T_{1/2}$ of 61 minutes and a Cl_{int} of 23 μL/min/mg. These values are well within the range of other antidepressant drugs, signaling that metabolic stability is not a likely cause of the poor bioavailability of aplysinopsin analogs. Based on in silico and in vitro studies, a second library of twelve aplysinopsin analogs was designed, synthesized, and evaluated for their serotonin and MAO activities. *N*-benzyl aplysinopsin analogs possessed moderate affinity for serotonin receptor subyptes 5-HT_{2B} and 5-HT_{2C}, with the lowest affinity being that of compound **83** for 5-HT_{2C} (K_i = 493 nM). Similar to the first library of analogs analyzed, the most active compounds did not display significant selectivity between 5-HT_2 receptor subtypes, as compound **83** also had a K_i of 787 nM at 5-HT_{2B}. Several *N*-benzyl compounds also exhibited nanomolar level affinity for the 5-HT3 and KOR receptors. This is the first report of such affinities by aplysinopsin analogs.

Previous studies have shown the aplysinopsin scaffold to possess affinity for the 5-HT_2 receptor subfamily.[38, 44] These studies examined the selectivity among serotonin receptor subtypes 5-HT_{2A} and 5-HT_{2C}. It was shown that halogenation of the indole moiety and the

pattern of *N*-alkylations on the imidazolidinone moiety could not only improve K_i values for the 5-HT_2 family of receptors, but could also increase selectivity between subtypes 2A and 2C. The previous evaluations of aplysinopsin analogs' binding affinities for 5-HT_2 subtypes neglected to evaluate the affinity at 5-HT_{2B}. The 5-HT_{2B} subtype is an important subtype to consider when designing drug leads, as it has been known to cause serious cardiovascular side effects.[102] In addition, the 5-HT_2 receptor subfamily shares a highly conserved sequence of over 80% in transmembrane domains. Therefore, it is not surprising that many 5-HT_2 ligands possess high affinities for all three 5-HT_2 receptor subtypes. The current work examined a large library of aplysinopsin analogs (**31-92**), and revealed an overall selectivity for 5-HT_{2B} over 5-HT_{2A} and 5-HT_{2C} subtypes.

This initial expanded SAR study of 50 analogs (**30-80**) confirmed the previous findings that halogenation of the indole moiety could lead to an increase in the binding affinities at serotonin receptors. Whereas previous studies only examined brominations at C-5 and C-6, the current work also considered halogenation of C-4 and C-7, of which C-4 brominated analogs were among the most potent analogs in each group of compounds. In terms of the *N*-alkylation pattern, the results were inconclusive as to the effects on serotonin binding.

During the course of the current work, the first report of the 5-HT_{2B} crystal structure was published by Wacker *et al.*[78] The structure was elucidated with the LSD precursor ergotamine (ERG) bound, as shown in Figure 3-17. This work revealed several key structural features of the 5-HT_{2B} binding pocket which may explain the high affinity aplysinopsins have for this particular serotonin receptor subtype. Of note, the hydrogen bond between threonine (T140) and ERG and the salt bridge formation between the aspartic acid residue (D135) and ERG appear to be

important residues for potential aplysinopsin binding.

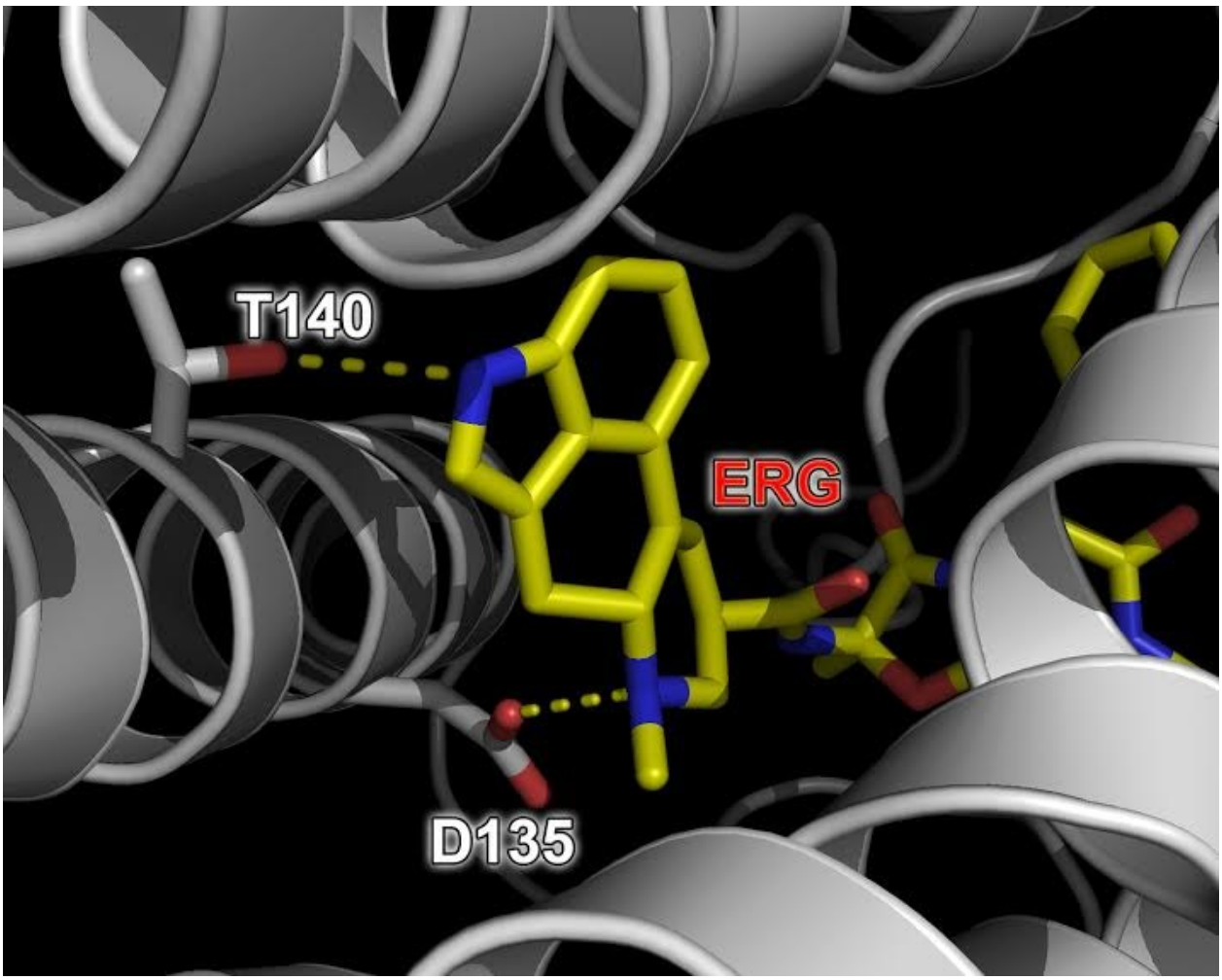

PDB ID: 4IB4

Figure 3-17 Crystal structure of 5-HT$_{2B}$ with ergotamine bound.

A two dimensional depiction of the binding site is shown below in Figure 3-18. Replacing ERG with the aplysinopsin scaffold reveals that the two critical binding residues (T140 and D135) are easily accessible for the aplysinopsin scaffold. This predicted binding model is in agreement with the previous reports that R2 and R4 should be alkylated to increase serotonin receptor affinity. When both R2 and R4 are alkylated, the resulting imine at R3 is easily protonated to allow for the salt bridge formation with D135. This aspartic acid residue is

conserved in all three 5-HT_2 receptor subtypes, possibly explaining the lack of selectivity of aplysinopsin analogs among this subfamily of receptors. This model of binding would also explain the lack of activity seen in analogs **81-85** and **87-92**, all of which are substituted at the indole nitrogen. The loss of the ability to form a hydrogen bond with the T140 residue could explain this loss of serotonin affinity compared to aplysinopsin analogs which are not substituted at the indole nitrogen.

Future studies will explore more in-depth three dimensional docking studies making use of the recently elucidated 5-HT_{2B} structure to determine which structural variations of aplysinopsin analogs are responsible for increasing selectivity among the 5-HT_2 receptor family.

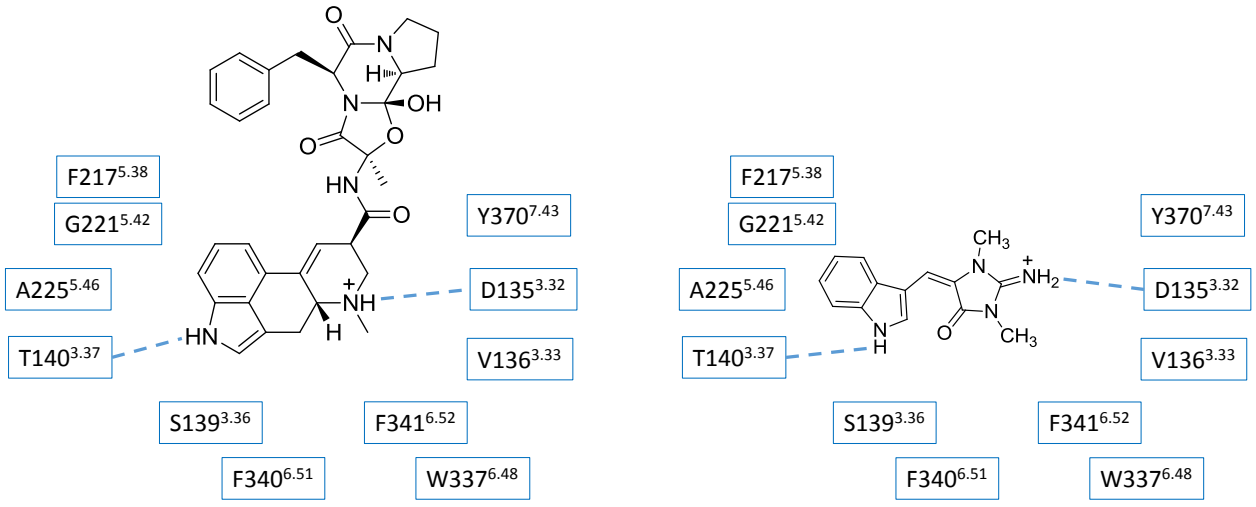

Figure 3-18 Two dimensional representation of ligand interactions in 5-HT2B binding pocket.

The second library of analogs (**81-92**) was also evaluated for its MAO inhibitory activities at isoforms A and B. Analogs substituted at C-5 showed low micromolar level IC_{50} values. Compounds **88** and **89** were the most potent, with IC_{50} values of 0.204 μM and 0.547 μM, respectively. These compounds also displayed high selectivity, with SI values of 99 and 53,

respectively. These results mirrored those seen with the first library of analogs (**30-80**), which showed increased MAO-A inhibitory activity and selectivity when C-5 or C-6 were halogenated. This suggests that substitution at C-5 or C-6 is important for MAO-A potency and selectivity. Furthermore, this enhanced potency was observed if the substituent was either electron withdrawing (halogens Br and F) or electron donating (methoxy, compound **89**).

The MAO isoforms A and B share a 70% sequence homology.[103] However, the active sites for each enzyme contain 20 enzymes, seven of which are different in MAO-A compared to MAO-B.[104] These changes in active site residues results in MAO-A having a hydrophobic cavity that is ~ 550 $Å^3$, which is smaller than the MAO-B active site cavity which is ~700 $Å^3$. This smaller active site cavity could account for the loss of MAO-A inhibitory activity in the second series of aplysinopsin analogs with bulky benzyl substitutions (**81-85**) and lengthy alkyl substitutions at the indole nitrogen (**91-92**). Another interesting difference between the two isoforms of MAO is that MAO-A crystalizes as a monomer, whereas MAO-B presents as a dimer, as shown in Figure 3-19. The binding of deprenyl and clorgyline reveal that the critical changes in active site residues are the change of Phe-208 in MAO-A to Ile-199 in MAO-B; and Ile-335 to Tyr-326 in MAO-B. As mentioned previously, the width and depth of the binding cavities varies widely from MAO-A to MAO-B. In an effort to explain why aplysinopsins are selective for MAO-A, we are currently designing docking and molecular dynamics studies to give insight into the selectivity between MAO-A and MAO-B.

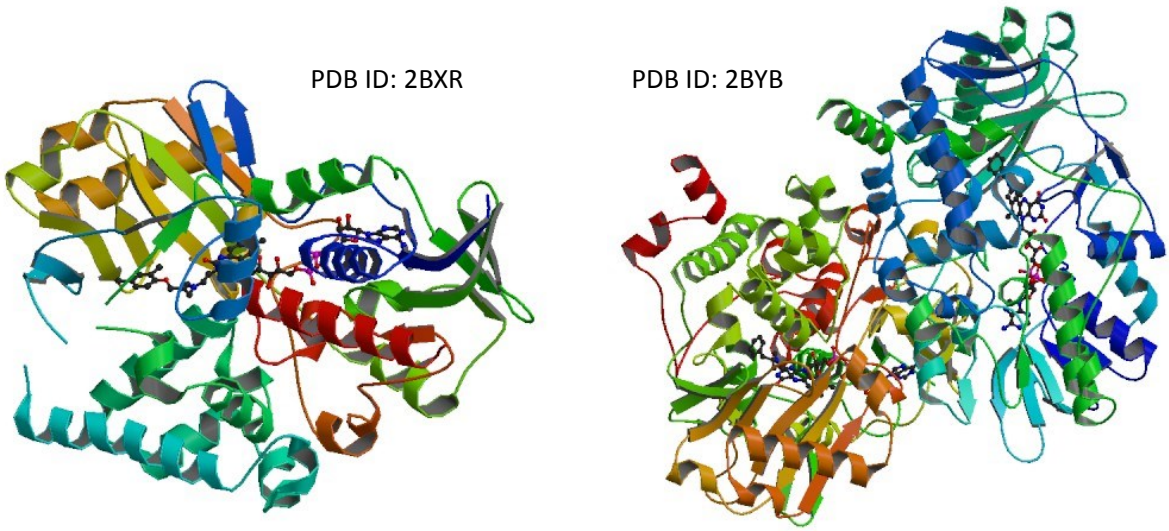

Figure 3-19 Crystal structures of MAO isoforms A and B in complex with inhibitors clorgyline and deprenyl.

Based on these in vitro screening findings, three lead compounds were further evaluated in an in vivo model. Compounds **83**, **88**, and **89** were evaluated in the chick-anxiety depression model. Compound **83**, the *p*-chloro-*N*-benzylaplysinopsin analog, showed a modest antidepressant effect at a dose of 10 mg/kg in the later phases of the assay. This delay in onset was seen previously with compound **33**, which also has a high affinity for serotonin receptor subtypes. Compound **89**, the 5-methoxyaplysinopsin analog, displayed potent antidepressant activity, attenuating behavioral despair at all doses. In contrast, the 5-fluoroaplysinopsin analog (**88**) showed no antidepressant activity across all doses.

Experimental

Chemistry

Unless specified all reagents were purchased from commercial sources and used without further purification. Compounds were purified via column chromatography using Sorbtech silica gel, 60A, 40-63um from Sorbent Technologies. Whatman silica gel F254 polyester backed plates were used for TLC and visualized with UV light and/or ninhydrin, vanillin, and anisaldehyde. NMR spectra were recorded on a 400 MHz Bruker instrument (400 UltraShield, 54 mm standard magnet bore, Billerica, MA) with 3mm direct carbon probe. ^{1}H-NMR and ^{13}C-NMR spectra were recorded at 400 MHz and 100 MHz, respectively. Chemical shifts were standardized to TMS and solvent signals. All biologically evaluated compounds were found to possess ≥ 95% purity by HPLC (UV detection at 210 and 254 nm). Purified samples were analyzed by LC-MS (Bruker Daltonic microTOF, Leipzig Germany) using a 150 x 4.6 mm C8 column (Luna Phenomenex). HR-ESI-MS analysis was done in positive ionization mode.

General procedures for the synthesis of each group of aplysinopsin analogs and full characterizations of three compounds evaluated in vivo are provided below. Analytical data for all other compounds can be found in Chapter 5.

General procedure for the synthesis of *N*-benzyl aplysinopsin analogs (81-85)

To a solution of 3-formylindole (2.4 mmol, 348 mg) in EtOH (20 mL) at room temperature, KOH pellets (3 mmol, 170 mg) were added and the mixture was stirred until maximum solubilization was achieved. The EtOH was removed under vacuum and 20 mL of acetone was added. This was followed by the addition of the appropriate benzyl bromide (2.4 mmol). A precipitate was formed instantly, and was filtered off and the solution concentrated to

yield the *N*-benzyl substituted 3-formylindoles. They were used in the next step without further purification.

Next, the appropriate *N*-benzyl-3-formylindoles (0.24 mmol) were dissolved in ethylene glycol (0.25 mL). A solution of imidazolidinone **28** (0.36 mmol, 91.8 mg) in ethylene glycol (0.25 mL) was added and the mixture was heated at 130°C for 2h. Additional **28** was added (0.12 mmol, 30.6 mg) in ethylene glycol (0.25 mL) and the reaction mixture heated for another 2h at 130°C. The mixture was cooled, diluted with H_2O (30 mL) and extracted with EtOAC (4 x 30 mL). The organic layers were combined, washed with H_2O (4 x 25 mL), and dried with $MgSO_4$. After filtering and concentration, the crude product was purified using flash chromatography (dichlormethane-methanol, 9:1) to yield the *N*-benzylaplysinopsin analogs **81-85**.

General procedure for the synthesis of analogs substituted on the indole moiety (86, 88, 89)

Equimolar amounts of the appropriate 3-formylindoles (5-cyano, 5-fluoro, 5-methoxy) and imidazolidinone **28** were mixed under nitrogen and heated over an open flame until the reaction mixture began effervescing. Several minutes after the mixture stopped effervescing it was cooled to room temperature. The crude mixture was extracted with MeOH and insoluble materials filtered off. The solution was concentrated and loaded on silica gel for purification using.

General procedure for the synthesis of analogs substituted at the indole nitrogen (87, 90-92)

For compounds **90-92**, 3-formylindole (2.5 mmol, 363 mg) and KOH (5 mmol, 280 mg) were dissolved in 10 mL DMSO. Appropriate alkyl iodide (5 mmol) was added, and the solution was stirred at room temperature and monitored via TLC until the total consumption of the

starting material. The solution was diluted with H_2O (10 mL) and extracted with EtOAc (3 x 15 mL). They solution was then concentrated and the *N*-substituted 3-formylindoles were crystallized and used in the following condensation step without further purification. These intermediates were then subjected to the condensation conditions.

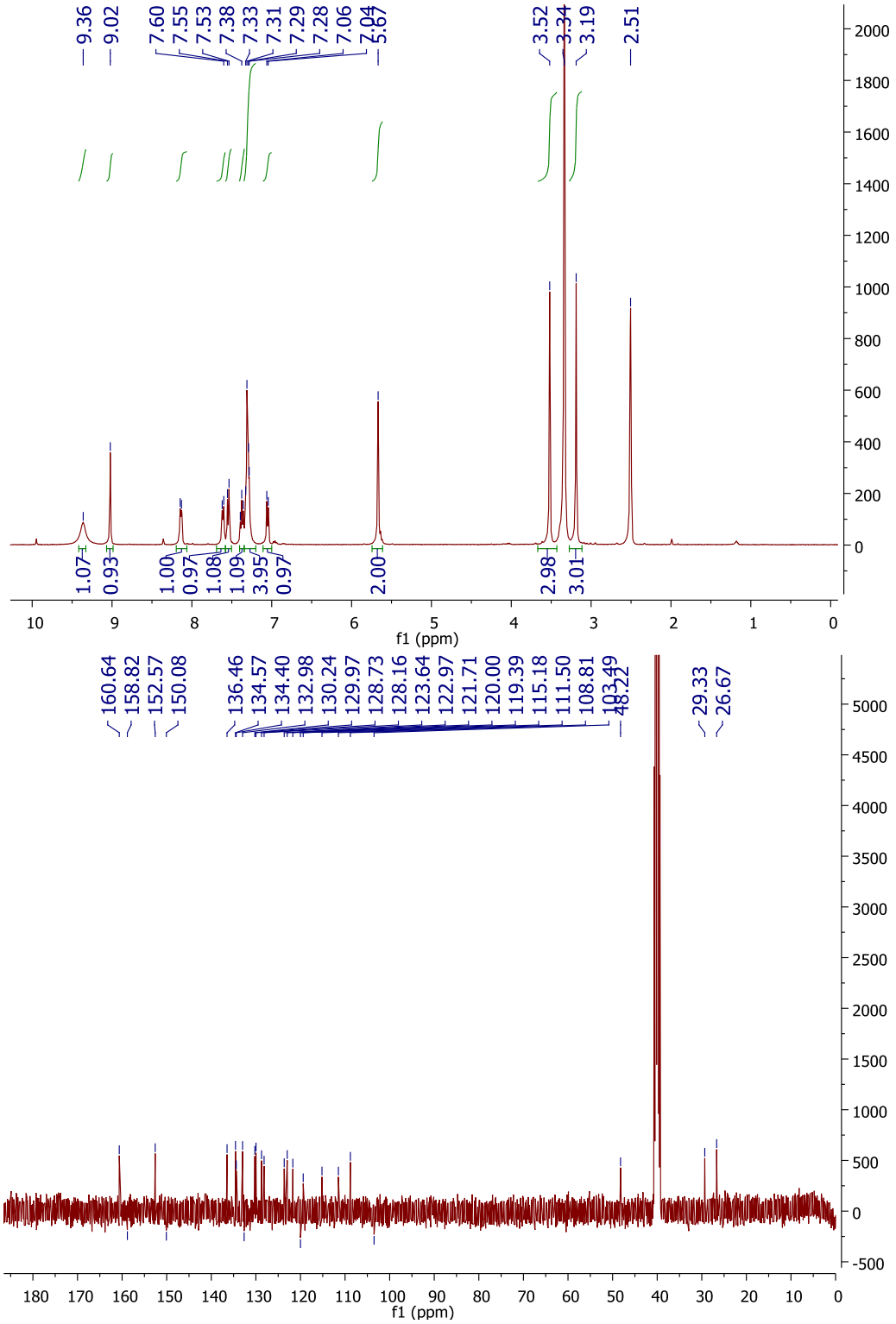

Figure 3-20 ^{1}H and ^{13}C NMR spectra of compound 83.

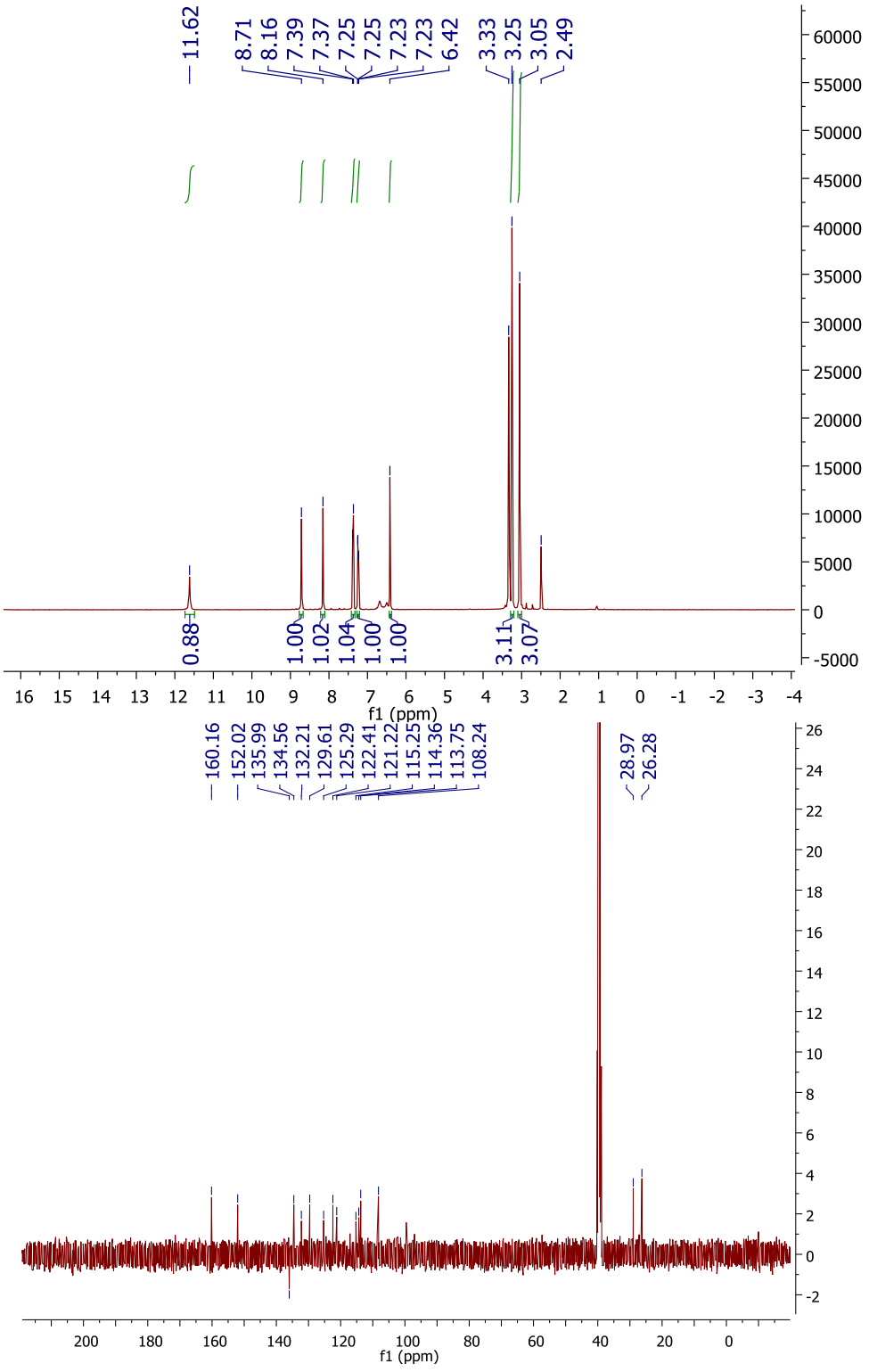

Figure 3-21 ^{1}H and ^{13}C NMR spectra of compound 88.

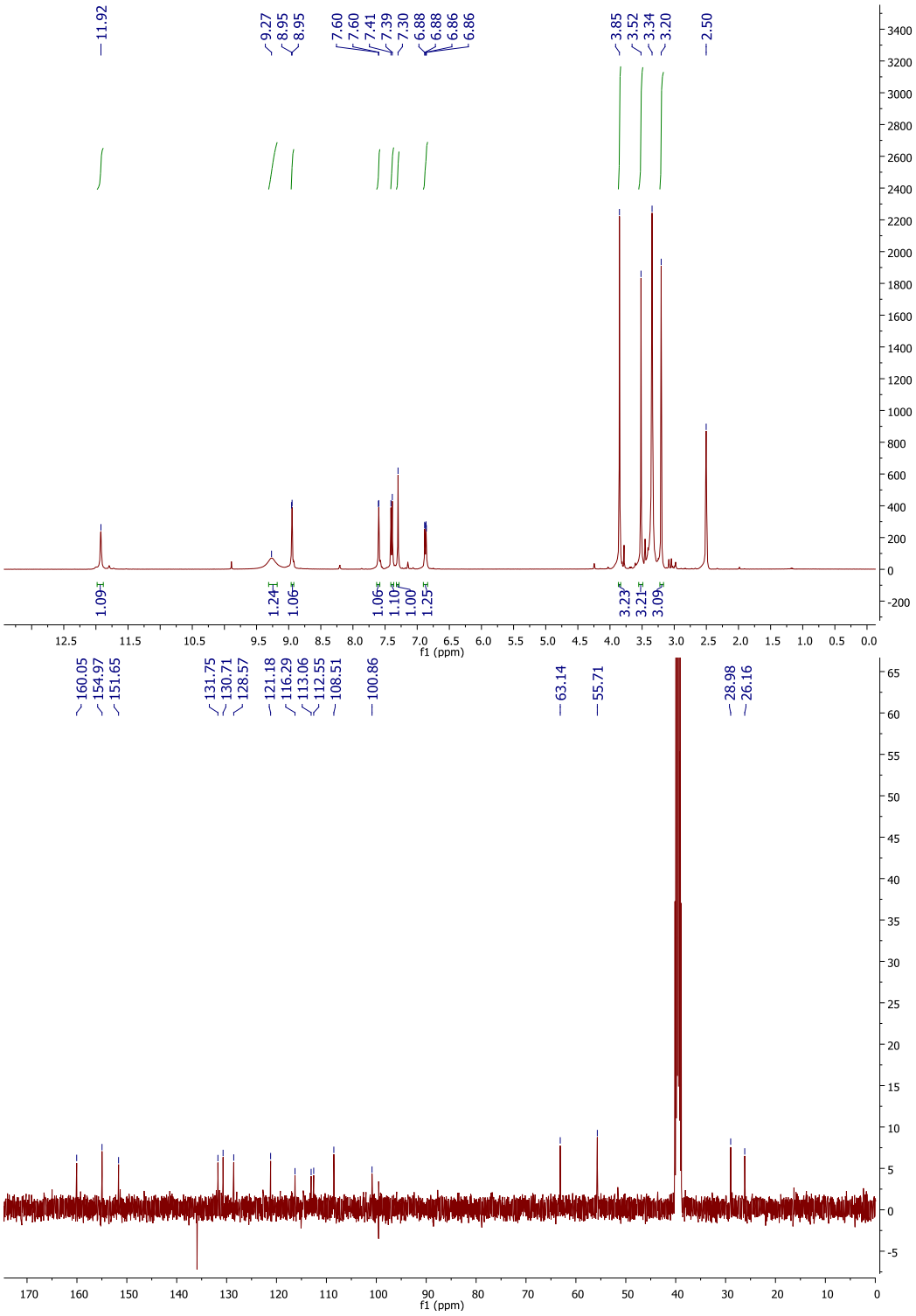

Figure 3-22 ^{1}H and ^{13}C NMR spectra of compound 89.

(E)-5-[(1-(2-chlorobenzyl)-*1H*-indol-3-yl)methylene]- 2-imino-1,3-dimethylimidazolidin-4-one (83)

^{1}H NMR (400 MHz, DMSO) δ 9.36 (s, 1H), 9.02 (s, 1H), 8.14 (d, *J* = 6.5 Hz, 1H), 7.61 (d, *J* = 7.8 Hz, 1H), 7.54 (d, *J* = 7.8 Hz, 1H), 7.38 (t, *J* = 7.4 Hz, 1H), 7.30 (dd, *J* = 12.7, 5.0 Hz, 4H), 7.05 (d, *J* = 7.5 Hz, 1H), 5.67 (s, 2H), 3.52 (s, 3H), 3.19 (s, 3H). ^{13}C NMR (101 MHz, DMSO) δ 160.64, 152.57, 136.46, 134.57, 134.40, 132.98, 130.33, 130.24, 129.97, 128.73, 128.16, 123.64, 122.97, 121.71, 119.39, 115.18, 111.50, 108.81, 48.22, 29.33, 26.67. HRESMS *m/z* calcd 379.1326 ($M^{\cdot+}$ +H); found: 379.1335.

(E)-5-[(5-fluoro-*1H*-indol-3-yl)methylene]-2-imino-1,3-dimethylimidazolidin-4-one (88)

^{1}H NMR (400 MHz, DMSO) δ 11.62 (s, 1H), 8.71 (s, 1H), 8.16 (s, 1H), 7.38 (d, *J* = 8.6 Hz, 1H), 7.24 (dd, *J* = 8.5, 1.4 Hz, 1H), 6.42 (s, 1H), 3.25 (s, 3H), 3.05 (s, 3H). ^{13}C NMR (101 MHz, DMSO) δ 160.16, 152.02, 134.56, 132.21, 129.61, 125.29, 122.41, 121.22, 115.25, 114.36, 113.75, 108.24, 28.97, 26.28. HRESMS *m/z* calcd 273.1152 ($M^{\cdot+}$ +H); found: 273.1148

(E)-5-[(5-methoxy-*1H*-indol-3-yl)methylene]-2-imino-1,3-dimethylimidazolidin-4-one (89)

^{1}H NMR (400 MHz, DMSO) δ 11.92 (s, 1H), 9.27 (s, 1H), 8.95 (d, *J* = 3.0 Hz, 1H), 7.60 (d, *J* = 2.0 Hz, 1H), 7.40 (d, *J* = 8.7 Hz, 1H), 7.30 (s, 1H), 6.87 (dd, *J* = 8.7, 2.3 Hz, 1H), 3.85 (s, 3H), 3.52 (s, 3H), 3.20 (s, 3H). ^{13}C NMR (101 MHz, DMSO) δ 160.05, 154.97, 151.65, 131.75, 130.71, 128.57, 121.18, 116.29, 113.06, 112.55, 108.51, 100.86, 55.71, 28.98, 26.16. HRESMS *m/z* calcd 285.1352 ($M^{\cdot+}$ +H); found: 285.1350.

Bioassay

In vitro stability study and metabolism profiling

Compound **53** was solubilized in DMSO at 10 mM, and incubated in duplicate with rat

liver microsomes at 37°C in 1000 μL volume. The reaction mixture contains 0.5 mg liver microsomal protein in 0.5 M potassium phosphate pH, NADPH Regenerating System Solution A and B (BD Biosciences) and 1 μL substrate in DMSO (5 μM final concentration). A control is run for each test compound without NADPH to detect NADPH-free degradation. At 15, 30, and 60 min, 100 μL is removed from each experimental and mixed with 100 μL acetonitrile containing internal standards. After centrifugation the supernatants are analyzed by LC-MS to quantitate the remaining parent. The sample analysis is performed by LC-MS with an Agilent 1100 HPLC equipped with a diode array detector and Micromass Quatro Micro API. Data were analyzed using masslynx and quanlynx. The LC conditions are as follows: flow rate: 0.5 mL/min; Accucore C18 2.1x50 mm column, gradient from 95% water (0.1% formic acid) to 95% acetonitrile (0.1% formic acid) over 8 minutes.

Data are converted to % remaining by dividing the time zero concentration value. Data are fit to a first-order decay model to determine half-life. Intrinsic clearance is calculated from the half-life and the protein concentration. Incubation samples were analyzed to detect metabolites. LC-MS data was processed using metabolynx software to generate structural hypothesis based on daughter ion data.

MDR-1 efflux pump

Modulation of MDR-1 activity is monitored in Caco-2 cells derived from the human colonic epithelium or HEK human kidney cells. The assay monitors the time-depenedent increase in calcein fluorescence in live cells in 96 well plates. Cells are seeded into 96-well culture plates 24h prior to assay at 80,000 cells per well. The medium is removed and 50 μL of D-PBS, 10 mM glucose (negative control), test compound (25 μM), or reference compound

(cyclosporin A) (25 μM). The cells are incubated at 37°C for 30 min. Next calcein-AM is added to the cells at a final concentration of 500 nM). Fluorescence is monitored over a 4 minute period by a FlexStation II fluorimeter (Molecular Devices). Compounds are assayed in quadruplicate and each assay will contain wells with no test compound (negative control) and wells with 25 μM cyclosporin A (positive control). Results for test compounds are calculated from the slope of fluorescence increase and are normalized so that the value for untreated cells is 0% and the value for cyclosporin A is 100%.

In vitro evaluation of CNS receptor binding affinity

K_i determinations were generously provided by the National Institute of Mental Health's Psychoactive Drug Screening Program. Briefly, compounds are initially evaluated in a primary binding assay, in which they are tested at a final concentration of 10 μM. They are tested in quadruplicate and compounds that show > 50% inhibition are deemed hits and advance to secondary radioligand binding assays. Here compounds are tested at 11 concentrations (0.1, 0.3, 1, 3, 10, 30, 100, 300 nM, 1, 3, 10 μM) to determine the K_i values at specific receptors. For complete experimental details please refer to the PDSP web site http://pdsp.med.unc.edu/ and click on "Binding Assay" on the menu bar.

In vitro evaluation of MAO inhibitory activity

An in vitro assay was designed to measure the effect of aplysinopsin analogs on MAO-A and B activity. Recombinant human MAO-A and B were obtained from BD Biosciences (Bedford, MA, USA). Kynuramine bromide, 4-hydroxyquinoline, clorgyline and R-(-)-deprenyl were purchased from Sigma (St Louis, MO, USA). Aplysinopsin analogs (10^{-9} to 10^{-2}M), clorgyline and deprenyl (10^{-12} to 10^{-5}M) were tested for inhibition of human MAO-A and B

activity. MAO-activity was assessed by a modification of the fluorometric method of Kralj[79] and was adopted for 96 well plate format. The 200 µL reaction mixtures containing recombinant human MAO-A or MAO-B (5 µg/ml) and the test compounds in KH_2PO_4 buffer (100 mM; pH 7.4) were pre-incubated at 37°C for 15 min. The reactions with positive control wells with standard MAO inhibitors and controls without inhibitors were also set up simultaneously. The reaction was initiated by addition of kynuramine (250 µM) in potassium phosphate buffer (100 mM; pH 7.4) and incubated further at 37°C for 20 min. After incubation the reaction was stopped by the addition of 75 µL of 2N NaOH. The deaminated product of kynuramine, which spontaneously cyclizes to 4-hydroxyquinoline, was determined fluorometrically at 320 nm excitation and 460 nm emission wavelengths in a plate reader (SpectraMax M5, Molecular Devices, Sunnyvale, CA, USA). Wells receiving no test compounds were used as controls to calculate the inhibition percentage. The IC-50 values were computed from the dose response inhibition curves prepared by GraphPad.

In vivo evaluation of aplysinopsin analogs

All procedures involving animals were performed as approved by the Institutional Animal Care and Use Committee of The University of Mississippi. Cockerels (Production Red, Ideal Poultry, Cameron, TX, USA) were received into the laboratory at 2 days post hatch and housed in 34 x 57 x 40 cm cages with 12 chicks per cage. Food and water are available ad libitum via gravity feeders. Daily maintenance that entails the replacement of tray liners and filling food and water gravity feeders is conducted during the hour that precedes the animal's dark cycle. Lights are operated on a 12:12 light dark cycle. Supplemental heating sources are provided to maintain appropriate housing temperatures in the range of 32 +/- 1°C.

Testing equipment

A six unit testing apparatus containing Plexiglas chambers (25 x 25 x 22 cm) surrounded by sound attenuating media is used to record separation-induced vocalizations. Each unit is lined with acoustical fiber media, illuminated by a 25-W light bulb, and ventilated by an 8-cm-diameter rotary fan (Model FP-108AX S1, Commonwealth Industrial Corp., Taipei, Taiwan). Miniature video cameras (Model PC60XP, SuperCircuits, Inc., Liberty Hill, TX) mounted in the sound-attenuating enclosures at floor level and routed through a multiplexor (Model PC47MC, SuperCircuits, Inc.) provided televised display of the chicks for behavioral observation. To record DVocs, microphones (Radio Shack Omnidirectional Model 33-3013 modified for AC current) are mounted at the top of the Plexiglas chamber. These vocalizations are routed to a computer equipped with custom designed software for data collection.

Methods

Squads of six chicks were taken from their home cage and placed within a lidded plastic transport container. To track subject assignment to treatment conditions, chicks are marked using colored felt pens and body weight is determined for each chick to determine dosing and identify outliers (i.e., low body weight). Drugs were administered IP 15 minutes prior to behavioral testing. Chicks were placed into individual testing units for a 60 minute session. Following the completion of the session chicks were removed from the testing apparatus and returned to their home cage.

LIST OF REFERENCES

1. Rozas, I., Improving antidepressant drugs: update on recently patented compounds. *Expert. Opin. Ther. Pat.* **2009,** *19* (6), 827-45.

2. (a) Holden, C., Future brightening for depression treatments. *Science* **2003,** *302* (5646), 810-3; (b) Krishnan, V.; Nestler, E. J., The molecular neurobiology of depression. *Nature* **2008,** *455* (7215), 894-902.

3. Lopez-Munoz, F.; Alamo, C.; Juckel, G.; Assion, H. J., Half a century of antidepressant drugs: on the clinical introduction of monoamine oxidase inhibitors, tricyclics, and tetracyclics. Part I: monoamine oxidase inhibitors. *J. Clin. Psychopharmacol.* **2007,** *27* (6), 555-9.

4. Gillman, P. K., Tricyclic antidepressant pharmacology and therapeutic drug interactions updated. *Br. J. Pharmacol.* **2007,** *151* (6), 737-748.

5. Cusack, B.; Nelson, A.; Richelson, E., Binding of antidepressants to human brain receptors: focus on newer generation compounds. *Psychopharmacology (Berlin).* **1994,** *114* (4), 559-565.

6. Sills, M. A.; Loo, P. S., Tricyclic antidepressants and dextromethorphan bind with higher affinity to the phencyclidine receptor in the absence of magnesium and L-glutamate. *Mol. Pharmacol.* **1989,** *36* (1), 160-5.

7. Narita, N.; Hashimoto, K.; Tomitaka, S.-i.; Minabe, Y., Interactions of selective serotonin reuptake inhibitors with subtypes of σ receptors in rat brain. *Eur. J. Pharmacol.* **1996,** *307* (1), 117-119.

8. Bie Shung, T.; Yellin, T. O., Differences in the interaction of histamine H2 receptor antagonists and tricyclic antidepressants with adenylate cyclase from guinea pig gastric mucosa. *Biochem. Pharmacol.* **1984,** *33* (22), 3621-3625.

9. Broquet, K. E., Status of Treatment of Depression. *South. Med. J.* **1999,** *92* (9), 845-857.

10. Gumnick, J. F.; Nemeroff, C. B., Problems with currently available antidepressants. *J. Clin. Psychiatry* **2000,** *61 Suppl 10*, 5-15.

11. Newman, D. J.; Cragg, G. M.; Snader, K. M., Natural products as sources of new drugs over the period 1981−2002. *J. Nat. Prod.* **2003,** *66* (7), 1022-1037.

12. Newman, D. J.; Cragg, G. M., Natural products as sources of new drugs over the 30 years from 1981 to 2010. *J. Nat. Prod.* **2012,** *75* (3), 311-335.

13. Gerwick, W. H.; Moore, B. S., Lessons from the past and charting the future of marine natural products drug discovery and chemical biology. *Chem. Biol.* **2012,** *19* (1), 85-98.

14. Cole, A.; Marmura, M., Triptans: Where things stand. *Curr. Treat. Options Neurol.* **2010,** *12* (5), 454-463.

15. Younes, A.; Bartlett, N. L.; Leonard, J. P.; Kennedy, D. A.; Lynch, C. M.; Sievers, E. L.; Forero-Torres, A., Brentuximab Vedotin (SGN-35) for Relapsed CD30-Positive Lymphomas. *N. Engl. J. Med.* **2010,** *363* (19), 1812-1821.

16. Grosso, F.; Jones, R. L.; Demetri, G. D.; Judson, I. R.; Blay, J.-Y.; Le Cesne, A.; Sanfilippo, R.; Casieri, P.; Collini, P.; Dileo, P.; Spreafico, C.; Stacchiotti, S.; Tamborini, E.; Tercero, J. C.; Jimeno, J.; D'Incalci, M.; Gronchi, A.; Fletcher, J. A.; Pilotti, S.; Casali, P. G., Efficacy of trabectedin (ecteinascidin-743) in advanced pretreated myxoid liposarcomas: a retrospective study. *The Lancet Oncology* **2007,** *8* (7), 595-602.

17. Löwenberg, B.; Pabst, T.; Vellenga, E.; van Putten, W.; Schouten, H. C.; Graux, C.; Ferrant, A.; Sonneveld, P.; Biemond, B. J.; Gratwohl, A.; de Greef, G. E.; Verdonck, L. F.; Schaafsma, M. R.; Gregor, M.; Theobald, M.; Schanz, U.; Maertens, J.; Ossenkoppele, G. J., Cytarabine dose for acute myeloid leukemia. *N. Engl. J. Med.* **2011,** *364* (11), 1027-1036.

18. Twelves, C.; Cortes, J.; Vahdat, L.; Wanders, J.; Akerele, C.; Kaufman, P., Phase III trials of eribulin mesylate (E7389) in extensively pretreated patients with locally recurrent or metastatic breast cancer. *Clinical Breast Cancer* **2010,** *10* (2), 160-163.

19. Schmidtko, A.; Lötsch, J.; Freynhagen, R.; Geisslinger, G., Ziconotide for treatment of severe chronic pain. *Lancet* **2010,** *375* (9725), 1569-1577.

20. Lee, J. H.; O'Keefe, J. H.; Lavie, C. J.; Marchioli, R.; Harris, W. S., Omega-3 fatty acids for cardioprotection. *Mayo Clin. Proc.* **2008,** *83* (3), 324-332.

21. Mayer, A. M. S.; Glaser, K. B.; Cuevas, C.; Jacobs, R. S.; Kem, W.; Little, R. D.; McIntosh, J. M.; Newman, D. J.; Potts, B. C.; Shuster, D. E., The odyssey of marine pharmaceuticals: a current pipeline perspective. *Trends Pharmacol. Sci.* **2010,** *31* (6), 255-265.

22. Nemeroff, C. B.; Owens, M. J., The role of serotonin in the pathophysiology of depression: as important as ever. *Clin. Chem.* **2009,** *55* (8), 1578-9.

23. Terry, A. V., Jr.; Buccafusco, J. J.; Wilson, C., Cognitive dysfunction in neuropsychiatric disorders: selected serotonin receptor subtypes as therapeutic targets. *Behav. Brain Res.* **2008,** *195* (1), 30-8.

24. Gillette, R., Evolution and function in serotonergic systems. *Integr. Comp. Biol.* **2006,** *46* (6), 838-46.

25. Nichols, D. E.; Nichols, C. D., Serotonin receptors. *Chem. Rev.* **2008,** *108* (5), 1614-41.

26. Youdim, M. B.; Collins, G. G.; Sandler, M.; Bevan Jones, A. B.; Pare, C. M.; Nicholson, W. J., Human brain monoamine oxidase: multiple forms and selective inhibitors. *Nature* **1972,** *236* (5344), 225-8.

27. Kaszlauskas, R.; Murphy, P. T.; Quinn, R. J.; Wells, R. J., Aplysinopsin, a new tryptophan derivative from a sponge. *Tetrahedron Lett.* **1977,** *18* (1), 61-64.

28. Djura, P.; Faulkner, D. J., Metabolites of the marine sponge Dercitus species. *J. Org. Chem.* **1980,** *45* (4), 735-737.

29. Bergquist, P. R.; Wells, R. J., *Marine Natural Products: Chemical and Biological Perspectives*. Academic Press: New York, 1983; Vol. V.

30. Fattorusso, E.; Lanzotti, V.; Magno, S.; Novellino, E., Tryptophan derivatives from a mediterranean anthozoan, *Astroides calycularis*. *J. Nat. Prod.* **1985,** *48* (6), 924-927.

31. Okuda, R. K.; Klein, D.; Kinnel, R. B.; Li, M.; Scheuer, P. J., Marine natural products: the past twenty years and beyond. *Pure & Appl. Chem.* **1982,** *54*, 1907-1914.

32. Murata, M.; Miyagawa-Kohshima, K.; Nakanishi, K.; Naya, Y., Characterization of compounds that induce symbiosis between sea anemone and anemone fish. *Science* **1986,** *234* (4776), 585-7.

33. Aoki, S.; Ye, Y.; Higuchi, K.; Takashima, A.; Tanaka, Y.; Kitagawa, I.; Kobayashi, M., Novel neuronal nitric oxide synthase (nnos) selective inhibitor, aplysinopsin-type indole alkaloid, from marine sponge *Hyrtios erecta*. *Chem. Pharm. Bull. (Tokyo).* **2001,** *49* (10), 1372-1374.

34. (a) Guella, G.; Mancini, I.; Zibrowius, H.; Pietra, F., Novel Aplysinopsin-type alkaloids from scleractinian corals of the family Dendrophylliidae of the Mediterranean and the Philippines. Configurational-assignment criteria, stereospecific synthesis, and photoisomerization. *Helv. Chim. Acta* **1988,** *71* (4), 773-782; (b) Guella, G.; Mancini, I.; Zibrowius, H.; Pietra, F., Aplysinopsin-type alkaloids from Dendrophyllia sp., a scleractinian coral of the family dendrophylliidae of the Philippines, facile photochemical (Z/E) photoisomerization and thermal reversal. *Helv. Chim. Acta* **1989,** *72* (7), 1444-1450.

35. Kondo, K.; Nishi, J.; Ishibashi, M.; Kobayashi, J. i., Two new tryptophan-derived alkaloids from the okinawan marine sponge *Aplysina* Sp. *J. Nat. Prod.* **1994,** *57* (7), 1008-1011.

36. Iwagawa, T.; Miyazaki, M.; Okamura, H.; Nakatani, M.; Doe, M.; Takemura, K., Three novel bis(indole) alkaloids from a stony coral, Tubastraea sp. *Tetrahedron Lett.* **2003,** *44* (12), 2533-2535.

37. Hollenbeak, K. H.; Schmitz, F. J., Aplysinopsin: antineoplastic tryptophan derivative

from the marine sponge *Verongia spengelii*. *Lloydia* **1977,** *40* (5), 479-81.

38. Hu, J. F.; Schetz, J. A.; Kelly, M.; Peng, J. N.; Ang, K. K.; Flotow, H.; Leong, C. Y.; Ng, S. B.; Buss, A. D.; Wilkins, S. P.; Hamann, M. T., New antiinfective and human 5-HT2 receptor binding natural and semisynthetic compounds from the Jamaican sponge *Smenospongia aurea*. *J. Nat. Prod.* **2002,** *65* (4), 476-80.

39. Ang, K. K.; Holmes, M. J.; Higa, T.; Hamann, M. T.; Kara, U. A., In vivo antimalarial activity of the beta-carboline alkaloid manzamine A. *Antimicrob. Agents Chemother.* **2000,** *44* (6), 1645-9.

40. Laport, M. S.; Santos, O. C. S.; Muricy, G., Marine sponges: potential sources of new antimicrobial drugs. *Curr. Pharm. Biotechnol.* **2009,** *10* (1), 86-105.

41. Tymiak, A. A.; Rinehart Jr, K. L.; Bakus, G. J., Constituents of morphologically similar sponges : Aplysina and smenospongia species. *Tetrahedron* **1985,** *41* (6), 1039-1047.

42. Gulati, D.; Chauhan, P.; Bhakuni, R.; Bhakuni, D., A new synthesis of aplysinopsin, a marine alkaloid and its analogues and their biological activities. *Indian J. Chem. B* **1993,** *33*, 4-9.

43. Baird-Lambert, J.; Davis, P. A.; Taylor, K. M., Methylaplysinopsin: a natural product of marine origin with effects on serotonergic neurotransmission. *Clin. Exp. Pharmacol. Physiol.* **1982,** *9* (2), 203-12.

44. Cummings, D. F.; Canseco, D. C.; Sheth, P.; Johnson, J. E.; Schetz, J. A., Synthesis and structure-affinity relationships of novel small molecule natural product derivatives capable of discriminating between serotonin 5-HT1A, 5-HT2A, 5-HT2C receptor subtypes. *Bioorg. Med. Chem.* **2010,** *18* (13), 4783-92.

45. Kochanowska, A. J.; Rao, K. V.; Childress, S.; El-Alfy, A.; Matsumoto, R. R.; Kelly, M.; Stewart, G. S.; Sufka, K. J.; Hamann, M. T., Secondary metabolites from three Florida sponges with antidepressant activity. *J. Nat. Prod.* **2008,** *71* (2), 186-9.

46. Cecchelli, R.; Berezowski, V.; Lundquist, S.; Culot, M.; Renftel, M.; Dehouck, M.-P.; Fenart, L., Modelling of the blood-brain barrier in drug discovery and development. *Nat. Rev. Drug Discov.* **2007,** *6* (8), 650-661.

47. Pigott, H. E.; Leventhal, A. M.; Alter, G. S.; Boren, J. J., Efficacy and effectiveness of antidepressants: current status of research. *Psychother. Psychosom.* **2010,** *79* (5), 267-279.

48. Current depression among adults---United States, 2006 and 2008. *MMWR. Morb. Mortal. Wkly. Rep.* **2010,** *59* (38), 1229-35.

49. Kennedy, S. H.; Rizvi, S. J., Emerging drugs for major depressive disorder. *Expert Opin.*

Emerg. Drugs **2009,** *14* (3), 439-53.

50. Berger, M.; Gray, J. A.; Roth, B. L., The expanded biology of serotonin. *Annu. Rev. Med.* **2009,** *60* (1), 355-366.

51. (a) Robichaud, A.; Largent, B. L., Recent advances in selective serotonin receptor modulation. *Annu. Rep. Med. Chem.* **2000,** *35*, 11-20; (b) Halford, J. C.; Blundell, J. E., Serotonin receptor modulation in the treatment of obesity. *Handbook of Obesity* **2008**, 375-388.

52. (a) Wang, B.; Chehab, F. F., Deletion of the serotonin 2c receptor from transgenic mice overexpressing leptin does not affect their lipodystrophy but exacerbates their diet-induced obesity. *Biochem. Biophys. Res. Commun.* **2006,** *351* (2), 418-23; (b) Tecott, L. H.; Sun, L. M.; Akana, S. F.; Strack, A. M.; Lowenstein, D. H.; Dallman, M. F.; Julius, D., Eating disorder and epilepsy in mice lacking 5-HT2c serotonin receptors. *Nature* **1995,** *374* (6522), 542-6.

53. Rothman, R. B.; Baumann, M. H.; Savage, J. E.; Rauser, L.; McBride, A.; Hufeisen, S. J.; Roth, B. L., Evidence for possible involvement of 5-HT(2B) receptors in the cardiac valvulopathy associated with fenfluramine and other serotonergic medications. *Circulation* **2000,** *102* (23), 2836-41.

54. Colman, E.; Golden, J.; Roberts, M.; Egan, A.; Weaver, J.; Rosebraugh, C., The FDA's Assessment of Two Drugs for Chronic Weight Management. *N. Engl. J. Med.* **2012,** *367* (17), 1577-1579.

55. Connolly, H. M.; Crary, J. L.; McGoon, M. D.; Hensrud, D. D.; Edwards, B. S.; Edwards, W. D.; Schaff, H. V., Valvular heart disease associated with fenfluramine-phentermine. *N. Engl. J. Med.* **1997,** *337* (9), 581-8.

56. Thomsen, W. J.; Grottick, A. J.; Menzaghi, F.; Reyes-Saldana, H.; Espitia, S.; Yuskin, D.; Whelan, K.; Martin, M.; Morgan, M.; Chen, W.; Al-Shamma, H.; Smith, B.; Chalmers, D.; Behan, D., Lorcaserin, a novel selective human 5-hydroxytryptamine2C agonist: in vitro and in vivo pharmacological characterization. *J. Pharmacol. Exp. Ther.* **2008,** *325* (2), 577-87.

57. Coutts, R. T.; Baker, G. B.; Danielson, T. J., New Developements in monoamine oxidase inhibitors. In *Dev. Drugs Mod. Med.*, Gorrod, J. W.; Gibson, G. G.; Mitchard, M., Eds. Horwood: Chichester, UK, 1986; pp 40-48.

58. Youdim, M. B.; Bakhle, Y. S., Monoamine oxidase: isoforms and inhibitors in Parkinson's disease and depressive illness. *Br. J. Pharmacol.* **2006,** *147 Suppl 1*, S287-96.

59. Youdim, M. B.; Edmondson, D.; Tipton, K. F., The therapeutic potential of monoamine oxidase inhibitors. *Nat. Rev. Neurosci.* **2006,** *7* (4), 295-309.

60. Prins, L. H.; Petzer, J. P.; Malan, S. F., Inhibition of monoamine oxidase by indole and benzofuran derivatives. *Eur. J. Med. Chem.* **2010,** *45* (10), 4458-66.

61. Sant' Anna Gda, S.; Machado, P.; Sauzem, P. D.; Rosa, F. A.; Rubin, M. A.; Ferreira, J.; Bonacorso, H. G.; Zanatta, N.; Martins, M. A., Ultrasound promoted synthesis of 2-imidazolines in water: a greener approach toward monoamine oxidase inhibitors. *Bioorg. Med. Chem. Lett.* **2009,** *19* (2), 546-9.

62. Warnick, J. E.; Wicks, R. T.; Sufka, K. J., Modeling anxiety-like states: pharmacological characterization of the chick separation stress paradigm. *Behav. Pharmacol.* **2006,** *17* (7), 581-7.

63. Stanovnik, B.; Svete, J., The synthesis aplysinopsins, meridianines, and related compounds. *Mini-Reviews in Organic Chemistry* **2005,** *2* (3), 211-224.

64. Clark, R. D.; Repke, D. B., The Leimgruber-Batcho indole synthesis. *Heterocycles* **1984,** *22* (1), 195-221.

65. Kenyon, G. L.; Rowley, G. L., Tautomeric preferences among glycocyamidines. *J. Am. Chem. Soc.* **1971,** *93*, 5552-5560.

66. Bengelsdorf, I. S., A reaction of guanidine with glyoxals in aqueous solution. The preparation of glycocyamidines. *J. Am. Chem. Soc.* **1953,** *75*, 3138-3140.

67. Dalkafouki, A.; Ardisson, J.; Kunesch, N.; Lacombe, L.; Poisson, J. E., Synthesis of 2-dimethylaminoimidazole derivatives: a new access to indolylimidazole alkaloids of marine origin. *Tetrahedron Lett.* **1991,** *32*, 5225-5328.

68. Porwal, S.; Chauhan, S. S.; Chauhan, P. M. S.; Shakya, N.; Verma, A.; Gupta, S., Discovery of Novel Antileishmanial Agents in an Attempt to Synthesize Pentamidine−Aplysinopsin Hybrid Molecule. *J. Med. Chem.* **2009,** *52* (19), 5793-5802.

69. Gadwood, R. C.; Kamdar, B. V.; Dubray, L. A.; Wolfe, M. L.; Smith, M. P.; Watt, W.; Mizsak, S. A.; Groppi, V. E., Synthesis and biological activity of spirocyclic benzopyran imidazolone potassium channel openers. *J. Med. Chem.* **1993,** *36* (10), 1480-7.

70. Cheng, Y. C.; Robison, B.; Parks, R. E., Jr., Demonstration of the heterogeneity of nucleoside diphosphokinase in rat tissues. *Biochemistry (Moscow).* **1973,** *12* (1), 5-10.

71. Bialonska, D.; Zjawiony, J. K., Aplysinopsins--marine indole alkaloids: chemistry, bioactivity and ecological significance. *Mar. Drugs* **2009,** *7* (2), 166-83.

72. Moron, J. A.; Campillo, M.; Perez, V.; Unzeta, M.; Pardo, L., Molecular determinants of MAO selectivity in a series of indolylmethylamine derivatives: biological activities, 3D-QSAR/CoMFA analysis, and computational simulation of ligand recognition. *J. Med. Chem.* **2000,** *43* (9), 1684-91.

73. Lehr, E., Distress call reactivation in isolated chicks: a behavioral indicator with high selectivity for antidepressants. *Psychopharmacology (Berlin).* **1989,** *97* (2), 145-6.

74. Sufka, K. J.; Feltenstein, M. W.; Warnick, J. E.; Acevedo, E. O.; Webb, H. E.; Cartwright, C. M., Modeling the anxiety-depression continuum hypothesis in domestic fowl chicks. *Behav. Pharmacol.* **2006,** *17* (8), 681-9.

75. Warnick, J. E.; Huang, C. J.; Acevedo, E. O.; Sufka, K. J., Modelling the anxiety-depression continuum in chicks. *J Psychopharmacol* **2009,** *23* (2), 143-56.

76. Sufka, K. J.; Warnick, J. E.; Pulaski, C. N.; Slauson, S. R.; Kim, Y. B.; Rimoldi, J. M., Antidepressant efficacy screening of novel targets in the chick anxiety-depression model. *Behav. Pharmacol.* **2009,** *20* (2), 146-54.

77. Lewellyn, K.; Bialonska, D.; Chaurasiya, N. D.; Tekwani, B. L.; Zjawiony, J. K., Synthesis and evaluation of aplysinopsin analogs as inhibitors of human monoamine oxidase A and B. *Bioorg. Med. Chem. Lett.* **2012,** *22* (15), 4926-4929.

78. Wacker, D.; Wang, C.; Katritch, V.; Han, G. W.; Huang, X. P.; Vardy, E.; McCorvy, J. D.; Jiang, Y.; Chu, M.; Siu, F. Y.; Liu, W.; Xu, H. E.; Cherezov, V.; Roth, B. L.; Stevens, R. C., Structural features for functional selectivity at serotonin receptors. *Science* **2013,** *340* (6132), 615-9.

79. Kralj, D.; Novak, A.; Dahmann, G.; Groselj, U.; Meden, A.; Svete, J., One-pot parallel solution-phase synthesis of 1-substituted 4-(2-aminoethyl)-*1H*-pyrazol-5-ols. *J. Comb. Chem.* **2008,** *10* (5), 664-70.

80. van De Waterbeemd, H.; Smith, D. A.; Beaumont, K.; Walker, D. K., Property-based design: optimization of drug absorption and pharmacokinetics. *J. Med. Chem.* **2001,** *44* (9), 1313-33.

81. Pajouhesh, H.; Lenz, G. R., Medicinal chemical properties of successful central nervous system drugs. *NeuroRx.* **2005,** *2* (4), 541-53.

82. Lipinski, C. A.; Lombardo, F.; Dominy, B. W.; Feeney, P. J., Experimental and computational approaches to estimate solubility and permeability in drug discovery and development settings. *Adv. Drug Del. Rev.* **1997,** *23* (1), 3-25.

83. (a) Wenlock, M. C.; Austin, R. P.; Barton, P.; Davis, A. M.; Leeson, P. D., A comparison of physiochemical property profiles of development and marketed oral drugs. *J. Med. Chem.* **2003,** *46* (7), 1250-6; (b) Vieth, M.; Siegel, M. G.; Higgs, R. E.; Watson, I. A.; Robertson, D. H.; Savin, K. A.; Durst, G. L.; Hipskind, P. A., Characteristic physical properties and structural fragments of marketed oral drugs. *J. Med. Chem.* **2004,** *47* (1), 224-232.

84. CA, L., Drew University Medical Chemistry Special Topics Course. July: 1999.

85. Clark, D. E., In silico prediction of blood-brain barrier permeation. *Drug Discov. Today* **2003,** *8* (20), 927-33.

86. Di, L.; Kerns, E. H.; Carter, G. T., Strategies to assess blood-brain barrier penetration. *Expert Opin. Drug Discov.* **2008,** *3* (6), 677-87.

87. Prentis, R. A.; Lis, Y.; Walker, S. R., Pharmaceutical innovation by the seven UK-owned pharmaceutical companies (1964-1985). *Br. J. Clin. Pharmacol.* **1988,** *25* (3), 387-96.

88. Rampe, D.; Murawsky, M. K.; Grau, J.; Lewis, E. W., The antipsychotic agent sertindole is a high affinity antagonist of the human cardiac potassium channel HERG. *J. Pharmacol. Exp. Ther.* **1998,** *286* (2), 788-93.

89. Fermini, B.; Fossa, A. A., The impact of drug-induced QT interval prolongation on drug discovery and development. *Nat. Rv. Drug Discov.* **2003,** *2* (6), 439-447.

90. Zheng, W.; Spencer, R. H.; Kiss, L., High throughput assay technologies for ion channel drug discovery. *Assay Drug Dev. Technol.* **2004,** *2* (5), 543-52.

91. Rowley, M.; Kulagowski, J. J.; Watt, A. P.; Rathbone, D.; Stevenson, G. I.; Carling, R. W.; Baker, R.; Marshall, G. R.; Kemp, J. A.; Foster, A. C.; Grimwood, S.; Hargreaves, R.; Hurley, C.; Saywell, K. L.; Tricklebank, M. D.; Leeson, P. D., Effect of plasma protein binding on in vivo activity and brain penetration of glycine/NMDA receptor antagonists. *J. Med. Chem.* **1997,** *40* (25), 4053-68.

92. Veronesi, B., Characterization of the MDCK cell line for screening neurotoxicants. *Neurotoxicology* **1996,** *17* (2), 433-43.

93. Venkatakrishnan, K.; Moltke, L. L.; Greenblatt, D. J., Human drug metabolism and the cytochrome P450s: application and relevance of in vitro models. *J. Clin. Pharmacol.* **2001,** *41* (11), 1149-1179.

94. Obach, R. S.; Baxter, J. G.; Liston, T. E.; Silber, B. M.; Jones, B. C.; MacIntyre, F.; Rance, D. J.; Wastall, P., The prediction of human pharmacokinetic parameters from preclinical and in vitro metabolism data. *J. Pharmacol. Exp. Ther.* **1997,** *283* (1), 46-58.

95. Penthala, N. R.; Yerramreddy, T. R.; Crooks, P. A., Synthesis and in vitro screening of novel N-benzyl aplysinopsin analogs as potential anticancer agents. *Bioorg. Med. Chem. Lett.* **2011,** *21* (5), 1411-3.

96. Ottoni, O.; Cruz, R.; Alves, R., Efficient and simple methods for the introduction of the sulfonyl, acyl and alkyl protecting groups on the nitrogen of indole and its derivatives. *Tetrahedron* **1998,** *54* (46), 13915-13928.

97. Boyd, E. M.; Sperry, J., Synthesis of the selective neuronal nitric oxide synthase (nnos) inhibitor 5, 6-dibromo-2′-demethylaplysinopsin. *Synlett* **2011,** *2011* (06), 826-830.

98. Rajkumar, R.; Mahesh, R., Review: The auspicious role of the 5-HT3 receptor in depression: a probable neuronal target? *J. Psychopharmacol. (Oxf).* **2010,** *24* (4), 455-469.

99. Thompson, A. J.; Lummis, S. C., The 5-HT3 receptor as a therapeutic target. *Expert Opin. Ther. Targets* **2007,** *11* (4), 527-40.

100. Kivell, B.; Prisinzano, T., Kappa opioids and the modulation of pain. *Psychopharmacology (Berlin).* **2010,** *210* (2), 109-119.

101. Bruchas, Michael R.; Schindler, Abigail G.; Shankar, H.; Messinger, Daniel I.; Miyatake, M.; Land, Benjamin B.; Lemos, Julia C.; Hagan, C. E.; Neumaier, John F.; Quintana, A.; Palmiter, Richard D.; Chavkin, C., Selective p38α MAPK deletion in serotonergic neurons produces stress resilience in models of depression and addiction. *Neuron* **2011,** *71* (3), 498-511.

102. Cowley, G.; Springen, K., After fen-phen. *Newsweek* **1997,** *130* (13), 46-8.

103. Bach, A. W.; Lan, N. C.; Johnson, D. L.; Abell, C. W.; Bembenek, M. E.; Kwan, S. W.; Seeburg, P. H.; Shih, J. C., cDNA cloning of human liver monoamine oxidase A and B: molecular basis of differences in enzymatic properties. *Proc. Natl. Acad. Sci. U. S. A.* **1988,** *85* (13), 4934-8.

104. De Colibus, L.; Li, M.; Binda, C.; Lustig, A.; Edmondson, D. E.; Mattevi, A., Three-dimensional structure of human monoamine oxidase A (MAO A): relation to the structures of rat MAO A and human MAO B. *Proc. Natl. Acad. Sci. U. S. A.* **2005,** *102* (36), 12684-9.

APPENDIX

4. NMR data for compounds 31-80

(Z)-5-[(1H-indol-3-yl)methylene]-2-amino-1H-imidazol-4(5H)-one **(31)**: ^{1}H NMR (400 MHz, DMSO) δ 11.69 (s, 1H), 8.07 (s, 1H), 7.81 (d, *J* = 7.7 Hz, 1H), 7.43 (d, *J* = 7.9 Hz, 1H), 7.18 – 7.13 (m, 1H), 7.10 (t, *J* = 7.4 Hz, 1H), 6.75 (s, 1H). ^{13}C NMR (101 MHz, DMSO) δ 172.65, 160.79, 136.36, 127.82, 127.24, 122.53, 120.38, 118.85, 118.20, 112.32, 110.61, 104.96. HRESMS *m/z* calcd 227.0933 ($M^{\cdot+}$ +H); found: 227.0940.

(Z)-2-amino-5-[(4-bromo-1H-indol-3-yl)methylene]-1H-imidazol-4(5H)-one (**32**): ^{1}H NMR (400 MHz, DMSO) δ 11.87 (s, 1H), 8.52 (s, 1H), 7.45 (d, *J* = 8.0 Hz, 1H), 7.27 (d, *J* = 8.0 Hz, 1H), 7.04 (t, *J* = 8.0 Hz, 1H), 6.87 (s, 1H). ^{13}C NMR (DMSO) δ (ppm): 172.35, 157.48, 137.24, 132.38, 130.98, 127.28, 125.76, 122.29, 115.87, 112.25, 110.13, 104.48. HRESMS *m/z* calcd 305.0038 ($M^{\cdot+}$ +H); found: 305.0069.

(Z)-2-amino-5-[(5-bromo-1H-indol-3-yl)methylene]-1H-imidazol-4(5H)-one (**33**): ^{1}H NMR (400 MHz, DMSO) δ 11.72 (s, 1H), 8.06 (s, 1H), 7.38 (d, *J* = 8.5 Hz, 1H), 7.24 (d, *J* = 8.5 Hz, 1H), 6.59 (s, 1H). ^{13}C NMR (101 MHz, DMSO) δ 168.36, 164.54, 137.31, 135.03, 128.95, 125.35, 124.79, 121.68, 119.28, 114.19, 112.78, 102.97. HRESMS *m/z* calcd 305.0038 ($M^{\cdot+}$ +H); found: 305.0040.

(Z)-2-amino-5-[(6-bromo-1H-indol-3-yl)methylene]-1H-imidazol-4(5H)-one (**34**): ^{1}H NMR (400 MHz, DMSO) δ 11.66 (s, 1H), 8.05 (s, 1H), 7.82 (d, *J* = 7.9 Hz, 1H), 7.61 (s, 1H), 7.19 (d, *J* = 8.1 Hz, 1H), 6.60 (s, 1H). ^{13}C NMR (101 MHz, DMSO) δ 173.60, 163.59, 137.06, 131.59, 129.78, 126.20, 123.89, 123.10, 114.49, 112.89, 110.63, 105.21. HRESMS *m/z* calcd 305.0038 ($M^{\cdot+}$ +H); found: 305.0035.

(Z)-2-amino-5-[(7-bromo-1H-indol-3-yl)methylene]-1H-imidazol-4(5H)-one (**35**): ^{1}H NMR (400 MHz, DMSO) δ 11.65 (s, 1H), 8.24 (s, 1H), 7.87 (s, 1H), 7.36 (d, *J* = 6.1 Hz, 1H), 7.08 – 6.97 (m, 1H), 6.60 (s, 1H). ^{13}C NMR (101 MHz, DMSO) δ 171.84, 158.03, 134.65, 132.20, 128.92, 124.90, 124.84, 121.48, 118.63, 113.42, 109.65, 104.89. HRESMS *m/z* calcd 305.0038 ($M^{\cdot+}$ +H); found: 305.0043.

(E)-5-[(1H-indol-3-yl)methylene]-2-amino-1-methyl-1H-imidazol-4(5H)-one (**36**): ^{1}H NMR (400 MHz, DMSO) δ 11.47 (s, 1H), 9.10 (d, *J* = 2.4 Hz, 1H), 7.89 (d, *J* = 7.6 Hz, 1H), 7.43 (d, *J* = 7.7 Hz, 1H), 7.20 – 7.04 (m, 2H), 6.55 (s, 1H), 3.29 (s, 3H). ^{13}C NMR (DMSO) δ (ppm): 175.96, 165.44, 136.02, 131.24, 129.07, 128.19, 122.07, 119.88, 118.42, 112.22, 109.45, 105.11, 28.27. HRESMS *m/z* calcd 241.1089 ($M^{\cdot+}$ +H); found: 241.1091.

(E)-2-amino-5-[(4-bromo-1H-indol-3-yl)methylene]-1-methyl-1H-imidazol-4(5H)-one (**37**): ^{1}H NMR (DMSO, 400 MHz) δ 11.82 (s, 1H), 9.21 (s, 1H), 7.47 (d, *J* = 8.0 Hz, 1H), 7.42 (s, 1H), 7.29 (d, *J* = 8.0 Hz, 1H), 7.04 (t, *J* = 8.0 Hz, 1H), 3.23 (s, 3H); ^{13}C NMR (101 MHz, DMSO) δ 175.73, 165.40, 137.80, 131.10, 130.93, 125.10, 124.35, 123.11, 113.21, 112.45, 109.65, 105.89, 28.30. HRESMS *m/z* calcd 319.0194 ($M^{\cdot+}$ +H); found: 319.0151.

(E)-2-amino-5-[(5-bromo-1H-indol-3-yl)methylene]-1-methyl-1H-imidazol-4(5H)-one (**38**): ^{1}H NMR (400 MHz, DMSO) δ 11.60 (s, 1H), 9.11 (d, *J* = 2.0 Hz, 1H), 8.17 (s, 1H), 7.39 (d, *J* = 8.5 Hz, 1H), 7.24 (dd, *J* = 8.5, 1.6 Hz, 1H), 6.53 (s, 1H), 3.28 (s, 3H). ^{13}C NMR (101 MHz, DMSO) δ 175.90, 165.58, 134.72, 133.13, 131.75, 130.07, 124.52, 121.13, 114.17, 112.80, 109.38, 104.56, 28.35. HRESMS *m/z* calcd 319.0194 ($M^{\cdot+}$ +H); found: 319.0198.

(E)-2-amino-5-[(6-bromo-1H-indol-3-yl)methylene]-1-methyl-1H-imidazol-4(5H)-one

(**39**): ^{1}H NMR (400 MHz, DMSO) δ 11.53 (s, 1H), 9.06 (s, 1H), 7.87 (d, *J* = 8.5 Hz, 1H), 7.60 (d, *J* = 1.3 Hz, 1H), 7.22 (dd, *J* = 8.5, 1.4 Hz, 1H), 6.48 (s, 1H), 3.26 (s, 3H). ^{13}C NMR (101 MHz, DMSO) δ 175.80, 165.48, 136.73, 131.38, 130.74, 125.29, 124.57, 124.10, 113.42, 112.30, 109.23, 105. 73, 28.29. HRESMS *m/z* calcd 319.0194 ($M^{\cdot+}$ +H); found: 319.0194.

(E)-2-amino-5-[(7-bromo-1H-indol-3-yl)methylene]-1-methyl-1H-imidazol-4(5H)-one (**40**): ^{1}H NMR (DMSO, 400 MHz) δ (ppm): 11.64 (s, 1H), 9.14 (s, 1H), 7.93 (d, *J* = 8.0 Hz, 1H), 7.36 (d, *J* = 8.0 Hz, 1H), 7.05 (t, *J* = 8.0, 1H), 6.48 (s, 1H), 3.27 (s, 3H) ; ^{13}C NMR (101 MHz, DMSO) δ 175.93, 165.74, 134.35, 132.15, 129.89, 124.63, 121.25, 118.19, 110.70, 104.89(d), 104.22, 28.28. HRESMS *m/z* calcd 319.0194 ($M^{\cdot+}$ +H); found: 319.0198.

(Z)-4-[(1H-indol-3-yl)methylene]-2-amino-1-methyl-1H-imidazol-5(4H)-one (**41**): ^{1}H NMR (400 MHz, DMSO) δ 11.50 (s, 1H), 8.21 (s, 1H), 7.91 (d, *J* = 7.7 Hz, 1H), 7.41 (d, *J* = 7.8 Hz, 1H), 7.21 – 6.99 (m, 2H), 6.76 (s, 1H), 3.05 (s, 3H). ^{13}C NMR (101 MHz, DMSO) δ 169.60, 157.84, 136.29, 129.26, 127.16, 122.32, 120.20, 119.13, 112.88, 112.21, 111.89, 107.53, 26.00. HRESMS *m/z* calcd 241.1089 ($M^{\cdot+}$ +H); found: 241.1084.

(Z)-2-amino-4-[(4-bromo-1H-indol-3-yl)methylene]-1-methyl-1H-imidazol-5(4H)-one (**42**): ^{1}H NMR (400 MHz, DMSO) δ 11.88 (s, 1H), 8.57 (s, 1H), 7.57 (s, 1H), 7.46 (d, *J* = 8.0 Hz, 1H), 7.27 (d, *J* = 7.5 Hz, 1H), 7.04 (t, *J* = 7.8 Hz, 1H), 3.04 (s, 3H). ^{13}C NMR (101 MHz, DMSO) δ 173.45, 158.36, 137.73, 136.39, 131.47, 124.84, 124.23, 123.23, 113.54, 112.40, 112.28, 107.30, 26.00. HRESMS *m/z* calcd 319.0194 ($M^{\cdot+}$ +H); found: 319.0196.

(Z)-2-amino-4-[(5-bromo-1H-indol-3-yl)methylene]-1-methyl-1H-imidazol-5(4H)-one (**43**): ^{1}H NMR (400 MHz, DMSO) δ 11.67 (s, 1H), 8.22 (s, 1H), 8.18 (s, 1H), 7.37 (d, *J* = 8.5 Hz,

1H), 7.24 (dd, *J* = 8.6, 1.4 Hz, 1H), 6.73 (s, 1H), 3.04 (s, 3H). ^{13}C NMR (101 MHz, DMSO) δ 163.45, 154.34, 134.68, 132.60, 129.02, 123.29, 121.98, 121.39, 114.58, 114.05, 113.89, 105.78, 26.69. HRESMS *m/z* calcd 319.0194 ($M^{\cdot+}$ +H); found: 319.0154.

(Z)-2-amino-4-[(6-bromo-1H-indol-3-yl)methylene]-1-methyl-1H-imidazol-5(4H)-one (**44**): ^{1}H NMR (400 MHz, DMSO) δ 11.58 (s, 1H), 8.19 (s, 1H), 7.95 (d, *J* = 8.5 Hz, 1H), 7.60 (s, 1H), 7.17 (dd, *J* = 8.5, 1.3 Hz, 1H), 6.70 (s, 1H), 3.04 (s, 3H). ^{13}C NMR (101 MHz, DMSO) δ163.34, 153.71, 137.39, 133.03, 127.02, 123.97, 123.31, 121.10, 115.78, 113.29, 112.75, 105.57, 26.10. HRESMS *m/z* calcd 319.0194 ($M^{\cdot+}$ +H); found: 319.0144.

(Z)-2-amino-4-[(7-bromo-1H-indol-3-yl)methylene]-1-methyl-1H-imidazol-5(4H)-one (**45**): ^{1}H NMR (400 MHz, DMSO) δ 11.66 (s, 1H), 8.28 (s, 1H), 7.94 (d, *J* = 7.9 Hz, 1H), 7.35 (d, *J* = 7.5 Hz, 1H), 7.02 (t, *J* = 7.7 Hz, 1H), 6.71 (s, 1H), 3.04 (s, 3H). ^{13}C NMR (101 MHz, DMSO) δ 165.85, 153.49.29, 134.60, 131.07, 129.10, 124.69, 122.38, 114.25, 112.69, 105.87, 105.34, 103.21, 25.88. HRESMS *m/z* calcd 319.0194 ($M^{\cdot+}$ +H); found: 319.0138.

(E)-5-[(1H-indol-3-yl)methylene]-1-methyl-2-(methylamino)-1H-imidazol-4(5H)-one (**46**): ^{1}H NMR (400 MHz, DMSO) δ 11.48 (s, 1H), 9.09 (s, 1H), 7.89 (d, *J* = 7.6 Hz, 1H), 7.43 (d, *J* = 7.8 Hz, 1H), 7.12 (dt, *J* = 14.7, 6.9 Hz, 2H), 6.55 (s, 1H), 3.26 (s, 3H), 2.91 (s, 3H). ^{13}C NMR (101 MHz, DMSO) δ 162.03, 153.21, 135.87, 130.91, 127.50, 122.48, 122.20, 120.75, 118.65, 115.08, 112.36, 108.56, 29.01, 26.24. HRESMS *m/z* calcd 255.1246 ($M^{\cdot+}$ +H); found: 255.1301.

(E)-5-[(4-bromo-1H-indol-3-yl)methylene]-1-methyl-2-(methylamino)-1H-imidazol-4(5H)-one (**47**): ^{1}H NMR (400 MHz, DMSO) δ 11.82 (s, 1H), 9.21 (s, 1H), 7.47 (d, *J* = 7.7 Hz, 1H), 7.43 (s, 1H), 7.29 (d, *J* = 7.5 Hz, 1H), 7.04 (t, *J* = 7.8 Hz, 1H), 3.20 (s, 3H), 2.90 (s, 3H).

^{13}C NMR (101 MHz, DMSO) δ 171.84, 159.82, 137.69, 133.18, 128.44, 125.89, 124.34, 115.44, 113.67, 112.19, 109.69, 102.01, 31.56, 28.16. HRESMS *m/z* calcd 333.0351 ($M^{\cdot+}$ +H); found: 333.0321.

(E)-5-[(5-bromo-1H-indol-3-yl)methylene]-1-methyl-2-(methylamino)-1H-imidazol-4(5H)-one (**48**): ^{1}H NMR (400 MHz, DMSO) δ 11.60 (s, 1H), 9.09 (s, 1H), 8.33 (s, 1H), 7.49 (d, *J* = 8.6 Hz, 1H), 7.24 (d, *J* = 8.5 Hz, 1H), 6.54 (s, 1H), 3.26 (s, 3H), 2.91 (s, 3H). ^{13}C NMR (101 MHz, DMSO) δ 169.35, 153.20, 136.00, 135.39, 133.71, 129.06, 122.88, 122.10, 114.05, 113.29, 108.38, 104.24, 30.11, 28.35. HRESMS *m/z* calcd 333.0351 ($M^{\cdot+}$ +H); found: 333.0358.

(E)-5-[(6-bromo-1H-indol-3-yl)methylene]-1-methyl-2-(methylamino)-1H-imidazol-4(5H)-one (**49**): ^{1}H NMR (400 MHz, DMSO) δ 11.53 (s, 1H), 9.05 (s, 1H), 8.67 (s, 1H), 7.86 (dd, *J* = 8.4, 4.8 Hz, 1H), 7.22 (d, *J* = 8.4 Hz, 1H), 6.50 (s, 1H), 3.24 (s, 3H), 2.91 (s, 3H). ^{13}C NMR (101 MHz, DMSO) δ 168.97, 151.08, 136.89, 136.39, 132.20, 129.63, 122.75, 120.59, 114.79, 114.75, 109.43, 101.64, 28.11, 27.53. HRESMS *m/z* calcd 333.0351 ($M^{\cdot+}$ +H); found: 333.0298.

(E)-5-[(7-bromo-1H-indol-3-yl)methylene]-1-methyl-2-(methylamino)-1H-imidazol-4(5H)-one (**50**): ^{1}H NMR (400 MHz, DMSO) δ 11.62 (s, 1H), 9.11 (s, 1H), 7.93 (d, *J* = 7.9 Hz, 1H), 7.36 (d, *J* = 7.2 Hz, 1H), 7.05 (t, *J* = 7.7 Hz, 1H), 6.49 (s, 1H), 3.25 (s, 3H), 2.92 (s, 3H). ^{13}C NMR (101 MHz, DMSO) δ 169.22, 153.59, 137.97, 135.02, 128.74, 130.19, 127.25, 125.38, 120.19, 115.23, 108.34, 104.34, 31.07, 28.20. HRESMS *m/z* calcd 333.0351 ($M^{\cdot+}$ +H); found: 333.0348.

(E)-5-[(1H-indol-3-yl)methylene]-2-imino-1,3-dimethylimidazolidin-4-one (**51**): ^{1}H NMR (400 MHz, DMSO) δ 11.46 (s, 1H), 8.70 (s, 1H), 7.86 (d, *J* = 7.7 Hz, 1H), 7.42 (d, *J* = 7.8 Hz,

1H), 7.12 (dt, *J* = 14.5, 7.0 Hz, 2H), 6.42 (s, 1H), 3.25 (s, 3H), 3.06 (s, 3H). ^{13}C NMR (101 MHz, DMSO) δ 160.53, 152.24, 136.22, 131.67, 128.14, 123.24, 122.25, 121.20, 118.95, 116.21, 112.80, 108.94, 29.30, 26.65. HRESMS *m/z* calcd 255.1246 ($M^{\cdot+}$ +H); found: 255.1290.

(E)-5-[(4-bromo-1H-indol-3-yl)methylene]-2-imino-1,3-dimethylimidazolidin-4-one (**52**): ^{1}H NMR (400 MHz, DMSO) δ 11.79 (s, 1H), 8.68 (s, 1H), 7.46 (d, *J* = 8.0 Hz, 1H), 7.28 (d, *J* = 7.6 Hz, 1H), 7.25 (s, 1H), 7.03 (t, *J* = 7.8 Hz, 1H), 3.20 (s, 3H), 3.04 (s, 3H). ^{13}C NMR (101 MHz, DMSO) δ 169.03, 157.38, 137.08, 136.34, 129.04, 128.81, 127.44, 123.95, 120.21, 114.63, 110.05, 105.24, 30.82, 26.30. HRESMS *m/z* calcd 333.0351 ($M^{\cdot+}$ +H); found: 333.0348.

(E)-5-[(5-bromo-1H-indol-3-yl)methylene]-2-imino-1,3-dimethylimidazolidin-4-one (**53**): ^{1}H NMR (400 MHz, DMSO) δ 12.17 (s, 1H), 8.96 (s, 1H), 8.37 (s, 1H), 7.47 (d, *J* = 8.5 Hz, 1H), 7.34 (d, *J* = 8.5 Hz, 1H), 7.28 (s, 1H), 3.48 (s, 3H), 3.19 (s, 3H). ^{13}C NMR (101 MHz, DMSO) δ 160.56, 152.42, 134.96, 132.62, 130.02, 125.69, 122.81, 121.62, 115.65, 114.76, 114.15, 108.64, 29.37, 26.69. HRESMS *m/z* calcd 333.0351 ($M^{\cdot+}$ +H); found: 333.0351.

(E)-5-[(6-bromo-1H-indol-3-yl)methylene]-2-imino-1,3-dimethylimidazolidin-4-one (**54**): ^{1}H NMR (400 MHz, DMSO) δ 12.07 (s, 1H), 8.93 (s, 1H), 8.04 (d, *J* = 8.5 Hz, 1H), 7.69 (s, 1H), 7.34 (d, *J* = 8.4 Hz, 1H), 7.23 (s, 1H), 3.48 (s, 3H), 3.19 (s, 3H). ^{13}C NMR (101 MHz, DMSO) δ 160.53, 152.49, 137.09, 132.25, 127.21, 123.90, 122.92, 120.94, 115.84, 115.47, 115.35, 109.00, 29.37, 26.70. HRESMS *m/z* calcd 333.0351 ($M^{\cdot+}$ +H); found: 333.0352.

(E)-5-[(7-bromo-1H-indol-3-yl)methylene]-2-imino-1,3-dimethylimidazolidin-4-one (**55**): ^{1}H NMR (DMSO, 400 MHz) δ 11.63 (s, 1H), 8.73 (s, 1H), 7.90 (d, *J* = 8 Hz, 1H), 7.36 (d, *J* = 7.6 Hz, 1H), 7.04 (t, *J* = 7.6 Hz, 1H), 6.37 (s, 1H), 3.24 (s, 3H), 3.05 (s, 3H). ^{13}C NMR (101 MHz, DMSO) δ 169.27, 163.99, 137.34, 134.68, 129.65, 129.40, 127.84, 125.12, 121.83, 118.53,

109.32, 104.91, 31.17, 25.80. HRESMS *m/z* calcd 333.0351 ($M^{\cdot+}$ +H); found: 333.0352.

(Z)-4-[(1H-indol-3-yl)methylene]-1-methyl-2-(methylamino)-1H-imidazol-5(4H)-one (**56**): ^{1}H NMR (400 MHz, DMSO) δ 11.46 (s, 1H), 8.40 (s, 1H), 7.86 (d, *J* = 8.0 Hz, 1H), 7.44 (d, *J* = 7.8 Hz, 1H), 7.10 (m, 2H), 6.67 (s, 1H), 3.06 (s, 3H), 2.98 (s, 3H). ^{13}C NMR (101 MHz, DMSO) δ 166.33, 154.84, 135.22, 135.68, 131.67, 128.14, 127.24, 121.70, 119.90, 114.50, 111.80, 109.94, 27.24, 25.30. HRESMS *m/z* calcd 255.1246 ($M^{\cdot+}$ +H); found: 255.1187.

(Z)-4-[(4-bromo-1H-indol-3-yl)methylene]-1-methyl-2-(methylamino)-1H-imidazol-5(4H)-one (**57**): ^{1}H NMR (400 MHz, MeOD) δ 8.58 (s, 1H), 7.97 (s, 1H), 7.42 (d, *J* = 8.1 Hz, 1H), 7.30 (d, *J* = 7.5 Hz, 1H), 7.04 (t, *J* = 7.9 Hz, 1H), 3.14 (s, 3H), 3.09 (s, 3H). ^{13}C NMR (101 MHz, DMSO) δ 170.05, 156.76, 138.04, 136.87, 131.66, 125.18, 124.09, 120.29, 112.97, 112.30, 110.92, 104.34, 27.19, 25.01. HRESMS *m/z* calcd 333.0351 ($M^{\cdot+}$ +H); found: 333.0367.

(Z)-4-[(5-bromo-1H-indol-3-yl)methylene]-1-methyl-2-(methylamino)-1H-imidazol-5(4H)-one (**58**): ^{1}H NMR (400 MHz, MeOD) δ 8.26 (s, 1H), 8.17 (s, 1H), 7.33 (d, *J* = 8.5 Hz, 1H), 7.27 (d, *J* = 8.6 Hz, 1H), 6.96 (s, 1H), 3.14 (s, 3H), 3.11 (s, 3H). ^{13}C NMR (101 MHz, DMSO) δ 171.31, 167.27, 135.12, 134.21, 127.55, 126.25, 123.29, 120.88, 115.20, 114.23, 110.62, 105.01, 28.03, 26.12. HRESMS *m/z* calcd 333.0351 ($M^{\cdot+}$ +H); found: 333.0321.

(Z)-4-[(6-bromo-1H-indol-3-yl)methylene]-1-methyl-2-(methylamino)-1H-imidazol-5(4H)-one (**59**): ^{1}H NMR (DMSO, 400 MHz) δ (ppm): ^{1}H NMR (400 MHz, MeOD) δ 8.22 (s, 1H), 7.82 (d, *J* = 8.5 Hz, 1H), 7.58 (s, 1H), 7.24 (d, *J* = 7.3 Hz, 1H), 7.00 (s, 1H), 3.14 (s, 3H), 3.10 (s, 3H). ^{13}C NMR (101 MHz, DMSO) δ 163.03, 153.56, 136.79, 134.55, 128.21, 123.45, 123.29, 121.03, 113.98, 113.47, 112.25, 108.89, 27.37, 25.40. HRESMS *m/z* calcd 333.0351 ($M^{\cdot+}$ +H); found: 333.0329.

(Z)-4-[(7-bromo-1H-indol-3-yl)methylene]-1-methyl-2-(methylamino)-1H-imidazol-5(4H)-one (**60**): ^{1}H NMR (400 MHz, MeOD) δ 8.33 (s, 1H), 7.88 (d, *J* = 7.7 Hz, 1H), 7.36 (d, *J* = 7.6 Hz, 1H), 7.06 (t, *J* = 7.8 Hz, 1H), 7.01 (s, 1H), 3.15 (s, 3H), 3.11 (s, 3H). ^{13}C NMR (101 MHz, DMSO) δ 167.72, 155.58, 135.20, 130.18, 127.98, 125.41, 125.05, 123.56, 118.23, 110.39, 108.34, 104.38, 26.89, 25.07. HRESMS *m/z* calcd 333.0351 ($M^{\cdot+}$ +H); found: 333.0339.

(5E)-5-[(1H-indol-3-yl)methylene]-1,3-dimethyl-2-(methylimino)imidazolidin-4-one (**61**): ^{1}H NMR (400 MHz, DMSO) δ 8.75 (s, 1H), 7.77 (d, *J* = 8.0 Hz, 1H), 7.44 (d, *J* = 8.0 Hz, 1H), 7.22 (m, 2H), 6.99 (s, 1H), 3.30 (s, 3H), 3.15 (s, 3H), 3.10 (s, 3H). ^{13}C NMR (DMSO) δ (ppm): 175.22, 163.68, 136.34, 132.45, 128.11, 125.67, 123.18, 121.06, 119.24, 112.14, 110.01, 108.87, 32.87, 31.23, 26.80. HRESMS *m/z* calcd 269.1402 ($M^{\cdot+}$ +H); found: 269.1402.

(5E)-5-[(4-bromo-1H-indol-3-yl)methylene]-1,3-dimethyl-2-(methylimino)imidazolidin-4-one (**62**): ^{1}H NMR (400 MHz, DMSO) δ 11.83 (s, 1H), 8.69 (s, 1H), 7.47 (d, *J* = 8.0 Hz, 1H), 7.28 (d, *J* = 7.5 Hz, 1H), 7.25 (s, 1H), 7.04 (t, *J* = 7.8 Hz, 1H), 3.18 (s, 3H), 3.06 (s, 3H), 2.73 (s, 3H). ^{13}C NMR (101 MHz, DMSO) δ 165.24, 156.45, 137.75, 130.63, 129.84, 124.94, 124.43, 123.11, 113.26, 112.41, 109.32, 102.20, 34.41, 34.27, 28.49. HRESMS *m/z* calcd 347.0507 ($M^{\cdot+}$ +H); found: 347.0508.

(5E)-5-[(5-bromo-1H-indol-3-yl)methylene]-1,3-dimethyl-2-(methylimino)imidazolidin-4-one (**63**): ^{1}H NMR (400 MHz, DMSO) δ 11.64 (s, 1H), 8.73 (s, 1H), 8.16 (s, 1H), 7.38 (d, *J* = 8.5 Hz, 1H), 7.25 (d, *J* = 8.5 Hz, 1H), 6.42 (s, 1H), 3.36 (s, 3H), 3.23 (s, 3H), 2.99 (s, 3H). ^{13}C NMR (101 MHz, DMSO) δ 162.39, 152.07, 134.70, 130.05, 129.07, 124.59, 121.23, 114.11, 113.30, 112.77, 109.23, 103.51, 33.03, 31.23, 26.80. HRESMS *m/z* calcd 347.0507 ($M^{\cdot+}$ +H); found: 347.0512.

(5E)-5-[(6-bromo-1H-indol-3-yl)methylene]-1,3-dimethyl-2-(methylimino)imidazolidin-4-one (**64**): ^{1}H NMR (400 MHz, DMSO) δ 11.77 (s, 1H), 8.82 (s, 1H), 7.94 (d, *J* = 7.7 Hz, 1H), 7.65 (s, 1H), 7.27 (d, *J* = 8.1 Hz, 1H), 6.74 (s, 1H), 3.32 (s, 3H), 3.23 (s, 3H), 3.00 (s, 3H). ^{13}C NMR (101 MHz, DMSO) δ 163.20, 153.12, 137.45, 130.91, 130.02, 124.22, 123.07, 114.46, 113.72, 113.08, 110.11, 105.14, 34.01, 30.29, 23.30. HRESMS *m/z* calcd 347.0507 ($M^{\cdot+}$ +H); found: 347.0514.

(5E)-5-[(7-bromo-1H-indol-3-yl)methylene]-1,3-dimethyl-2-(methylimino)imidazolidin-4-one (**65**): ^{1}H NMR (400 MHz, DMSO) δ 11.86 (s, 1H), 8.35 (s, 1H), 7.99 (d, *J* = 7.9 Hz, 1H), 7.40 (d, *J* = 7.5 Hz, 1H), 7.09 (t, *J* = 7.8 Hz, 1H), 6.71 (s, 1H), 3.23 (s, 3H), 2.99 (s, 3H), 2.96 (s, 3H). ^{13}C NMR (101 MHz, DMSO) δ 162.44, 153.30, 141.59, 129.83, 126.62, 126.24, 125.95, 124.11, 120.70, 110.20, 107.78, 105.03, 35.80, 26.73, 24.86. HRESMS *m/z* calcd 347.0507 ($M^{\cdot+}$ +H); found: 347.0513.

(Z)-5-[(1H-indol-3-yl)methylene]-2-thioxoimidazolidin-4-one (**66**): ^{1}H NMR (400 MHz, DMSO) δ 8.40 (s, 1H), 7.79 (d, *J* = 7.6 Hz, 1H), 7.43 (d, *J* = 7.9 Hz, 1H), 7.16 (ddd, *J* = 14.2, 7.7, 3.8 Hz, 2H), 6.67 (s, 1H). ^{13}C NMR (101 MHz, DMSO) δ 177.19, 165.91, 136.35, 129.33, 127.56, 123.69, 123.07, 121.13, 118.49, 112.54, 108.73, 105.93. HRESMS *m/z* calcd 266.0363 ($M^{\cdot+}$ +Na); found: 266.0359.

(Z)-5-[(4-bromo-1H-indol-3-yl)methylene]-2-thioxoimidazolidin-4-one (**67**): ^{1}H NMR (400 MHz, DMSO) δ 12.03 (s, 1H), 8.43 (s, 1H), 7.66 (s, 1H), 7.49 (d, *J* = 8.0 Hz, 1H), 7.33 (d, *J* = 7.5 Hz, 1H), 7.09 (t, *J* = 7.8 Hz, 1H). ^{13}C NMR (101 MHz, DMSO) δ 177.69, 166.04, 138.05, 131.38, 125.74, 124.27, 124.07, 123.93, 113.39, 112.61, 109.21, 106.49. HRESMS *m/z* calcd 343.9468 ($M^{\cdot+}$ +Na); found: 343.9476.

(Z)-5-[(5-bromo-1H-indol-3-yl)methylene]-2-thioxoimidazolidin-4-one (**68**): ^{1}H NMR (400 MHz, DMSO) δ 12.16 (s, 1H), 8.46 (s, 1H), 8.04 (d, *J* = 1.2 Hz, 1H), 7.41 (d, *J* = 8.6 Hz, 1H), 7.30 (dd, *J* = 8.6, 1.5 Hz, 1H), 6.82 (s, 1H). ^{13}C NMR (101 MHz, DMSO) δ 177.49, 165.86, 135.10, 130.40, 129.37, 125.59, 124.32, 121.28, 114.48, 113.80, 108.55, 105.29. HRESMS *m/z* calcd 343.9468 ($M^{\cdot+}$ +Na); found: 343.9458.

(Z)-5-[(6-bromo-1H-indol-3-yl)methylene]-2-thioxoimidazolidin-4-one (**69**): ^{1}H NMR (400 MHz, DMSO) δ 8.42 (s, 1H), 7.78 (d, *J* = 8.5 Hz, 1H), 7.63 (d, *J* = 1.5 Hz, 1H), 7.23 (dd, *J* = 8.5, 1.6 Hz, 1H), 6.70 (s, 1H). ^{13}C NMR (101 MHz, DMSO) δ 178.11, 167.27, 137.22, 129.78, 127.05, 126.55, 123.62, 120.58, 115.48, 115.03, 109.59, 104.30. HRESMS *m/z* calcd 343.9468 ($M^{\cdot+}$ +Na); found: 343.9460.

(Z)-5-[(7-bromo-1H-indol-3-yl)methylene]-2-thioxoimidazolidin-4-one (**70**): ^{1}H NMR (400 MHz, DMSO) δ 11.97 (s, 1H), 8.53 (s, 1H), 7.83 (d, *J* = 7.9 Hz, 1H), 7.40 (d, *J* = 7.5 Hz, 1H), 7.07 (t, *J* = 7.8 Hz, 1H), 6.76 (s, 1H). ^{13}C NMR (101 MHz, DMSO) δ 177.72, 166.09, 134.83, 130.11, 129.28, 125.60, 124.97, 122.38, 118.19, 109.95, 105.13, 104.80. HRESMS *m/z* calcd 343.9468 ($M^{\cdot+}$ +Na); found: 343.9455.

(Z)-5-[(1H-indol-3-yl)methylene]-2-(methylthio)-1H-imidazol-4(5H)-one (**71**): ^{1}H NMR (400 MHz, DMSO) δ 11.85 (s, 1H), 8.37 (s, 1H), 8.15 (d, *J* = 7.6 Hz, 1H), 7.46 (d, *J* = 7.8 Hz, 1H), 7.22 – 7.13 (m, 2H), 7.11 (s, 1H), 2.68 (s, 3H). ^{13}C NMR (101 MHz, DMSO) δ 170.62, 159.79, 136.78, 136.40, 135.36, 132.46, 127.15, 122.87, 120.99, 116.30, 112.57, 111.58, 12.67. HRESMS *m/z* calcd 280.0521 ($M^{\cdot+}$ +Na); found: 280.0505.

(Z)-5-[(4-bromo-1H-indol-3-yl)methylene]-2-(methylthio)-1H-imidazol-4(5H)-one (**72**): ^{1}H NMR (400 MHz, DMSO) δ 11.64 (s, 1H), 8.75 (s, 1H), 7.94 (s, 1H), 7.52 (d, *J* = 8.0 Hz, 1H),

7.34 (d, *J* = 7.5 Hz, 1H), 7.08 (t, *J* = 7.8 Hz, 1H), 2.66 (s, 3H). ^{13}C NMR (101 MHz, DMSO) δ 170.64, 161.07, 138.01, 135.52, 133.94, 125.75, 124.45, 123.79, 115.56, 113.44, 112.72, 111.57, 12.69. HRESMS *m/z* calcd 357.9626 ($M^{\cdot+}$ +Na); found: 357.9614.

(Z)-5-[(5-bromo-1H-indol-3-yl)methylene]-2-(methylthio)-1H-imidazol-4(5H)-one (**73**): ^{1}H NMR (400 MHz, DMSO) δ 11.57 (s, 1H), 8.92 (s, 1H), 8.27 (s, 1H), 7.42 (d, *J* = 8.6 Hz, 1H), 7.30 (d, *J* = 8.6 Hz, 1H), 7.07 (s, 1H), 2.72 (s, 3H). ^{13}C NMR (101 MHz, DMSO) δ 170.74, 159.91, 136.04, 135.26, 134.60, 128.30, 125.42, 124.52, 116.90, 114.46, 113.65, 111.96, 12.88. HRESMS *m/z* calcd 357.9626 ($M^{\cdot+}$ +Na); found: 357.9610.

(Z)-5-[(6-bromo-1H-indol-3-yl)methylene]-2-(methylthio)-1H-imidazol-4(5H)-one (**74**): ^{1}H NMR (400 MHz, DMSO) δ 11.71 (s, 1H), 8.34 (s, 1H), 8.20 (d, *J* = 8.5 Hz, 1H), 7.65 (d, *J* = 1.6 Hz, 1H), 7.25 (dd, *J* = 8.5, 1.7 Hz, 1H), 7.07 (s, 1H), 2.67 (s, 3H). ^{13}C NMR (101 MHz, DMSO) δ 170.66, 160.55, 137.74, 135.83, 133.28, 126.05, 123.71, 122.24, 115.74, 115.53, 115.14, 111.84, 12.75. HRESMS *m/z* calcd 357.9626 ($M^{\cdot+}$ +Na); found: 357.9612.

(Z)-5-[(7-bromo-1H-indol-3-yl)methylene]-2-(methylthio)-1H-imidazol-4(5H)-one (**75**): ^{1}H NMR (400 MHz, DMSO) δ 12.03 (s, 1H), 8.39 (s, 1H), 8.19 (d, *J* = 7.9 Hz, 1H), 7.39 (d, *J* = 7.6 Hz, 1H), 7.10 (s, 1H), 7.07 (t, *J* = 7.8 Hz, 1H), 2.67 (s, 3H). ^{13}C NMR (101 MHz, DMSO) δ 170.58, 161.01, 136.28, 135.13, 132.93, 128.87, 125.47, 122.30, 119.61, 115.42, 112.77, 105.13, 12.69. HRESMS *m/z* calcd 357.9626 ($M^{\cdot+}$ +Na); found: 357.9619.

(Z)-5-[(1H-indol-3-yl)methylene]-2-(methylamino)-1H-imidazol-4(5H)-one (**76**): ^{1}H NMR (400 MHz, DMSO) δ 8.16 (s, 1H), 7.85 (d, *J* = 7.1 Hz, 1H), 7.41 (d, *J* = 8.0 Hz, 1H), 7.16 – 7.11 (m, 1H), 7.10 – 7.05 (m, 1H), 6.65 (s, 1H), 2.92 (s, 3H). ^{13}C NMR (101 MHz, DMSO) δ 166.72, 159.00, 136.32, 132.32, 130.41, 127.22, 122.24, 120.06, 118.98, 112.18, 112.05, 109.39,

28.41. HRESMS *m/z* calcd 263.0909 ($M^{\cdot+}$ +Na); found: 263.0906.

(Z)-5-[(4-bromo-1H-indol-3-yl)methylene]-2-(methylamino)-1H-imidazol-4(5H)-one (**77**): ^{1}H NMR (400 MHz, DMSO) δ 12.18 (s, 1H), 8.74 (s, 1H), 7.93 (s, 1H), 7.53 (d, *J* = 7.9 Hz, 1H), 7.37 (d, *J* = 7.5 Hz, 1H), 7.11 (t, *J* = 7.9 Hz, 1H), 2.68 (s, 3H). ^{13}C NMR (101 MHz, DMSO) δ 171.84, 157.01, 138.02, 137.03, 127.37, 124.43, 123.83, 122.83, 121.88, 121.70, 112.76, 111.53, 28.15. HRESMS *m/z* calcd 341.0014 ($M^{\cdot+}$ +Na); found: 341.0002.

(Z)-5-[(5-bromo-1H-indol-3-yl)methylene]-2-(methylamino)-1H-imidazol-4(5H)-one (**78**): ^{1}H NMR (400 MHz, DMSO) δ 11.63 (s, 1H), 8.51 (s, 1H), 8.14 (s, 1H), 7.36 (d, *J* = 8.6 Hz, 1H), 7.23 (d, *J* = 8.3 Hz, 1H), 6.60 (s, 1H), 2.92 (s, 3H). ^{13}C NMR (101 MHz, DMSO) δ 169.29, 155.11, 137.51, 135.19, 134.16, 132.29, 130.07, 122.25, 117.22, 114.15, 104.76, 104.36, 28.53. HRESMS *m/z* calcd 341.0014 ($M^{\cdot+}$ +Na); found: 341.0002.

(Z)-5-[(6-bromo-1H-indol-3-yl)methylene]-2-(methylamino)-1H-imidazol-4(5H)-one (**79**): ^{1}H NMR (400 MHz, DMSO) δ 11.59 (s, 1H), 8.14 (s, 1H), 7.90 (d, *J* = 6.2 Hz, 1H), 7.60 (s, 1H), 7.18 (d, *J* = 8.5 Hz, 1H), 6.60 (s, 1H), 2.91 (s, 3H). ^{13}C NMR (101 MHz, DMSO) δ 167.35, 154.29, 137.26, 136.33, 132.23, 126.16, 126.12, 122.93, 114.94, 114.75, 114.34, 100.19, 25.97. HRESMS *m/z* calcd 341.0014 ($M^{\cdot+}$ +Na); found: 341.0007.

(Z)-5-[(7-bromo-1H-indol-3-yl)methylene]-2-(methylamino)-1H-imidazol-4(5H)-one (**80**): ^{1}H NMR (400 MHz, DMSO) δ 11.62 (s, 1H), 8.29 (s, 1H), 7.95 (d, *J* = 7.4 Hz, 1H), 7.36 (d, *J* = 7.2 Hz, 1H), 7.03 (t, *J* = 7.5 Hz, 1H), 6.62 (s, 1H), 2.92 (s, 3H). ^{13}C NMR (101 MHz, DMSO) δ 168.13, 151.53, 138.79, 136.39, 134.67, 128.92, 124.77, 118.82, 117.42, 110.12, 108.13, 104.86, 28.14. HRESMS *m/z* calcd 341.0014 ($M^{\cdot+}$ + Na); found: 340.999

CMPD	5-HT1A	5-HT1B	5-HT1D	5-HT1E	5-HT2A	5-HT2B	5-HT2C	5-HT3	5-HT4	5-HT5A	5-HT6	5-HT7
31					1169	232	349			101		
32					4617	447	604			123		
33					58	51	35			89	742	512
34				>10,000	3128	269	201			184		
35				>10,000	2147	457	841			112	1405	
36						964	4778					
37					1413	784	2013					799
38	3215			>10,000		852	2454					
39						1378	3883					
40				>10,000	>10,000	1422	4129			1323		
41				>10,000		1284	10000					
42	3445				8669	228	1698			1282		
43	7361				279	94	1271			2332		1223
44	>10,000				4158	190	1916			5355		
45	7269			>10,000		593	10000			1550		
46						716	2354					
47	4608	>10,000	>10,000		662	99	320	5916		1454	1409	
48	2624					883	1078	6178				4114
49						489	2275					
50	>10,000			>10,000	7971	661	2208			1425	2306	
51	>10,000					4449	10000	3029			8768	
52	315	>10,000	6835	>10,000	>10,000	589	2762	656		7828		
53	527					1248	1265	1000		6725		
54	>10,000	0				2671	1704			9621		
55	1812	>10,000	>10,000	>10,000		349	3013	1223				
56				>10,000		5055	10000					
57		>10,000	>10,000			774	2339					

CMPD	5-HT1A	5-HT1B	5-HT1D	5-HT1E	5-HT2A	5-HT2B	5-HT2C	5-HT3	5-HT4	5-HT5A	5-HT6	5-HT7
58					>10,000	520	133					3350
59				>10,000		1274	10000					
60				>10,000		839	10000					
61				>10,000	>10,000	4554	10000	1511			1716	
62	6927		2552	>10,000	>10,000	897	1856	591		5080	7523	
63	2513					1620	2430	2624		9118		5367
64	>10,000					2468	1239			4681		
65	>10,000	>10,000	8867			965	6470			6913	7300	
66												
67												
68						287	970		928			
69						369	1870		2359			
70						780	885		1063			
71					470	50	80		472	3372	3733	
72	2753					1676	4348					
73						1346	2094		3799			
74					676	93	426		226		860	
75						2714						
76						1136	4367		5308			
77						154	980		1156			
78									2214			
79						993			2345			
80					3593	353	678		603	3324		

Table 4-1 Secondary in vitro binding data from compounds 31-80 at all 12 5-HT subtypes

NMR data for compounds 81-92

*(E)-5-[(1-benzyl-1H-indol-3-yl)methylene]-2-imino-1,3-dimethylimidazolidin-4-one (**81**):* ^{1}H NMR (400 MHz, $CDCl_3$) δ 9.03 (s, 1H), 7.78 (d, *J* = 8.0 Hz, 1H), 7.34 – 7.24 (m, 7H), 7.19 (d, *J* = 7.3 Hz, 2H), 6.63 (s, 1H), 5.42 (s, 2H), 3.34 (s, 3H), 3.18 (s, 3H). ^{13}C NMR (101 MHz, $CDCl_3$) δ 153.42, 145.37, 136.61, 136.14, 132.69, 128.86 (d), 127.83, 126.75 (d), 124.74, 122.71, 120.77, 120.04, 117.77, 110.59, 108.94, 108.73, 50.85, 26.34, 24.60. HRESMS *m/z* calcd 345.1715 ($M^{\cdot+}$ +H); found: 345.1710.

*(E)-5-[(1-(4-chlorobenzyl)-1H-indol-3-yl)methylene]-2-imino-1,3-dimethylimidazolidin-4-one (**82**):* ^{1}H NMR (400 MHz, DMSO) δ 9.51 (s, 1H), 9.07 (s, 1H), 8.11 (d, J = 6.2 Hz, 1H), 7.60 (d, J = 6.6 Hz, 1H), 7.41 (d, J = 7.5 Hz, 2H), 7.27 (m, 5H), 5.61 (s, 2H), 3.54 (s, 3H), 3.22 (s, 3H). ^{13}C NMR (101 MHz, DMSO) δ 161.58, 151.42, 138.28, 135.83, 134.12, 133.29, 129.93, 130.48, 130.20, 128.83, 128.24, 122.95, 122.35, 120.72, 118.88, 115.11, 110.73, 108.46, 48.18, 30.45, 28.28. HRESMS *m/z* calcd 379.1326 ($M^{\cdot+}$ +H); found: 379.1319.

*(E)-5-[(1-(2-chlorobenzyl)-1H-indol-3-yl)methylene]-2-imino-1,3-dimethylimidazolidin-4-one (**83**):* ^{1}H NMR (400 MHz, DMSO) δ 9.36 (s, 1H), 9.02 (s, 1H), 8.14 (d, *J* = 6.5 Hz, 1H), 7.61 (d, *J* = 7.8 Hz, 1H), 7.54 (d, *J* = 7.8 Hz, 1H), 7.38 (t, *J* = 7.4 Hz, 1H), 7.30 (dd, *J* = 12.7, 5.0 Hz, 4H), 7.05 (d, *J* = 7.5 Hz, 1H), 5.67 (s, 2H), 3.52 (s, 3H), 3.19 (s, 3H). ^{13}C NMR (101 MHz, DMSO) δ 160.64, 152.57, 136.46, 134.57, 134.40, 132.98, 130.33, 130.24, 129.97, 128.73, 128.16, 123.64, 122.97, 121.71, 119.39, 115.18, 111.50, 108.81, 48.22, 29.33, 26.67. HRESMS *m/z* calcd 379.1326 ($M^{\cdot+}$ +H); found: 379.1335.

*(E) -5-[(1-(4-nitrobenzyl)-1H-indol-3-yl)methylene]- 2-imino-1,3-dimethylimidazolidin-4-one (**84**):* ^{1}H NMR (400 MHz, DMSO) δ 8.83 (s, 1H), 8.19 (d, *J* = 8.4 Hz, 2H), 7.95 (d, *J* = 7.2 Hz, 1H), 7.47 (d, *J* = 7.5 Hz, 1H), 7.40 (d, *J* = 8.4 Hz, 2H), 7.24 – 7.11 (m, 3H), 6.44 (s, 1H), 5.69 (s, 2H), 3.27 (s, 3H), 3.06 (s, 3H). ^{13}C NMR (101 MHz, DMSO) δ 162.67, 150.98, 147.33, 146.16, 135.96, 130.88, 128.84, 128.41(d), 127.58, 124.34(d), 122.77, 120.50, 119.10, 110.83, 109.69, 102.19, 49.19, 27.43, 25.33. HRESMS *m/z* calcd 390.1566 ($M^{\cdot+}$ +H); found: 390.1572.

*(E) -5-[(1-(2-nitrobenzyl)-1H-indol-3-yl)methylene]- 2-imino-1,3-dimethylimidazolidin-4-one (**85**):* ^{1}H NMR (400 MHz, DMSO) δ 8.88 (s, 1H), 8.18 (dd, J = 7.8, 1.2 Hz, 1H), 8.07 – 8.00 (m, 1H), 7.58 (tt, J = 7.4, 6.2 Hz, 2H), 7.51 – 7.46 (m, 1H), 7.21 (p, J = 5.3 Hz, 2H), 6.78 (s, 1H), 6.55 (d, J = 7.5 Hz, 1H), 5.93 (s, 2H), 3.26 (s, 3H), 2.97 (s, 3H). ^{13}C NMR (101 MHz, DMSO) δ 162.35, 153.32, 147.71, 136.39, 134.76, 133.84, 132.34, 129.27, 128.69, 128.32, 125.75, 125.61, 123.16, 121.02, 119.16, 111.12, 109.45, 107.54, 47.60, 26.73, 24.76. HRESMS *m/z* calcd 390.1566 ($M^{\cdot+}$ +H); found: 390.1563.

*(E)-5-[(5-cyano-1H-indol-3-yl)methylene]-2-imino-1,3-dimethylimidazolidin-4-one (**86**):* ^{1}H NMR (400 MHz, DMSO) δ 12.16 (s, 1H), 8.89 (s, 1H), 8.63 (s, 1H), 7.61 (d, J = 8.4 Hz, 1H), 7.52 (d, J = 8.4 Hz, 1H), 6.86 (s, 1H), 3.36 (s, 3H), 3.11 (s, 3H). ^{13}C NMR (101 MHz, DMSO) δ 161.79, 158.16, 137.84, 136.40, 131.15, 128.02, 126.34, 125.21, 124.89, 121.03, 113.74, 109.94, 102.44, 28.36, 25.97. HRESMS *m/z* calcd 280.1198 ($M^{\cdot+}$ +H); found: 280.1201.

*(E)-5-[(1-acetyl-1H-indol-3-yl)methylene]-2-imino-1,3-dimethylimidazolidin-4-one (**87**):*

^{1}H NMR (400 MHz, DMSO) δ 9.67 (s, 1H), 9.22 (s, 1H), 8.36 (dd, J = 6.5, 2.4 Hz, 1H), 8.14 (dd, J = 6.2, 2.5 Hz, 1H), 7.53 – 7.36 (m, 2H), 7.18 (s, 1H), 3.51 (s, 3H), 3.23 (s, 3H), 2.73 (s, 3H). ^{13}C NMR (101 MHz, DMSO) δ 168.83, 162.30, 150.18, 136.40, 127.08, 126.23, 124.39, 124.08, 120.86, 119.84, 113.68, 109.14, 102.83, 33.36, 29.47, 24.51. HRESMS *m/z* calcd 297.1352 ($M^{\cdot+}$ +H); found: 297.1345.

*(E)-5-[(5-fluoro-1H-indol-3-yl)methylene]-2-imino-1,3-dimethylimidazolidin-4-one (**88**):* ^{1}H NMR (400 MHz, DMSO) δ 11.62 (s, 1H), 8.71 (s, 1H), 8.16 (s, 1H), 7.38 (d, *J* = 8.6 Hz, 1H), 7.24 (dd, *J* = 8.5, 1.4 Hz, 1H), 6.42 (s, 1H), 3.25 (s, 3H), 3.05 (s, 3H). ^{13}C NMR (101 MHz, DMSO) δ 160.16, 152.02, 134.56, 132.21, 129.61, 125.29, 122.41, 121.22, 115.25, 114.36, 113.75, 108.24, 28.97, 26.28. HRESMS *m/z* calcd 273.1152 ($M^{\cdot+}$ +H); found: 273.1151.

*(E)-5-[(5-methoxy-1H-indol-3-yl)methylene]-2-imino-1,3-dimethylimidazolidin-4-one (**89**):* ^{1}H NMR (400 MHz, DMSO) δ 11.92 (s, 1H), 9.27 (s, 1H), 8.95 (d, *J* = 3.0 Hz, 1H), 7.60 (d, *J* = 2.0 Hz, 1H), 7.40 (d, *J* = 8.7 Hz, 1H), 7.30 (s, 1H), 6.87 (dd, *J* = 8.7, 2.3 Hz, 1H), 3.85 (s, 3H), 3.52 (s, 3H), 3.20 (s, 3H). ^{13}C NMR (101 MHz, DMSO) δ 160.05, 154.97, 151.65, 131.75, 130.71, 128.57, 121.18, 116.29, 113.06, 112.55, 108.51, 100.86, 55.71, 28.98, 26.16. HRESMS *m/z* calcd 285.1352 ($M^{\cdot+}$ +H); found: 285.1358.

*(E) -5-[(1-methyl-1H-indol-3-yl)methylene]- 2-imino-1,3-dimethylimidazolidin-4-one (**90**):* ^{1}H NMR (400 MHz, DMSO) δ 8.81 (s, 1H), 7.98 (d, J = 7.9 Hz, 1H), 7.52 (d, J = 8.0 Hz, 1H), 7.26 (t, J = 7.5 Hz, 1H), 7.19 (t, J = 7.4 Hz, 1H), 6.76 (s, 1H), 3.88 (s, 3H), 3.25 (s, 3H), 3.01 (s, 3H). ^{13}C NMR (101 MHz, $CDCl_3$) δ 162.66, 152.69, 136.57, 132.11, 128.56, 125.85,

122.23, 120.17, 117.72, 109.74, 108.34, 104.23, 33.26, 27.03, 24.90. HRESMS *m/z* calcd 269.1402 ($M^{\cdot+}$ +H); found: 269.1397.

*(E) -5-[(1-ethyl-1H-indol-3-yl)methylene]- 2-imino-1,3-dimethylimidazolidin-4-one (**91**):* ^{1}H NMR (400 MHz, DMSO) δ 8.88 (s, 1H), 7.97 (d, J = 7.8 Hz, 1H), 7.55 (d, J = 8.1 Hz, 1H), 7.21 (dt, J = 25.3, 7.2 Hz, 2H), 6.75 (s, 1H), 4.29 (q, J = 7.2 Hz, 2H), 3.23 (s, 3H), 3.00 (s, 3H), 1.41 (t, J = 7.2 Hz, 3H). ^{13}C NMR (101 MHz, DMSO) δ 162.37, 153.23, 135.75, 131.18, 128.76, 124.84, 122.62, 120.58, 118.97, 110.78, 108.46, 108.22, 41.35, 26.68, 24.76, 15.66. HRESMS *m/z* calcd 283.1559 ($M^{\cdot+}$ +H); found: 283.1554.

*(E) -5-[(1-propyl-1H-indol-3-yl)methylene]- 2-imino-1,3-dimethylimidazolidin-4-one (**92**):* ^{1}H NMR (400 MHz, DMSO) δ 8.86 (s, 1H), 7.97 (d, *J* = 7.8 Hz, 1H), 7.56 (d, *J* = 8.0 Hz, 1H), 7.28 – 7.14 (m, 2H), 6.76 (s, 1H), 4.23 (t, *J* = 6.9 Hz, 2H), 3.24 (s, 3H), 3.01 (s, 3H), 1.89 – 1.75 (m, 2H), 0.87 (t, *J* = 7.3 Hz, 3H). ^{13}C NMR (101 MHz, DMSO) δ 162.39, 153.24, 136.40, 136.09, 131.95, 128.67, 124.90, 122.61, 120.54, 118.95, 110.91, 108.30, 48.05, 26.69, 24.77, 23.45, 11.60. HRESMS *m/z* calcd 297.1715 ($M^{\cdot+}$ +H); found: 297.1709.

VITA

Kevin Lewellyn was born and raised in Clarksdale, MS. He graduated from the University of Mississippi with a B.S. in Forensic Chemistry in May 2006. He worked as an analytical chemist at the Coy Waller Laboratory in Oxford, MS from 2006 – 2007.

Publications related to dissertation project:

- Lewellyn K, White SW, Sufka K, Tekwani, B, Chaurasiya, N, Zjawiony JK., Design and synthesis of aplysinopsin analogs with improved in vivo efficacy. (In preparation)

- Lewellyn, K, Bialonska, D, Loria, MJ, White, SW; Sufka, K, Zjawiony, J. K., In vitro structure–activity relationships of aplysinopsin analogs and their in vivo evaluation in the chick anxiety–depression model. *Biorg. Med. Chem.* **2013,** *21* (22), 7083-7090.

- Lewellyn K, Bialonksa D, Chaurasiya N, Tekwani B, Zjawiony J: Synthesis and evaluation of aplysinopsin analogs as inhibitors of human monoamine oxidase A and B. *Bioorg. Med. Chem. Lett.* **2012,** *22* (15): 4926-9.

Other Publications:

- Sufka KJ, Loria MJ, Lewellyn K, Zjawiony JK ,Ali Z, Abe N, Khan IA (in press). The effect of *Salvia divinorum* and *Mitragyna speciosa* extracts, fraction and major constituents on place aversion and place preference in rats. *Journal of Ethnopharmacology.*

- Fichna J, Dicay M, Lewellyn K, Janecka A, Zjawiony JK, Macnaughton WK, Storr MA: Salvinorin A has antiinflammatory and antinociceptive effects in experimental models of colitis in mice mediated by KOR and CB1 receptors. *Inflamm. Bowel Dis.* **2011,** 18(6):1137-45.

- Aviello G, Borrelli F, Guida F, Romano B, Lewellyn K, De Chiaro M, Luongo L, Zjawiony JK, Maione S, Izzo AA *et al*: Ultrapotent effects of salvinorin A, a hallucinogenic compound from Salvia divinorum, on LPS-stimulated murine macrophages and its anti-inflammatory action in vivo. *J. Mol. Med. (Berlin)* **2011**, 89(9):891-902.

- Fichna J, Lewellyn K, Yan F, Roth BL, Zjawiony JK: Synthesis and biological evaluation of new salvinorin A analogues incorporating natural amino acids. *Bioorg. Med. Chem. Lett.* **2011**, 21(1):160-163.